Anorganisch-chemisches Institut der Technischen Universität München

Contributions to the Chemistry of Gold(I) Cyanide, Isocyanide and Acetylide Complexes

Ruei-Yang Liau

Vollständiger Abdruck der von der Fakultät für Chemie
der Technischen UniversitätMünchen zur Erlangung des akademischen Grades eines

Doktors der Naturwissenschaften

genehmigten Dissertation.

Vorsitzender : Univ.-Prof. Dr. M. Schuster

Prüfer der Dissertation :

1. Univ.-Prof. Dr. H. Schmidbaur, em.
2. Univ.-Prof. Dr. Dr. h. c. St. Veprek

Die Dissertation wurde am 08.07.2003 bei der Technischen Universität München eingereicht und durch die Fakultät für Chemie am 30.07.2003 angenommen.

Die vorliegende Arbeit entstand in der Zeit von April 2001 bis Mai 2003 unter der Leitung von Herrn Prof. Dr H. Schmidbaur am Anorganisch-chemischen Institut der Technischen Universität München.

Meinem verehrten Lehrer

HERRN PROFESSOR DR H. SCHMIDBAUR

DANKE ICH FÜR DAS INTERESSANTE THEMA DIESER DISSERTATION, FÜR DAS MIR STETS ENTGEGENGEBRACHTE WOHLWOLLEN SOWIE FÜR DIE UNTERSTÜTZUNG MEINER ARBEIT IN EINER ATMOSPHÄRE GRÖSSTMÖGLICHER WISSENSCHAFTLICHER FREIHEIT.

To my parents, my wife and my son
with deep love and gratitude

ACKNOWLEDGEMENTS

I would like to express my sincere gratitude to Prof. Dr H. Schmidbaur for giving me the opportunity to work in his group. It is with great appreciation that I acknowledge him as a congenial supervisor.

I sincerely appreciate Mrs H. Froh and Mrs M. Donaubauer, the secretaries of the institute, for their generous help with organization and other tedious matters.

My sincere thanks also to Dr A. Schier for her patience and magnificence with the crystal structural determinations included in this work.

Mr M. Barth, Mrs S. Emmer, Mr T. Tafelmaier and Mrs U. Ammari are acknowledged for the elemental analysis presented in this work.

Ms R. Dumitrescu and Ms I. Werner are acknowledged for the measurements of mass spectra.

Mrs M. Bauer is acknowledged for her measurements of the Raman spectra by a Renishaw Raman Spectrometer Serie 1000 instrument.

Dr T. Mathieson, Dr J. Wilton-Ely, Dr A. Hamel and Dr H. Ehlich are gratefully acknowledged for an introduction into the field of gold chemistry.

Dr G. Wegner is especially acknowledged from my commencement in the working group as a good advisor because of his personality.

Prof. N. W. Mitzel, Dr R. Berger and Dr C. Lustig are acknowledged for their great discussions and suggestions in this work.

Mr A. Enthart and Mr M. Schulte-Bockholt are acknowledged for their collaboration and discussions by the Anorganisch-chemischen Fortgeschrittenpraktikum.

Dr G. Wegner and Mr F. Wiesbrock, my lab-colleagues are greatly acknowledged for the friendly working atmosphere and many useful suggestions.

The help of Miss S. Thwaite, Dr K. Porter and Dr K. Kemper is deeply appreciated for proof

reading this thesis.

To Miss D. Arnold, Dr E. Schmidt, Mrs G. Bassioni, Mr B. Djordjevic, Mrs G. Krutsch, Mr O. Minge, Mr U. Monkowius, Mr S. Nogai, Dr G. Rabe, Mr S. Reiter, Dr A. Rether, Mr P. Roembke, Mr D. Schneider, Mr O. Schuster, Mr T. Segmüller, Mr K. Vojinovic and all the friends that in some way contributed to this thesis, I am thankful for their great cooperativeness and friendly working atmosphere.

Finally I would like to express my affectionate gratitude to my parents, my wife and my son for their love, understanding and warm encouragement that enabled me to go through this journey.

ABBREVIATION

Et	ethyl
Fc	ferrocenyl
IR	Infrared
- s	strong (IR / Raman)
- vw	very weak (IR / Raman)
- w	weak (IR / Raman)
L	neutral ligand
Me	methyl
m. p.	melting point
MS	Mass Spectroscopy
NMR	Nuclear Magnetic Resonance
- δ	chemical shift (ppm, NMR)
- s	singlet (NMR)
- d	doublet (NMR)
- t	triplet (NMR)
- q	quartet (NMR)
Np	naphthyl
NQR	Nuclear Quadrupole Resonance
ppm	parts per million
PPN	Bis(triphenylphosphoranylidene)ammonium
Ph	phenyl
m-Tol	meta-tolyl
p-Tol	para-tolyl
RT	room temperature
^{t}Bu	tertiary butyl
THF	tetrahydrofuran
tht	tetrahydrothiophene
Vi	vinyl
ν	stretching frequency
X	mono-anionic ligand
XRD	X-ray diffraction
Z	atomic number

CONTENTS

1 General Introduction

The chemical symbol Au for gold derives from the Latin word *aurum* meaning 'shining dawn'. Auroa was the Roman goddess of dawn. From this etymological connection it appears that gold was from early times for humans a symbol of light and beauty, materializing the immortality of the gods.[1]

As the king of the elements gold is one of the most noble of the metals and has a unique position among the elements in the Periodic Table. Through history the possession of elemental gold has provided power and prestige to many nations, societies and individuals. In its various forms - as pure gold with glittering yellow color, or as a component of alloys or chemical compounds - it is used extensively in jewellery and decorative pieces but practical usage has for a long time been limited to applications such as dental fillings.

Gold, together with silver and copper are found in the IB subgroup of the Periodic Table of the Elements. These three metals were the first metals known to man as noble metals. The reactivity of Cu, Ag and Au decreases down the group, and in its inertness gold resembles the platinum group metals. The average relative abundances of the three coinage metals in the earth's crust are estimated to be: Cu = 68 ppm, Ag = 0.08 ppm and Au = 0.004 ppm. Gold belongs to a group of 23 trace elements that form only 0.0003 % of all elements present in the earth's crust. In seawater gold is present to the extent of about 0.001 ppm. In primary deposits gold is often chemically associated with tellurium or bismuth, and elemental gold is mainly found in pyrite and arsenopyrite. In secondary deposits, i.e. fluviatile or marine sediments, gold is found in elementary form as grains in so-called placer deposits.[1]

According to modern analysis, the gold content in the human lung is 0.1 - 400 ng/g[2]. The horns of the rhinoceros and antelopes and other animals contain traces of gold. For example, the gold content in the ashes of deer horn is 60 - 80 µg/g[2] and 0.3 - 28.3 ng/g in ashed horn of *odocoileus hemious*[3]. Boyle considered that the gold concentrates mainly in protein (e.g. horn,

---

[1] Morteani, G., in Schmidbaur, H. (ed.): Gold, Progress in Chemistry, Biochemistry and Technology, p.40, Wiley & Sons, Chichester, **1999**.

[2] Brooks, P. R.,"Noble Metals and Biological Systems", (Their Role in Medicine, Mineral Exploration and Enviroment), CRC Press Inc, **1992**.

[3] Jones, R. S., U.S. Geol. Surv. Circ., **1969**, 610.

hair) possibly as gold-protein complexes.[4] Many medicinal herbs contain a trace of gold[5] and their extracts might contain a trace of a gold complex that could cure sickness.[6]

From ancient cultures, such as those in India and Egypt, until current use as Auranofin, gold has been used in medicines of various kinds. The use of gold to cure sickness could date back as far as 2500 BC in China.[6-10] The modern use of gold complexes in medicine traces the experimental work of the German physician Robert Koch, who discovered the bacteriostatic effects of $Au(CN)_2^-$. In 1929, the French physician Jacques Forestier was the first to report the anti-arthritic activity of gold complexes (sodium aurothiopropanol sulfonate) to cure rheumatic arthritis.[11-13] Today the biochemistry of gold has developed primarily in response to the prolonged use of gold compounds in treating rheumatoid arthritis and in response to efforts to develop complexes with anti-tumor and anti-HIV activity.[13] Furthermore, specific gold complexes are used in the therapeutic treatment of rheumatoid arthritis and the potential of gold drugs as anti-tumour agents is receiving some attention.[14]

In addition to the development of gold compounds in medicine, the trend has changed significantly during the latter decades of the 20th century for the use of gold compounds in other areas. For example, this is especially apparent in the electronic industry which makes use of gold for specialized applications due to the high electrical conductivity and the high corrosion resistance of gold and many of its alloys.[15] Attributable to the lack of reactivity, the high cost

---

[4]Boyle, R. W., Geol. Surv. Can. Bull. **1979**, 280.

[5] Zhao, H., Ning, Y., Precious Metals (in Chinese). **1999**, 20(1), 45.

[6] Zhao, H., Ning, Y., Gold Bull. **2001**, 34(1), 24.

[7] Needham, J. M., "Science and Civilization in China, Vol. 5", Cambridge University Press, **1974**, 285.

[8] Fricker, S. P., Gold Bull., **1996**, 29(2), 53.

[9] Wigley, R. A., Brooks, R. R., "Gold and Silver in Medicine", in "Noble Metals and Biological Systems" CRC Press Inc., **1992**, pp 277-279.

[10] Dyson, G. M., J. Pharm., **1929**, 123, 249-250, 266-267.

[11] Higby, G. J., Gold Bull. **1982**, 15, 130.

[12] Kean, W. F., Lock, C. J., Howard-Lock, Inflammopharmacology, **1991**, 1, 103-114.

[13] Shaw III, C. F., in Schmidbaur, H. (ed.): Gold, Progress in Chemistry, Biochemistry and Technology, p.260, Wiley & Sons, Chichester, **1999**

[14] a) Brown, D. H., Smith, W. E., Chem. Soc. Rev., 1980, 9, 217. b) Sadler, P. J., Adv. Inorg. Chem., **1991**, 36, 1. c) Shaw III,C. F., in Metal Compounds in Cancer Therapy, ed. Fricker,, S. P., Chapman & Hall, London, **1994**, p. 47-64.

[15] a) Okinaka, Y., Hoshino, M., Gold Bull., 1998, 31, 3; b) Puddephatt, R. J., Treurnicht, I., J. Organomet. Chem. **1987**, 319, 129.

and the ease with which gold compounds decompose, the chemistry of gold was not studied in depth in the past.

In a typical modern gold recovery plant, the ore is first crushed and milled to render the gold available for leaching, which is achieved by cyanidation. Once the gold is in solution, it is recovered by adsorption onto activated carbon (carbon-in-pulp process), or by cementration on to zinc powder (Merrill-Crowe process), followed by subsequent recovery and smelting. It is noteworthy that these processes have all been known for at least 100 years, and are still used to this day. Due to improvements in the materials and engineering and more, the carbon-on-pulp process has only recently been applied on a commercial scale and the knowledge of the chemistry has been forthcoming in the last decade. In recent years because of the increase in environmental pressure, the minimization of cyanide released to backfill streams, plant effluents and tailings dam overflows is a topic of increasing international concern. Many plants are currently treating these streams by various methods, e.g. natural degradation (ponding), oxidation with hydrogen peroxide (or alkaline chlorination, SO_2/air, biological), adsorption using activated carbon or on ion-exchange resins.[16]

The natural degradation by "ponding" is the most common method of cyanide destruction that is currently used in gold plants. The processes that occur naturally in tailings dams include volatilization of HCN, bio-degradation, photo-decomposition of metal-cyanide complexes by UV light, and subsequent precipitation of the metals as hydroxides. The natural degradation is suitable in favorable climate with intensive UV light, otherwise the process using hydrogen peroxide oxidation a favorable alternative (shown in following processes).[17]

$$2\ Au\ +\ ½\ O_2\ +\ 4\ NaCN \xrightarrow{H_2O} 2\ Na(AuCN)_2\ +\ 2\ NaOH$$

$$2\ Na(AuCN)_2\ +\ 2\ e^- \xrightarrow[E1.]{2\ Na^+} 2\ Au\ +\ 4\ NaCN$$

[16] Adams, M. D., Jones, M. W., Dew, D. W., in Schmidbaur, H. (ed.): Gold, Progress in Chemistry, Biochemistry and Technology, p.40, Wiley & Sons, Chichester, **1999**.

[17] Schmidbaur, H., Naturw. Rdsch. **1995**, 48, 443.

$$2\ NaCN \xrightarrow[H_2O\ /\ O_2\ /\ h\nu]{H_2O\ /\ H_2O_2} 2\ NH_3 + 2\ NaHCO_3$$

Gold is the least reactive of all the metals, being the only one not chemically attacked by either oxygen or sulphur at any temperature. Gold(0) has the electronic configuration [Xe] $4f^{14}$ $5d^{10}$ $6s^1$. The inorganic and coordination compounds of gold are unique and form remarkable complexes in oxidation states from –I to +V, often with unusual stereochemistry. As expected from the electronic configuration, the oxidation states +1 and +3, corresponding to the electron configurations [Xe] $4f^{14}$ $5d^{10}$ $6s^0$ $6p^0$ and [Xe] $4f^{14}$ $5d^8$ $6s^0$ $6p^0$, are the most common and stable. The gold(I) complexes are usually two-coordinate, linear, diamagnetic 14-electron species. Three-coordinate trigonal-planar complexes and tetrahedrally four-coordinate complexes of monovalent gold have been characterized but are not as numerous.[18-20] Gold(III) complexes are almost always four-coordinate 16-electron species with square-planar stereochemistry, and hence are diamagnetic.

Physical methods have played an important role in studies of structure and bonding in gold compounds. These methods can be divided into spectroscopic and non-spectroscopic methods. Of the non-spectroscopic methods, the most important is X-ray diffraction which has been used to determine the structures of numerous gold compounds. The types of spectroscopic methods, e.g. vibrational (IR, Raman) spectroscopy, electronic (absorption, luminescence) spectroscopy, magnetic resonance spectroscopy (EPR, NMR and NQR) and Mössbauer spectroscopy, which are applicable is dictated to some extent by the electronic properties of the gold atom in its two most common oxidation states, +1 and +3.[21]

Gold has a single isotope, ^{197}Au, which is 100 percent abundant. It is a quadrupolar nucleus (I = 3/2) and as a result of rapid relaxation, the signals are extremely weak and broad. The consequence is that ^{197}Au NMR or NQR detection is not an effective spectroscopic tool. As a

---

[18] Crespo, O., Gimeno, M. C., Laguna, A., Jones, P. G., J. Chem. Soc., Dalton Trans., **1992**, 1601.

[19] Balch, A. L., Fung, E. Y., Inorg. Chem., **1990**, 29, 4764.

[20] Viotte, M., Gautheron, B., Kubicki, M. M., Mugnier, Y., Parish, R. V., Inorg. Chem. **1995**, 34, 3465.

[21] Bowmaker, G. A., in Schmidbaur, H. (ed.): Gold, Progress in Chemistry, Biochemistry and Technology, p.841, Wiley & Sons, Chichester, **1999.**

practical matter, NMR studies of gold complexes, whether inorganic, organometallic or biological on nature, are based on other isotopes such as ^{31}P, ^{13}C or ^{1}H, which are present in the ligands.[22] However, ^{197}Au is one of the most favorable nuclei for the observation of Mössbauer spectra, and such spectra have played an important role in the characterization of gold compounds.

1.1 Gold(I) and Aurophilicity

Gold(I) complexes generally take the form of LAuX (L = neutral ligand; X = anionic ligand). The ionic species $[LAuL]^+$ and $[XAuX]^-$ have also been observed. These linear complexes are characterized by a strong preference for large polarisable donor atoms. This is consistent with the perception that gold(I) ion is a particularly soft Lewis acid and forms strong associations with soft Lewis bases.[23] Gold(I) complexes of the type $(R_3P)AuX$ have been characterized extensively. Thiol (R_2S) and isonitrile (RNC) complexes are reasonably well documented. This trend is a general reflection on the stability afforded to the gold(I) center by the neutral ligand. Gold(I) complexes are usually prepared by treating the tetrachloroauric ion $[AuCl_4]^-$ with oxidisable ligands, for example, R_3P, R_2S or RNC. The reaction generally proceeds by way of reductive elimination of a neutral $LAuCl_3$ intermediate.

In recent years there have been more investigations into the application of crystallography in gold complexes. From structural and spectroscopic studies of gold compounds in general extensive evidence has emerged for the existence of closer-than-normal Au--Au distances, indicating an attractive interaction between the metal centers.[24-30] It has been established that these energetically favorable Au--Au contacts can result in the formation of dimeric, oligomeric and polymeric aggregations of gold(I) complexes.

---

[22] Shaw III, C. F., in The chemistry of organic derivatives of gold and silver, Patai, S., Rappoport, Z., editors, John Willey & Sons Ltd., **1999**.

[23] Schmidbaur, H., Chem. Soc. Rev., **1995**, 24, 391.

[24] Pathaneni, S. S., Desiraju, G. R., J. Chem. Soc., Dalton Trans., **1993**, 319.

[25] Parish, R. V., Hyperfine Interact. **1988**, 40, 159.

[26] Melnik, M., Parish, R. V., Coor, Chem. Rev., **1986**, 70, 157.

[27] Jones, P. G., Gold Bull., **1981**, 14, 102.

[28] Jones, P. G., Gold Bull., **1981**, 14, 159.

[29] Jones, P. G., Gold Bull., **1983**, 16, 114.

[30] Jones, P. G., Gold Bull., **1986**, 19, 46.

1.1.1 Aurophilic Attraction

The gaseous diatomic molecule Au_2 with extreme stability has a bond length of 2.47 Å with a bond dissociation energy of 288 kJ/mol.[31] The bond length is likely to represent the shortest distance possible between two gold atoms. The inter-atomic distance in bulk metallic gold is 2.88 Å with a bond energy of the order of 100 kJ/mol. This unexpected short lattice constant Au--Au is shorter than the corresponding Ag--Ag contact in metallic silver.[32] Intermolecular Au--Au interaction distances of greater than 3.0 Å are associated with energy of ~ 30 kJ/mol, which is comparable to that of hydrogen bonding.[33] From crystal structure investigations, Au--Au contacts shorter than twice the van der Waals radius of gold atoms (4 Å) have been observed, shorter than the bond length in element gold. This unexpected interatomic attractive force between gold atoms appears to be weak but turned out to determine, at least in part, molecular configurations and crystal lattices of gold compounds.[34] This phenomenon appeared not only with gold metal in the zero oxidation state [Au(0)],[32] but also in gold clusters with mixed valence characteristics,[35,36] for compounds of classical Au(I) and Au(III) oxidation states,[37-39] and even for the $[Au(II)]_2$ species.[40,41]

Classical theories of chemical bonding cannot provide a sound explanation for the short Au--Au interactions.[42] It would normally be expected that two gold(I) centers would repel each

---

[31] a) Spiro, T. G., Progr. Inorg. Chem.**1970**, 11,1; b) Gingerich , K. A., J. Cryst. Growth., **1971**, 9, 31.; c)Kordis, J., Gingerich, K. A., Seyse,, R. J., J. Chem. Int. Ed. Engl., **1974**, 61, 5114.

[32] Wells, A. F., Structural Inorganic Chemistry, 5th Ed. Clarendon Press, Oxford, **1987**.

[33] Mingos, D. M. P., J. Chem. Soc., Dalton Trans., **1996**, 561.

[34] Schmidbaur, H. in 'Gold 100', Vol. 3, ASIMM, Johannesburg, **1986**.

[35] Mingos, D. M. P., Gold Bull., **1984**, 17,5.

[36] Mingos, D. M. P., J. Chem. Soc., Dalton Trans., **1976**, 1163.

[37] a) Puddephatt, R. J. in Comprehensive Coordination Chemistry, (Wilkinson, G., Gillard, R. D., McLeverty, J. A., Eds.) Vol. 5, Pergamon, Oxford, **1987**; b) Puddephatt, R. J. in Comprehensive Organometallic Chemistry, (Wilkinson, G., Stone, F. G. A., Abel, E. W., Eds.) Vol. 5, Pergamon, Oxford, **1985**.

[38] Puddephatt, R. J. in The Chemistry of Gold, Elsevier, Amsterdam, **1978**.

[39] Schmidbaur, H. in Organogold Compounds, Gmelin Handbook of Inorganic Chemistry, Springer-Verlag, Berlin **1980**.

[40] Schmidbaur, H., Wohlleben, A., Wagner, F., van der Vondel, D. F., van der Kelen, G. P., Chem. Ber., **1977**, 110.

[41] Schmidbaur, H., Mandl, J. R., Frank, A., Huttner, G., Chem. Ber. **1976**, 109 ,466.

[42] Pyykkö, P., Mendizabel, F., Chem. Eur. J., **1997**, 3, 1458.

other on close contact.[43] This phenomenon established by crystallographic analysis of gold(I) complexes was described as " … the unprecedented affinity between gold atoms even with closed shell electron configurations and equivalent electrical charges, … "[44] and is known as aurophilicity, a term coined by H. Schmidbaur.[45]

1.1.2 Relativistic Effect

Gold(0) has the electronic configuration [Xe] $4f^{14}$ $5d^{10}$ $6s^{1}$ and the gold(I) cation has the formal electronic configuration [Xe] $4f^{14}$ $5d^{10}$ $6s^{0}$ $6p^{0}$. The attractive Au--Au contacts have been interpreted as a donation of electron density from filled d-orbitals on one metal center to empty p-orbitals on another. The phenomena are accounted for by the influence of relativity and correlations effect on the orbitals of the large gold nucleus.[46,47]

The electrons in atoms with high atomic numbers, under the influence of the increased nuclear point charge, reach velocities that approach the velocity of light and therefore have to be treated according to Einstein's theories of relativity. With the term v_e/v_l (where v_e and v_l are the velocities of the electron and the light, respectively) close to unity, the 'relativistic mass' of the electron is strongly increased, with a consequence also for the orbital radii of these electrons. The ratio of the relativistic radius of the valence electrons to their non-relativistic radius is shown as a function of the atomic number (Z) in **Figure 1-1.**[48,49] It is clear that this ratio strongly deviates from unity as Z is increased, and that $\langle r \rangle_{rel} / \langle r \rangle_{non\text{-}rel}$ reaches a pronounced local minimum for the element gold. Thus without any other special assumptions having to be made, this theoretical approach leads to the conclusion that gold occupies, in fact, a unique position among the elements.

---

[43] Pyykkö, P., Li, J., Runeberg, N., Chem. Phys. Lett. **1994**, 218, 133.

[44] Schmidbaur, H., Gold Bull., **1990**, 23 ,11.

[45] Schmidbaur, H., Chem. Soc. Rev., **1995**, 24, 391.

[46] Pyykkö, P., Desclaux, J. P., Accounts Chem. Res., **1979**, 12, 276.

[47] Pitzer, K. S., Accounts Chem. Res., **1979**, 12, 271, and literature therein.

[48] Pyykkö, P., Adv. Quantum Chem. **1978**, 11, 353.

[49] Pyykkö, P., Chem. Rev., **1988**, 88, 563, and refs. therein.

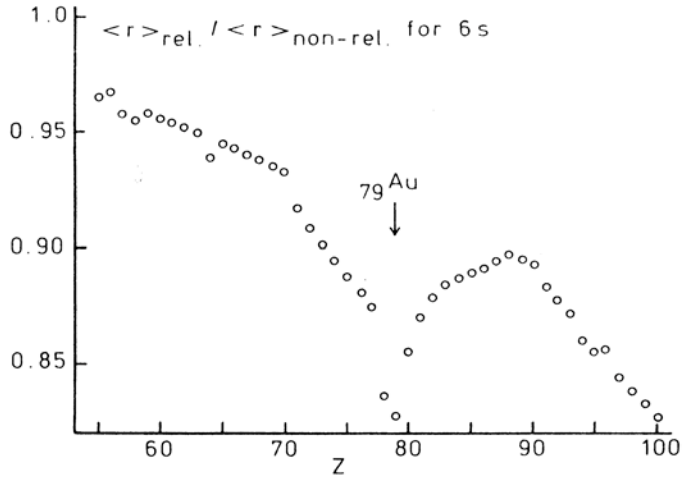

Figure 1-1 . The relativistic contraction of the 6s shell of elements Cs (Z = 55) to Fm (Z = 100), calculated as $\langle r_{6s} \rangle_{rel} / \langle r_{6s} \rangle_{non\text{-}rel.}$[48] The element gold (Z = 79) represents a pronounced local minimum.

In order to characterize the relativistic effect, it is often split into three (interrelated) 'symptoms':

a) s-orbital and - to a smaller extent - p-orbital contraction,

b) spin-orbit coupling, and

c) d-orbital expansion.

Taken together, these points mean that valence shell electrons of different orbital momentum (s, p, d) are brought much together in energy, especially with respect to the gap between the 6s and 5d states. Calculations have shown that through these drastic changes (as compared with the Ag homologue or other neighboring elements) the block of the so-called $5d^{10}$ 'closed shell' electrons of the Au(0) or Au(I) oxidation states can be 'broken up' and 'mobilized' for chemical bonding.[50-52] The calculated non-relativistic and relativistic (n-1)d and ns orbital energies for Ag (n = 5) and Au (n = 6) are shown in **Figure 1-2**.[48,53,54] The position of gold in the Periodic Table is such that the relativistic effects are at a maximum. Many of the anomalous properties of Au as compared with Ag and Cu are ascribed to such effects.

---

[50] a) Rösch, N., Görling, A., Ellis, D. E., Schmidbaur, H., Angew. Chem. **1989**, 101, 1410. b) Rösch, N., Görling, A., Ellis, D. E., Schmidbaur, H., Angew. Chem. Int. Ed. Engl. **1989**, 28, 1357.

[51] Jiang , Y., Alvarez, S., Hoffmann, R., Inorg. Chem., **1985**, 24, 749.

[52] a) Merz, K. M., Hoffmann, R., Inorg. Chem., **1988**, 27, 2120. b) Mehrotra, P. K., Hoffmann, R., Inorg. Chem., **1978**, 17, 2187. c) Dedieu, A., Hoffmann, R., J. Amer. Soc. **1978**, 100, 2074.

[53] Desclaux, J. P., At. Data Nucl. Data Tables, **1973**, 12, 311.

[54] Kaltsoyannis, N., J. Chem. Soc., Dalton Trans., **1997**, 1.

The tendency of gold(I) to form linear two-coordinate complexes through particularly efficient s/p or s/d hybridization is shown in Figure 1-3.[32-39] The promotion of hybridization by relativistic effects has been invoked to explain the predominance of gold(I) linear two-coordinate species. Hybridisation of $5d_Z^2$ and 6s allows the electron pair from $5d_Z^2$ to be placed in ψ_1 (see A in **Figure 1-3**). Mixing of ψ_2 and $6p_Z$ gives the ψ_3 and ψ_4 hybrid orbitals (see B in **Figure 1-3**),[55] and donor ligands will interact with these orbitals along the molecular z-axis.[56]

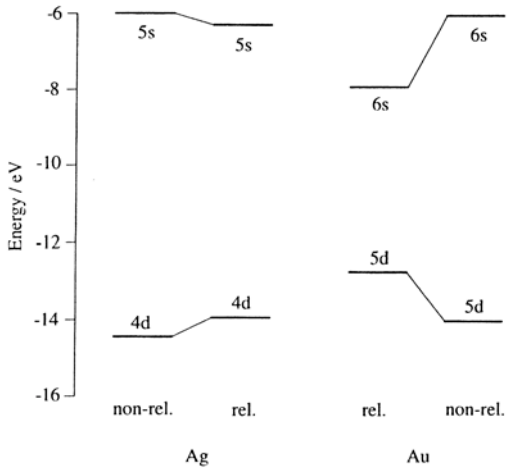

Figure 1-2. Calculated non-relativistic and relativistic (n-1)d and ns orbital energies for Ag (n = 5) and Au (n = 6). Relativistic d-orbital energies are the weighted average of the $d_{3/2}$ and $d_{5/2}$ spin-orbit components.

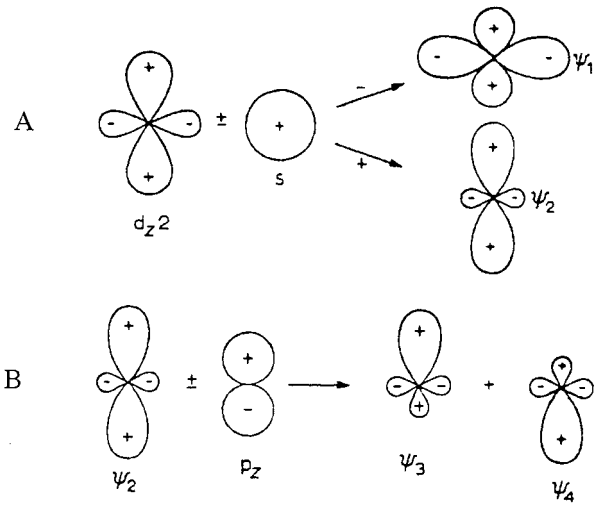

Figure 1-3. Formation of gold(I) linear complexes. (A): Hybridisation of $5d_Z^2$ and 6_s, (B) Mixing of ψ_2 and $6p_Z$.

[55] Puddephatt, R. J. in The Chemistry of Gold, Elsevier, Amsterdam, **1978**, p. 17.

[56] Cotton, F. A., Wilkinson, G., Advanced Inorganic Chemistry, J. Wiley & Sons, London, **1988**, p. 941.

1.1.3 LAuX Crystallography

Gold(I) complexes of the type L-Au-X (L = neutral donor ligand, X = anionic ligand like halide or pseudohalide) can be aggregated into dimers, oligomers or polymers. The degree of oligomerization is clearly determined by a number of factors, among which the steric and electronic effects of the ligands are most obvious. Large ligands, for example Ph_3P, tend to completely preclude the formation of Au--Au contacts.[57] The aggregation of the complexes generally involves one of three principal modes (**Figure 1-4**).[58] On rare occasions, combinations of these modes are observed in the crystal structure. A is a parallel interaction with a head-to-head ligand arrangement. B is described as an anti-parallel interaction with a head-to-tail ligand arrangement. C is an interaction with crossed ligands which are not necessarily perpendicular.

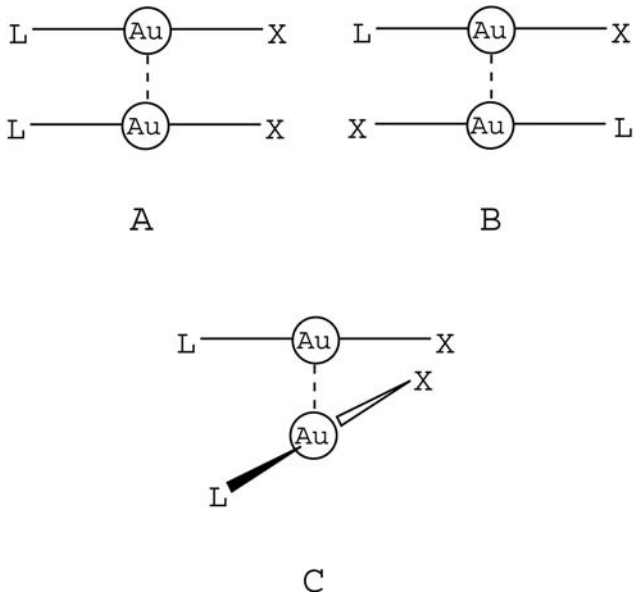

Figure 1-4. The interaction modes of LAuX aggregation.

The association leads to shorter intermolecular, sub-van-der-Waals contacts between the gold atoms in the range of d(Au--Au) 2.90 – 3.50 Å, and indicates a stronger interaction in the order of 5-10 kcal/mol for a dimeric unit. The crossed ligand dimers of LAuX molecules often have relatively shorter Au--Au contacts than the parallel dimers. For a series of hypothetical $(H_3P)AuX$ dimers, Pyykkö has carried out extensive theoretical calculations on Au--Au inter-

[57] Ahrland, S., Dreisch, K., Noren, B., Oskarsson, Å., Acta Chem. Scand., **1987**, 41a, 173.

[58] Schneider, W., Angermaier, K., Sladek, A., Schmidbaur, H., Z. Naturforsch. **1996**, 51b, 790.

actions and concluded that polarisable anions result in a stronger Au--Au attraction.[59]

As example (1,3,5-triaza-7-phosphaadamantane)AuX (X = Cl or Br) have been characterized as isostructural dimeric 'crossed lollipops' (**Figure 1-5**).[60] The relatively short intermolecular Au--Au distances are 3.092 Å and 3.107 Å, respectively. This result does not support the theory of soft anions (Br > Cl) enhancing the Au--Au attraction.

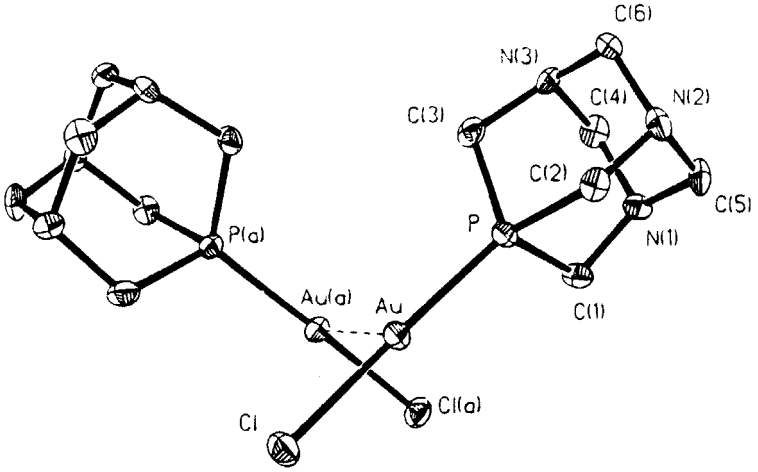

Figure 1-5. (1,3,5-triaza-7-phosphaadamantane)AuCl dimer.

The series of $(Me_2PhP)AuX$ (X = Cl,[61] Br[61] or I[61]) crystal structures have been determined, each forming a crossed dimer [**Figure 1-6**, $(Me_2PhP)AuCl$]. The Au--Au contact distances are 3.230(2) Å, 3.119(2) Å and 3.104(2) Å respectively, supporting Pyykkö's theoretical calculations. The calculated Au--Au distances for such dimers with perpendicular orientation of the two linear units are 3.366(2) Å (Cl), 3.338 Å (Br) and 3.315 Å (I).[62] The chloro complex crystallized in two separate polymorphic forms, i.e. colorless hexagonal blocks of trimeric $[(Me_2PhP)AuCl]_3$ and colorless prisms of dimeric $[(Me_2PhP)AuCl]_2$ molecules. The dimeric $[(Me_2PhP)AuCl]_2$ was reported by Tiekink *et al.* with apparent close Au--Au interaction.[63] In the report of Balch *et al.*[61] the two nearly linear P-Au-Cl units are staggered and connected through a Au--Au bond of length 3.230(2) Å.

---

[59] Pyykkö, P., Runeberg, N., Mendizabal, F., Chem. Eur. J., **1997**, 3, 1451.

[60] Assefa, Z., McBurnett, B. G., Staples, R. J., Fackler Jr., J. P., Assmann, B., Angermaier, K., Schmidbaur, H., Inorg. Chem. **1995**, 34, 75.

[61] Toronto, D. V., Weissbart, B., Tinti, D. S., Balch, A. L., Inorg. Chem. **1996**, 35, 2484.

[62] Li, J., Pyykkö, P., Chem. Phys. Lett. **1992**, 197, 586.

[63] Cookson, P. D., Tiekink, E. R. T., Acta Crystallogr. **1993**, C49, 1602.

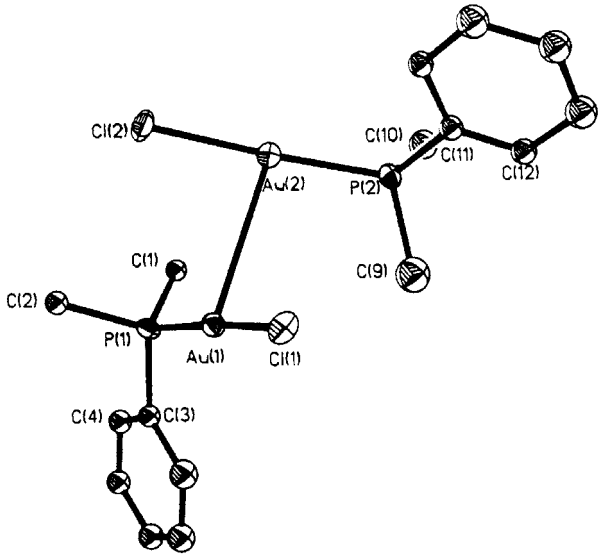

Figure 1-6. $[(Me_2PhP)AuCl]_2$ dimer.

Trimeric $[(Me_2PhP)AuCl]_3$ is a rare aurophilic polymorph (**Figure 1-7**). These linear units are connected by the interactions of pairs of gold atoms at relatively short distances [Au(1)-Au(2), 3.091(2) Å; Au(2)-Au(3), 3.120(2) Å)].[61]

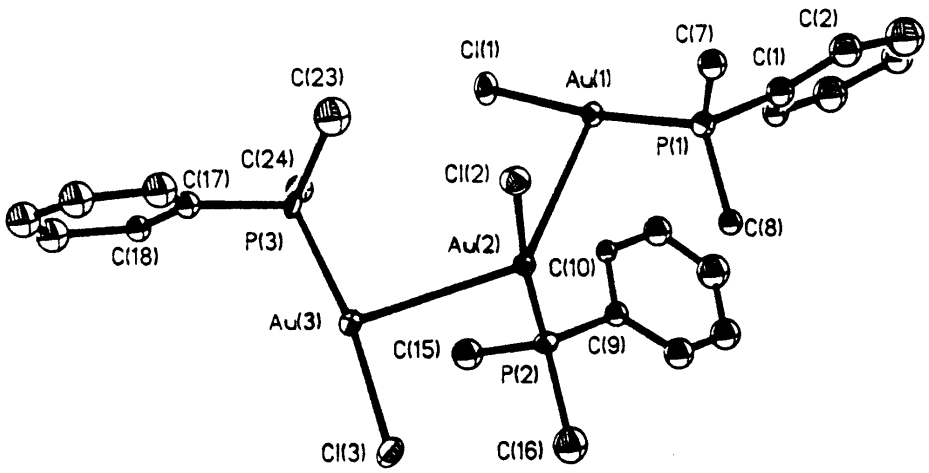

Figure 1-7. $[(Me_2PhP)AuCl]_3$ trimer.

The $(Me_3P)AuX$ (X = Cl,[64] Br[65] or CN[66]) complexes have been found to crystallize as isostructural polymeric chains with the crossed ligands forming helices. The structures of

---

[64] Angermaier, K., Zeller, E., Schmidbaur, H., J. Organomet. Chem. **1994**, 472, 371.

[65] Angermaier, K., Bowmaker, G. A., de Silva, E. N., Healy, P. C., Jones, B. E., Schmidbaur, H., Acta Chem. Scand. **1992**, 46a, 262.

[66] Ahrland, S., Dreisch, K., Noren, B., Oskarsson, Å., Acta Chem. Scand. **1987**, 41a, 173.

(Me_3P)AuCl and (Me_3P)AuCN are depicted in **Figure 1-8** and **Figure 1-9**, respectively. The mean Au--Au contact distances are 3.34 Å (Cl), 3.73 Å (Br) and 3.29 Å (CN). The (Me_3P)AuBr chain appears to be broken into a series of trimers with a long Au(1)'--Au(3) distance of 3.980(2) Å in between.

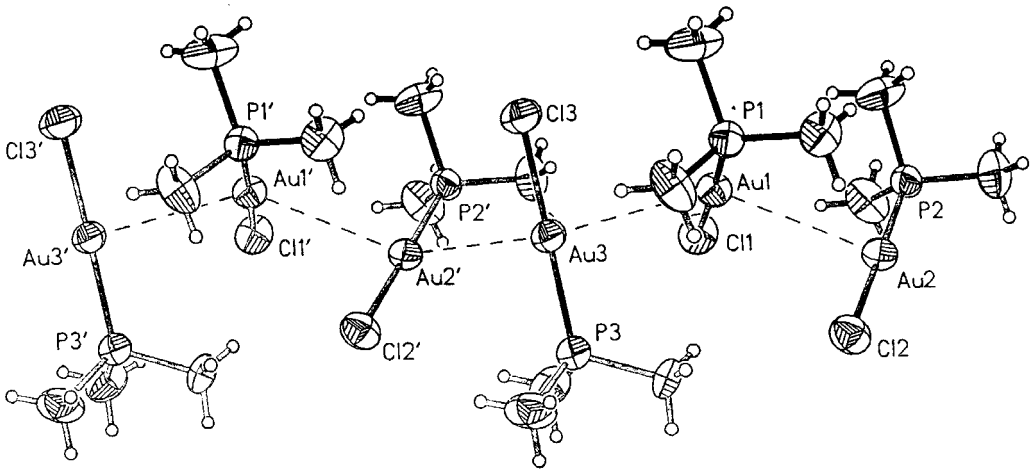

Figure 1-8. Chain of (Me_3P)AuCl molecules.

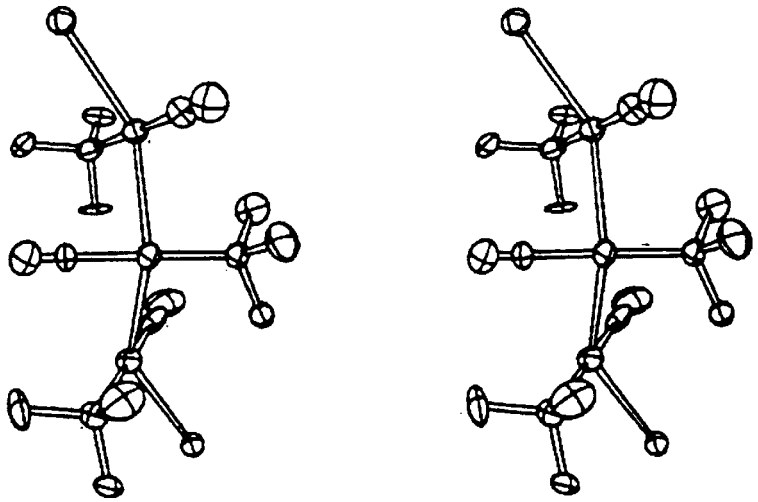

Figure 1-9. Stereoview of (Me_3P)AuCN crystal packing.

(Me_3P)AuI relinquishes the polymeric structure completely and exhibits dimers with a single crossed Au--Au interaction of 3.168 Å (**Figure 1-10**).[66] The short Au--Au distance of the dimer does not indicate that the iodide is enhancing the aurophilic interaction.

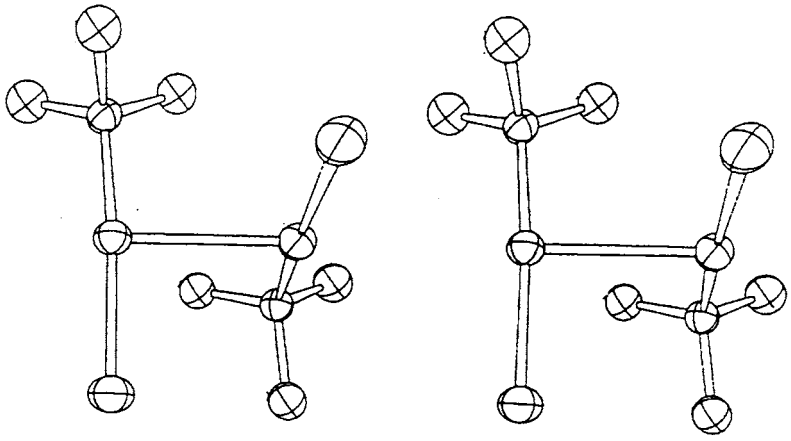

Figure 1-10. Steroview of $(Me_3P)AuI$ dimers.

1.2 Organogold Chemistry

The organometallic chemistry of gold is defined as the chemistry of compounds containing at least one direct gold to carbon bond. In step with the modern developments in gold chemistry, the pace of research on the organic chemistry of gold has quickened significantly in recent years. Major advances have been made not only in the characterization of unusual new compounds, but also in their application to practical purposes, such as surface coating and chemical vapor deposition. The repeated confirmation of the existence of attractive gold-gold interactions in such compounds has proved highly stimulating in the quest for a sound theoretical description of these phenomena.[67-69]

1.2.1 Gold(I) Cyanides and Cyano Complexes

By heating the acid $H[Au(CN)_2]$ at 110 °C gold(I) cyanide is obtained as a yellow powder sparingly soluble in water but readily soluble in aqueous cyanide solutions. It has a macromolecular structure related to that of Ag(CN)[70] in which the cyanide ion functions as a bridging ligand (Au-C = 2.12(14) Å, C-N = 1.17(2) Å).

In aqueous cyanide solution Au(CN) dissolves and the cyanide anion $[Au(CN)_2]^-$ is produced. For Cu(I) and Ag(I) the stable species are $[Cu(CN)_4]^{3-}$ and $[Ag(CN)_2]^-$ illustrating the ten-

[67]Görling, A., Rösch, N., Ellis, D. E., Schmidbaur, H., Inorg. Chem. **1991**, 30, 3986.

[68] Pyykkö, P., Zhao, Y., Angew. Chem. Int. Ed. Engl. **1991**,30, 604.

[69] Calhorda, M., J., Veiros, L. F., J. Organomet. Chem., **1994**, 478, 37.

[70] Zhdanov, G. S., Shugam, E. A., Acta Physicochem. URSS **1945**, 20, 253.

dency towards lower coordination numbers on descending the triad. The stability of $[Au(CN)_2]^-$ forms the basis for the process of leaching gold-bearing ores with cyanide in the presence of oxygen, which depends on the reaction:

$$4\ Au\ +\ 8\ CN^-\ +\ 2\ H_2O + O_2 \rightleftharpoons 4\ [Au(CN)_2]^-\ +\ 4\ OH^-$$

The overall formation constant of $[Au(CN)_2]^-$, estimated as 10^{38} from E° for the reaction

$$[Au(CN)_2]^-\ +\ e^- \rightleftharpoons Au\ +\ 2\ CN^-$$

is very high compared to 10^{24} for $[Cu(CN)_2]^-$ and 10^{20} for $[Ag(CN)_2]^-$. This difference in stabilities between the silver and gold complexes is also revealed by a substantial difference in the M-C stretching frequencies and the conclusion that metal-carbon π-bonding is stronger in $[Au(CN)_2]^-$ (**Table 1-1**).[71-73]

Table 1-1. M-C Stretching Frequencies and Force Constants for $[Ag(CN)_2]^-$ and $[Au(CN)_2]^-$.[73]

	ν_{MC}(Raman) (cm^{-1})	ν_{MC}(IR) (cm^{-1})	$k_{M\text{-}C} \times 10^{-5}$ (dynes·cm^{-1})
$[Ag(CN)_2]^-$	360	390	1.8
$[Au(CN)_2]^-$	452	427	2.8

The potassium salt, $K[Au(CN)_2]$, is best prepared by treating a solution of gold(III)chloride with ammonia and dissolving the precipitate in potassium cyanide solution.[74] It is also the only compound isolable in the system KCN-AuCN-H_2O.[75] The anion $[Au(CN)_2]^-$ is diamagnetic and linear, and although the structure of $K[Au(CN)_2]$ is basically like that of $K[Ag(CN)_2]$, the stacking of layers of anions and cations is slightly different.[76] Rosenzweig and Cromer determined the structure of $K[Au(CN)_2]$ in 1959. This structure consists of alternating layers of potassium and dicyanoaurate components in which the gold atoms of one layer are 3.64 Å away from the nearest neighbor in the same layer.

---

[71] Johnson, B. F. G., Davis, R., in The Chemistry of Copper, Silver and Gold, **1973**, 145.

[72] Jones, L. J., J. Chem. Phys. **1965**, 43, 594.

[73] Stammreich, H., Chadwick, B. M., Frankiss, S. G., J. Mol. Spec., **1968**, 1, 191.

[74] Latimer, W. M., The Oxidation States of the Elements and Their Potentials in Aqueous Solution, 2nd edn. Prentice-Hall, Englewood Cliffs, New Jersey, **1952**.

[75] Bassett, H., Corbett, A. S., J. Chem. Soc. **1924**, 1660.

[76] Rosenzweig, A., Cromer, D. T., Acta Cryst. **1959**, 12, 709.

1.2.2 (Isonitrile)gold(I) Complexes - (RNC)AuX

(Isonitrile)gold(I) complexes have attracted increasing attention because of their use in new domains of application. (Isonitrile)gold(I)alkyl complexes can be used as MOCVD precursors for the deposition of thin gold films,[77-79] and (isonitrile)gold(I) alkynes and halides were shown to form a new type of liquid crystalline phase.[80-85] The ability of (isonitrile)gold(I) halides to form liquid crystalline phases is thought to arise from the presence of weak gold-gold interactions, which can be compared in strength to hydrogen bonds,[86-88] in the systems.[85]

The synthesis of (isonitrile)gold(I) complexes was first reported by Sacco *et al.* in 1955.[89] From tetrachlorogold(III) acid and isonitrile they obtained compounds of the type $(RNC)AuCl_3$, and of the type (RNC)AuCl in low (< 40%) yield for the (isonitrile)gold(I) chlorides with excess of the isonitrile. Today the (isonitrile)gold(I) chlorides are generally obtained from the following modified synthetic route using $(Me_2S)AuCl$ or (tht)AuCl:

$$(tht)AuCl + RNC \longrightarrow (RNC)AuCl + tht$$

(MeN≡C)AuC≡N is one representative example with the combination of parallel (head-to-head) and antiparallel (head-to-tail) interactions in the crystal (**Figure 1-11**).[90] The structure is built up from monomeric units linked together in two-dimensional polymeric layers through very weak Au--Au interactions of distance d(Au--Au) = 3.52 – 3.72 Å.[91]

---

[77] Puddephatt, R. J., Treurnicht, I., J. Organomet. Chem. **1987**, 319, 129.

[78] Dryden, N. H., Shapter, J. G., Coatsworth. L. L., Norton, P. R., Puddephatt, R. J., Chem. Mater. **1992**, 4, 979.

[79] Norton, P. R., Young, P. A., Cheng, Q., Dryden, N., Puddephatt, R. J., Surf. Sci. **1994**, 307, 172.

[80] Alejos, P., Coco, S., Espinet, P., New J. Chem. **1995**, 19, 799.

[81] Benouazzane, M., Coco, S., Espinet, P., Martin-Alvarez, J. M., J. Mater. Chem. **1995**, 5, 441

[82] Coco, S., Espinet, P., Martin-Alvarez, J. M., New J. Chem. **1995**, 19, 959.

[83] Ishii, R., Kaharu, T., Pirio, N., Zhang, S.-W., Takahashi, S., J. Chem. Soc., Chem. Commun. 1995, 1215.

[84] Kaharu, T., Ishii, R., Adachi, T., Yoshida, T., Takahashi, S., J. Mater. Chem. **1995**, 5, 687.

[85] Kaharu, T., Ishii, R., Takahashi, S., J. Chem. Soc., Chem. Commun. **1994**, 1349.

[86] Schmidbaur, H., Graf, W., Müller, G. Angew. Chem. Int. Ed. Engl. **1988**, 24, 417.

[87] Schmidbaur, H., Dziwok, K., Grohmann, A., Müller, G., Chem. Ber. **1989**, 122, 893.

[88] Dziwok, K., Lachmann, J., Wilkinson, D. L., Müller, G., Schmidbaur, H., Chem. Ber. **1990**, 122, 893.

[89] Sacco, A., Freni, M., Gazz. Chim. Ital. **1955**, 85, 989.

[90] Esperas, S. Acta Chem. Scand. **1976**, A30, 527.

[91] Schmidbaur, H. "Gold-Organic Compounds", in Gmelin Handbuch der Anorganischen Chemie, Slawisch, A., editor, 8. edition, Springer-Verlag, Berlin **1980**,162.

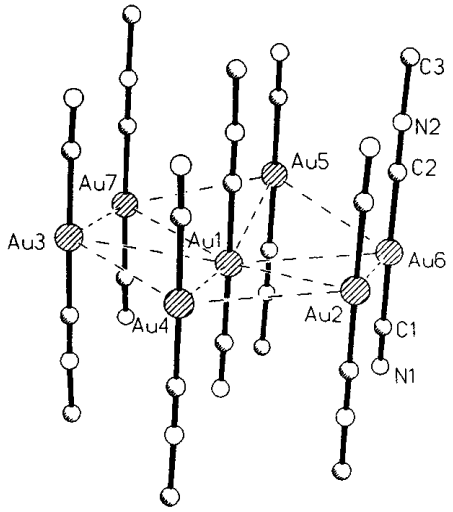

Figure 1-11. Crystal packing of methylisocyanide gold(I) cyanide molecules (MeN≡CAuC≡N). The gold atoms are arranged in puckered sheets with Au--Au contacts.

The cell packing of methylisonitrilegold(I) chloride, (MeNC)AuCl, leads to zig-zag chains with the monomeric units arranged in an antiparallel fashion (**Figure 1-12**). The Au--Au contacts are surprisingly long [3.637(1) Å],[92-94,58] probably due to the close antiparallel packing in layers, which forces the metal atoms into alternating position above and below the plane defining the center of the layer.

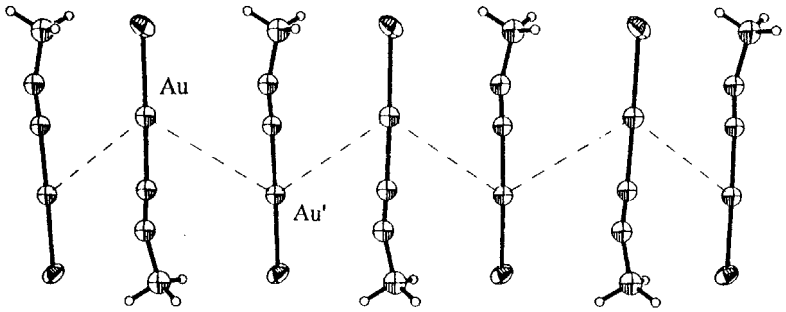

Figure 1-12. Supramolecular structure of (MeNC)AuCl - Polymeric zig-zag chains with antiparallel arrangement of the molecules [Au--Au' 3.637(1) Å].

The (^{t}BuNC)AuCl monomeric units form zig-zag chains with a sequence of anti-parallel arrangements (**Figure 1-13**). The relatively short gold-carbon (isocyanide) bond of 1.92(1) Å may indicate significant gold-ligand back-bonding. The closest approach of Au atoms is

---

[92] Browning, J., Goggin, P. L., Goodfellow, R. J., J. Chem. Research (S) **1978**, 328.

[93] Browning, J., Goggin, P. L., Goodfellow, R. J., J. Chem. Research (M) **1978**, 4201.

[94] Perreault, D., Drouin, M., Michel, A., Harvey, P. D., Inorg. Chem. **1991**, 30, 2.

3.695(1) Å indicating no significant Au--Au bonding within this structure.[95]

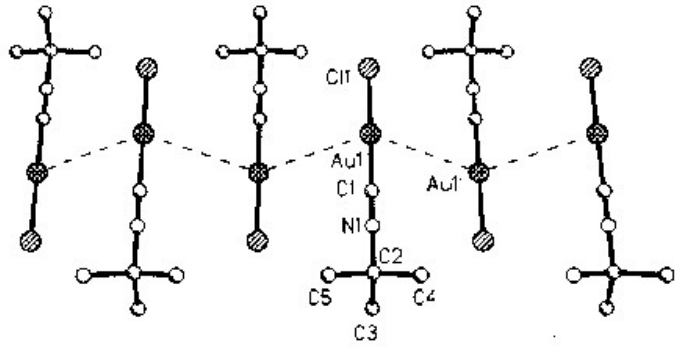

Figure 1-13. Infinite zigzag chain structure of (^{t}BuNC)AuCl.[94]

(^{t}BuNC)AuBr is isostructural to the chloride analogue (^{t}BuNC)AuCl. The monomeric units form zig-zag chains with a sequence of anti-parallel arrangements (**Figure 1-14**), but there are only very weak Au--Au interactions as suggested by long [Au--Au = 3.689(1) Å] distances.[96]

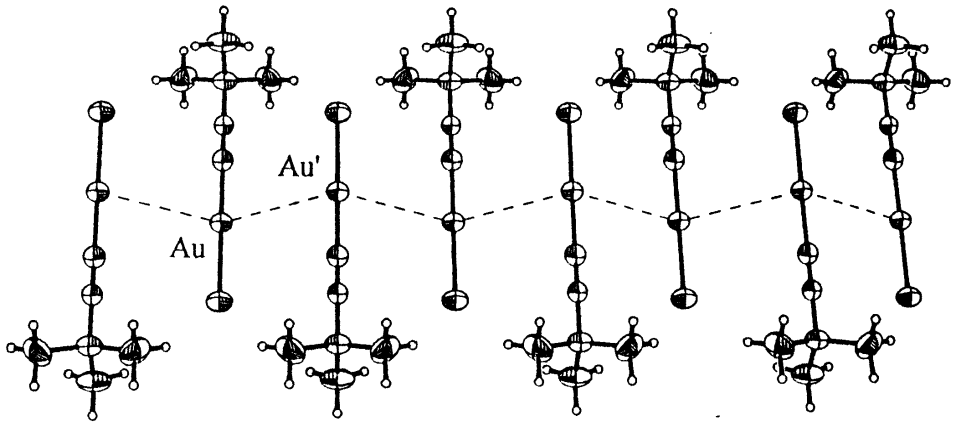

Figure 1-14. Supramolecular structure of (^{t}BuNC)AuBr - Polymeric zig-zag chains with antiparallel arrangement of the molecules [Au--Au' 3.689(1) Å].

With more bulky molecules like mesitylisonitrile as ligands, no chain or layer structure is formed, and for (MesNC)AuCl only dimers with shorter intermolecular Au--Au contacts of 3.336(1) Å are observed (**Figure 1-15**).

[95] Eggleston, D. S., Chodosh, D. F., Webb, R. L., Davis, L. L., Acta Cryst. **1986**, C42, 36.

[96] Schneider, W., Angermaier, K., Sladek, A., Schmidbaur, H., Z. Naturforsch. **1996**, 51b, 790.

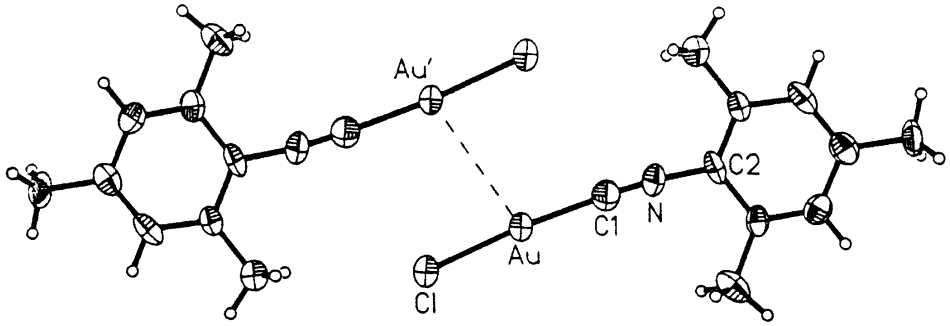

Figure 1-15. Dimer of (MesNC)AuCl, with an intermolecular distance Au--Au' 3.336(1) Å.

Most gold compounds have a linear, rod-like structure. Bachman *et al.* have provided the first evidence with n-alkylisocyanide complexes of the type (R-NC)AuCl, (where R = C_nH_{2n+1} and n = 1-11), that aurophilic bonding can be used to induce the formation of mesomorphic phases in the absence of traditional mesogenic (liquid-crystal) units such as aromatic rings.[97] In this work they made the first observation of rotator phases induced by direct metal-metal bonding.[98] Rotator phases are intermediate between the ordered crystal and the isotropic (disordered) melt. In this phase, the molecules have additional freedom of rotator motion. These peculiar structural features generally lead to anomalously large thermal expansion, isothermal compressibility and heat capacity. With (R-NC)AuCl molecules they found that above 50 °C the crystalline (isocyanide)gold chloride complexes have physical properties characteristic of rotator phases.

The linear array of the atoms Cl-Au-C-N in the metal complex causes the molecules to behave like flexible hydrocarbon chains with a rod-like end group containing the aurophilic gold atom. When crystallized, the arrangement of the molecules follows a pattern that brings the gold atoms of neighboring molecules close together (about 3.5 Å apart) with adjacent molecules aligned in opposite directions (**Figure 1-16**). These zigzag chains pack in what is referred to as a herring-bone structure, as seen for other long-chain hydrocarbons bearing functional groups. Several of these zigzag chains stack together to create a bilayer structure similar to the bilayers formed by hydrogen-bonded chains of alcohols. Similar structures with a well defined bilayer motif are formed by unbranched alcohols, $C_nH_{2n+1}OH$, but in this case the

[97] Bachman, R. E., Fioritto, M. S., Fetics, S. K. & Cocker, T. M. J., Am. Chem. Soc. **2001**, 123, 5376.

[98] Schmidbaur, H. Nature, **2001**, 413, 31.

chains are attached to each other through hydrogen bonds between the hydroxyl groups.[99]

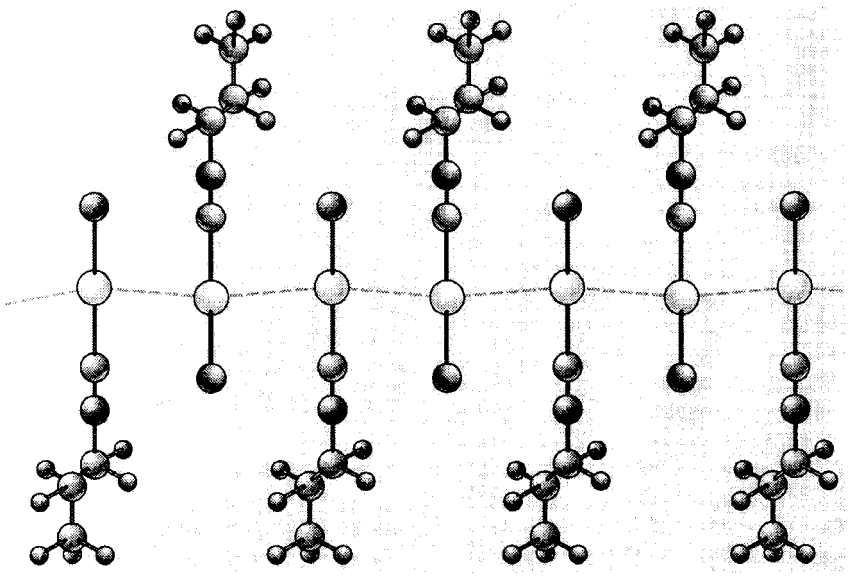

Figure 1-16. View of the antiparallel chains formed by aurophilic bonding (dashed lines) in $C_3H_7NCAuCl$.

1.2.3 Alkynylgold(I) Complexes

The main interest in acetylide gold(I) complexes is based on the synthesis of rigid-rod gold(I) complexes. Previous routes to alkynylgold(I) complexes generally start with $HAuCl_4$, which is reduced by SO_2 in the presence of acetate, followed by addition of the terminal acetylene.[100] In this way polymeric gold(I) acetylides $[Au(C{\equiv}CR)]_n$ are obtained.[101]

Coates and Parkin synthesized $[Au(C{\equiv}C^tBu)]_n$ in 1962.[100] The pale yellow compound is soluble in inert non-polar solvents and resembles its copper(I) analogue, $Cu(C{\equiv}C^tBu)$, which is octameric in boiling benzene solution.[102,103] With coordination number two of the metal, the authors have suggested that the gold compound is likely to have the structure in **Figure 1-17** (I). An insoluble form of this compound was also obtained, for which another structure was proposed as shown in **Figure 1-17** (II). The compound has been characterized only by ele-

---

[99] Wang, J.-L., Leveiler, F., Jacquemain, D., Kjaer, K., Als-Nielsen, J., Lahav, M., Leiserowitz, L., J. Am. Chem. Soc. **1994**, 116,1192.

[100] Coates, G. E., Parkin, C., J. Chem. Soc., **1962**, 3220.

[101] Schmidbaur, H., Grohmann, A., Olmos, M. E., "Organogold Chemistry", in Gold: Progress in Chemistry, Biochemistry and Technology, Schmidbaur, H., editor, Wiley & Sons Ltd., Chichester, **1999**.

[102] Favorski, Morev, J., Russ. Phys. Chem. Soc. **1920**, 50, 571.

[103] Coates, G. E., Parkin, C., J. Inorg. Nuclear Chem., **1961**, 22, 59.

mental analyses and IR spectroscopy.

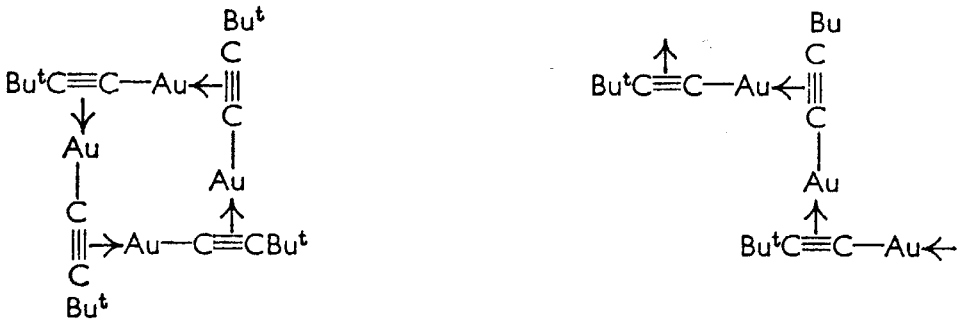

I **II**

Figure 1-17. Suggested structures of the [Au(C≡C^{t}Bu)] oligomer (I) and polymer (II).

In 1995 Mingos *et al.* prepared [Au(C≡C^{t}Bu)]$_n$ by treatment of [Au(NH$_3$)$_2$]$^+$ with ^{t}BuC≡CH. The X-ray crystallographic analysis has demonstrated that, contrary to the previously proposed tetrameric formula, the real formula is [Au(C≡C^{t}Bu)$_6$]$_2$.[104] The compound presents a highly unusual catenate structure based on two interlocked rings, each one containing six gold centers (**Figure 1-18**). The gold atoms are coordinated to the C≡C^{t}Bu ligands in three modes (η^1- η^1, η^1- η^2, η^2- η^2) (**Figure 1-19**), representing all possible coordination modes of two alkynyl ligands around a gold atom. This remarkable aurophilic motif features two interlocking hexagonal rings of gold atoms, which are stabilized by inter- and intramolecular Au--Au contacts of ~ 3.3 Å.

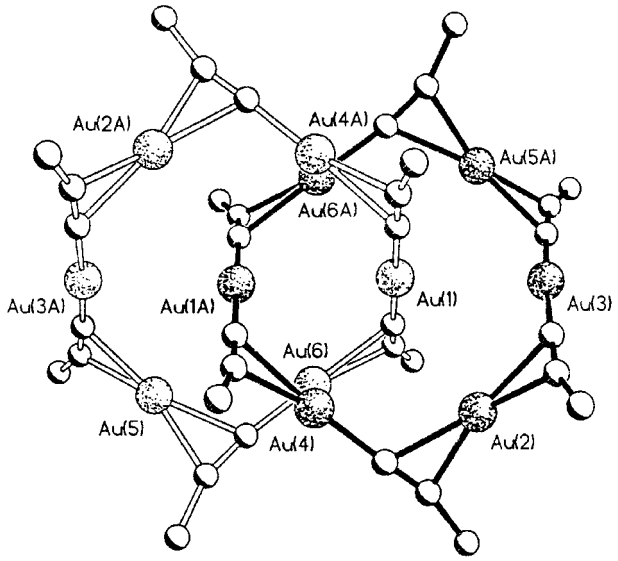

Figure 1-18. Crystal structure of [Au(C≡C^{t}Bu)$_6$]$_2$.

[104] Mingos, D. M., Yau, J., Menzer, S., Williams, D. J., Angew. Chem. Int. Ed. Engl. **1995**, 64, 1894.

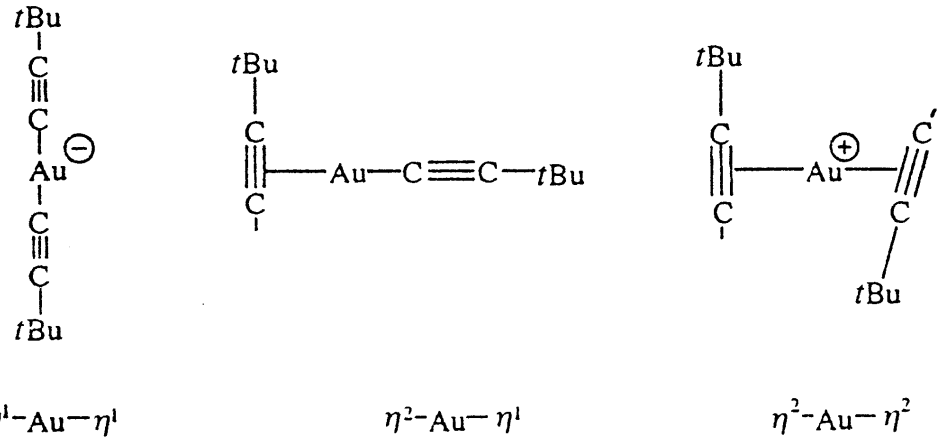

Figure 1-19. The different types of ligand arrangements and distribution of formal charges for $[Au(C{\equiv}C^tBu)_6]_2$.

The preparation of complexes of type [Au(C≡CR)(L)] often fails since the $[Au(C{\equiv}CR)]_n$ compounds initially formed may readily decompose, depending on the nature of the acetylide ligand. Several new synthetic routes to alkynylgold (I) compounds that circumvent this problem have been established. Complex gold(I) chlorides containing a variety of tertiary phosphines have been found to react with a wide range of terminal acetylenes, either in diethylamine in the presence of copper(I) halides,[105] or in alcoholic solution in the presence of sodium alkoxide,[105,106-108] to give the corresponding alkynylgold (I) complexes in good yield. These transformations are equally applicable to unsubstituted acetylene, which gives dinuclear gold(I) acetylides $[Au_2(C{\equiv}C)(PR_3)_2]$.[106-108]

In 1967 Corfield and Shearer reported the first structurally characterized gold(I) σ-acetylide derivative (^{i}PrNH$_2$)AuC≡CPh. The complexes formed by phenylethynylgold(I) with amines tend to be sparingly soluble in inert solvents. In the crystal the gold atoms lie in infinite zigzag chains.[109] Within a chain the Au--Au separations are 3.722 Å, but the pairs of chains interact with Au--Au separations of only 3.274 Å (**Figure 1-20**).

---

[105] Bruce, M. I., Horn, E., Matisons, J. G., Snow, M. R., Aust. J. Chem. **1984**, 37, 1163.

[106] Cross, R. J., Davidson, M. F., J., Chem. Soc., Dalton Trans., **1986**, 411.

[107] Cross, R. J., Davidson, M. F., McLennan, A. J., J. Organomet. Chem. **1984**, 265, C37.

[108] Müller, T. E., Choi, S. W.-K., Mingos, D. M. P., Murphy, D., Williams, D. J., Yam, V. W.-W., J. Organomet. Chem., **1994**, 484, 209.

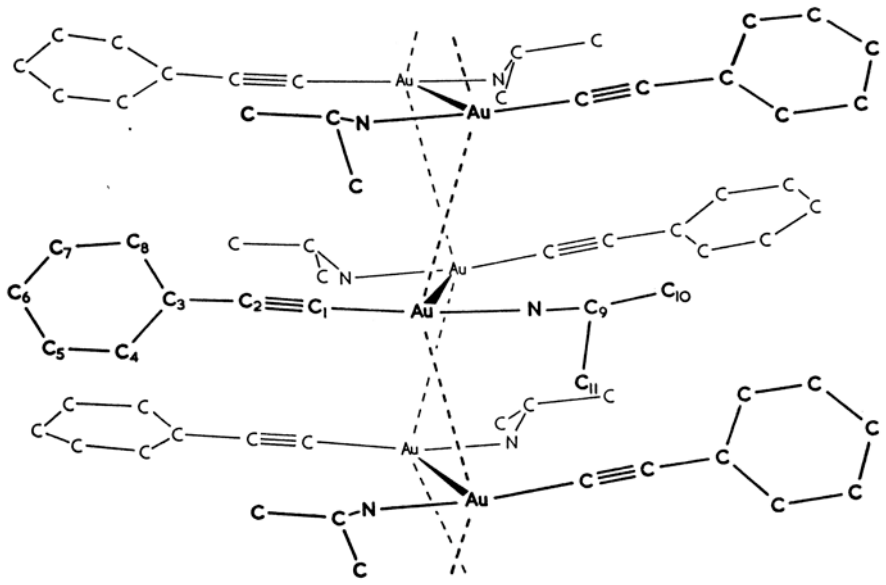

Figure 1-20. Perspective view of the crystal structure [(^{i}PrNH$_2$)AuC≡CPh].

In 1984 Bruce *et al.* reported an experimentally convenient synthesis of a series of gold(I) acetylide complexes containing tertiary phosphines, including reactions between AuCl(PR_3) [R_3 = Me_3, Ph_3, $Ph(OMe)_2$] and alk-1-ynes. They were carried out either in diethylamine in the presence of copper(I) halides, or with methanol/sodium methoxide and gave good to excellent yields.[105]

$$(Ph_3P)AuCl + HC{\equiv}CC_6F_5 \xrightarrow[-\,[Et_2NH_2]Cl]{Et_2NH\,/CuCl} Ph_3PAuC{\equiv}CC_6F_5$$

In this work they determined the crystal structure of $Ph_3PAuC{\equiv}CC_6F_5$ as the second structurally characterized gold(I) σ-acetylide derivative (**Figure 1-21**). The crystals contain only discrete molecules of the complex, with an Au--Au separation that exceeds 5.0 Å. This is due to the presence of the bulky C_6F_5 group, which prevents the second molecule to approach close enough to allow the Au--Au interaction to give a weakly bonded dimer.

[109] Corfield, P. W. R., Shearer, H. M. M., Acta Cryst. **1967**, 23, 156.

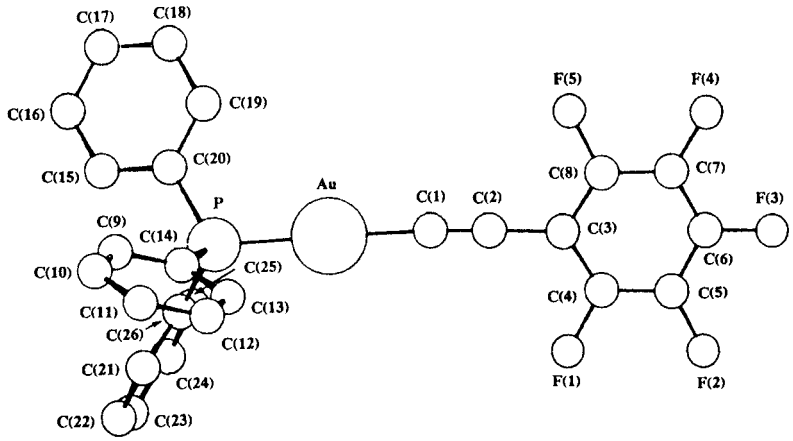

Figure 1-21. Molecular structure of $Ph_3PAuC{\equiv}CC_6F_5$.

Following the structures of (^{i}PrNH$_2$)AuC≡CPh and $Ph_3PAuC{\equiv}CC_6F_5$, Bruce *et al.* determined in 1986 a further crystal structure of $Ph_3PAu(C{\equiv}CPh)$.[110] The asymmetric unit contains two molecules, each consisting of a gold atom attached to a phenylethynyl group and a triphenylphosphine ligand (**Figure 1-22**). In the dimer with a relatively short Au--Au separation of 3.379(1) Å, the Au-C≡C-C moieties are nearly orthogonal.

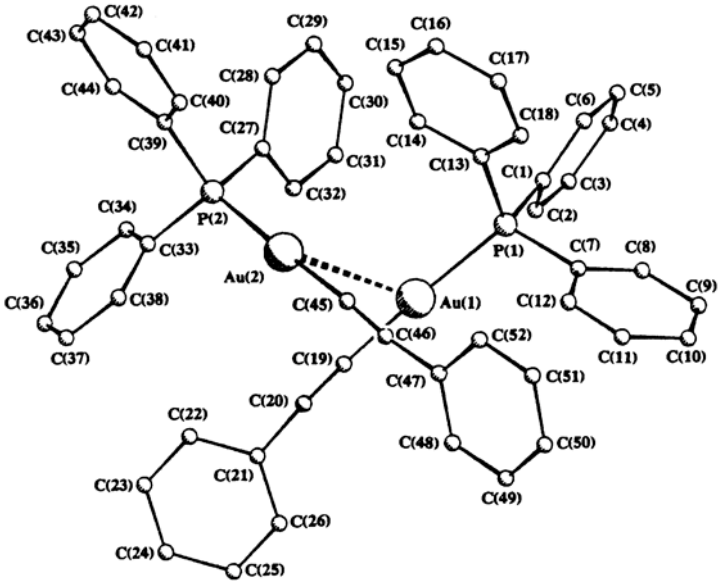

Figure 1-22. The two independent molecules in crystal of $Ph_3PAuC{\equiv}CPh$ showing Au--Au interaction at a distance of 3.379(1) Å.

In 1994 Müller *et al.* synthesized $Fc_2PhPAuC{\equiv}CPh$ in alcoholic solution using sodium alkoxide and PhC≡CH as the reagents and obtained the first crystal structure of a product obtained using this synthetic route.[108]

---

[110] Bruce, M. I., Duffy, D. N., Aust. J. Chem. **1986**, 39, 1697.

$$Fc_2PhPAuCl + PhC{\equiv}CH \xrightarrow[-\ NaCl]{EtOH/NaOEt,\ reflux,\ 1h} Fc_2PhPAuC{\equiv}CPh$$

The structure of the complex $Fc_2PhPAuC{\equiv}CPh$ is shown in **Figure 1-23**. Inspection of the packing of the molecules does not reveal any significant intermolecular interactions. The C≡C bond length with 1.172(21) Å is at the short end of the range found for transition metal acetylides.

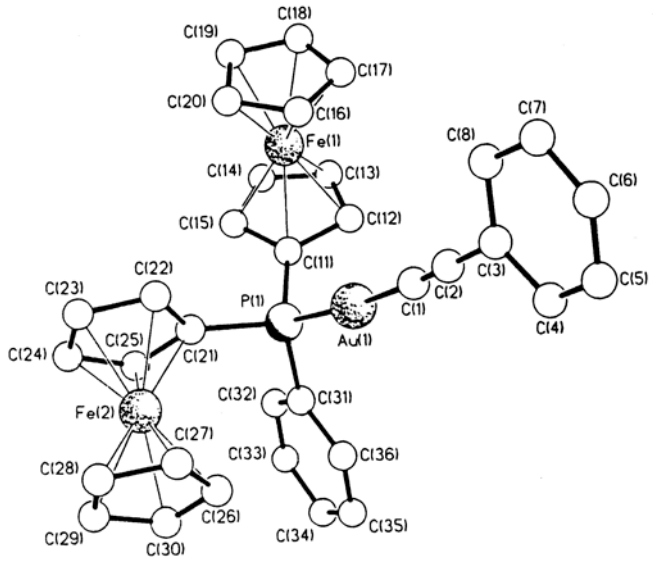

Figure 1-23. Molecular structure of $Fc_2PhPAuC{\equiv}CPh$.

An alternative high-yield method for preparing gold(I) phenylacetylides involves the electrochemical oxidation of gold metal in an acetonitrile solution of the acetylene,[111] with the target compounds precipitating during electrolysis. Other routes that have led to alkynylgold(I) complexes have employed acetylacetonatogold(I) derivatives,[112] alkylgold(I) complexes[113] and N-substituted (phosphine)gold(I) imidazoles,[114] respectively. The anionic ligands in these reagents are sufficiently basic to deprotonate the acetylene moiety, thus forming acetylide complexes.[104] NH_3 can act as a deprotonant, as demonstrated in the reaction of $[Au(NH_3)_2]^+$ with phenylacetylene to give $[Au(C{\equiv}CPh(NH_3)]$ in excellent yield.

---

[111] Casey, A. T., Vecchio, A. M., Appl. Organomet. Chem., **1990**, 4, 513.

[112] Vicente, J., Chicote, M.-T., Abrisqueta, M.-D., J. Chem. Soc., Dalton Trans. **1995**, 497.

[113] Muratami, M., Inouye, M., Suginome, M., Ito, Y., Bull. Chem. Soc. Jpn., **1988**, 61, 3649.

[114] Bonati, F., Burini, A., Pietrosi, B. R., Giorgini, E., Bovio, B., J. Organomet. Chem., **1988**, 66, 3176.

Regarding the specific area of the present work, alkynyl gold complexes of the types LAuC≡CAuL (**A**), LAuC≡CH (**B**, L = PR_3) and $R_3PAuC{\equiv}CR'$ (**C**) will be presented below in greater detail.

Amongst the previously reported alkynyl gold(I) complexes of type (**B**), Werner *et al.* reported in 1984 the synthesis of ($^{i}Pr_3P$)AuC≡CH as the first well characterized ethynyl gold(I) complex.[115] The other compounds of the type [$R_3PAuC{\equiv}CH$] (**B**), e.g. R = Ph, C_6H_4-OMe-4, have been obtained by treating the bis(acetylide)aurates(I) with bis(phosphine)gold(I) derivatives,[112] but no structure of a representative example for series **B** has been reported.

Apart from the neutral digold acetylides of the type LAuC≡CAuL (**A**), there are also anionic digold acetylides as shown in the species $[Ph_4P^+]_2[RAuC{\equiv}CAuR]^{2-}$ (R = CN, PhC≡C, MeC≡C, HC≡C), prepared from gold carbide by Nast *et al.* in 1981. These compounds were identified by vibrational and ^{31}P-NMR spectroscopy.

Because of their low solubility the bisaurated ethynes were less well studied. The ethynediyl compounds $Ph_3PAuC{\equiv}CAuPPh_3{\cdot}2C_6H_6$ and (*m*-Tol)$_3$PAuC≡CAuP(*m*-Tol)$_3{\cdot}nC_6H_6$ (n = 0 and 1) were the first to be structurally characterized (**Figure 1-24**).[116]

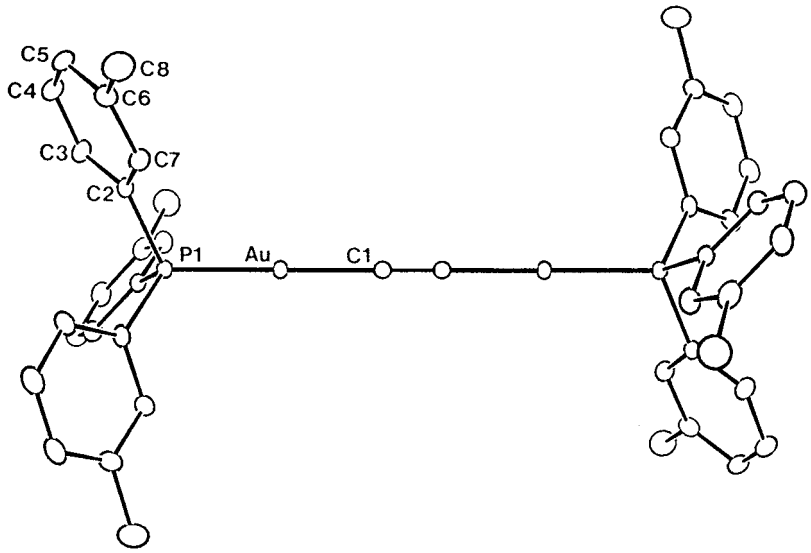

Figure 1-24. One molecule of (*m*-Tol)$_3$PAuC≡CAuP(*m*-Tol)$_3$ as found in (*m*-Tol)$_3$PAuC≡CAuP(*m*-Tol)$_3$ and (*m*-Tol)$_3$PAuC≡CAuP(*m*-Tol)$_3{\cdot}C_6H_6$.

---

[115] Werner, H., Otto, H., Ngo-Khac, T., Burschka, C., J. Organomet. Chem., **1984**, 262, 123.

[116] Bruce, M., Grundy, K. R., Liddell, M. J., Snow, M. R., Tiekink, E. R. T., J. Organomet. Chem. **1988**, 344, C49.

In (*m*-Tol)$_3$PAuC≡CAuP(*m*-Tol)$_3$, the benzene molecules reside in cavities defined by six methyl groups from six tertiary phosphine ligands of six symmetry-related dinuclear units (**Figure 1-25-a**). The structure of $Ph_3PAuC{\equiv}CAuPPh_3{\cdot}2C_6H_6$ (**Figure 1-25-b**) is virtually identical with those found in (*m*-Tol)$_3$PAuC≡CAuP(*m*-Tol)$_3{\cdot}nC_6H_6$ (n = 0 and 1). Although the host lattices are isomorphous, the cavities are different. The two benzene molecules in $Ph_3PAuC{\equiv}CAuPPh_3{\cdot}2C_6H_6$ are capped at either end by the PPh_3 groups and are apparently essential for the formation of the cubic lattice. In all cases there are no Au--Au interactions to be found in the crystal. Further information from fast atom-bombardment mass spectra showed these compounds to be associated in a series of major ions of the formulas $[M_n + Au]^+$, $[M_n + Au(PR_3)]^+$ and $[M_n + Au_2C_2)]^+$, [M = $R_3PAuC{\equiv}CAuPR_3$, n = 1-4]. The $[M_n + Au(PR_3)]^+$ cations are isolobal analogues of the often-observed $[M + H]^+$ ions in organic compounds.

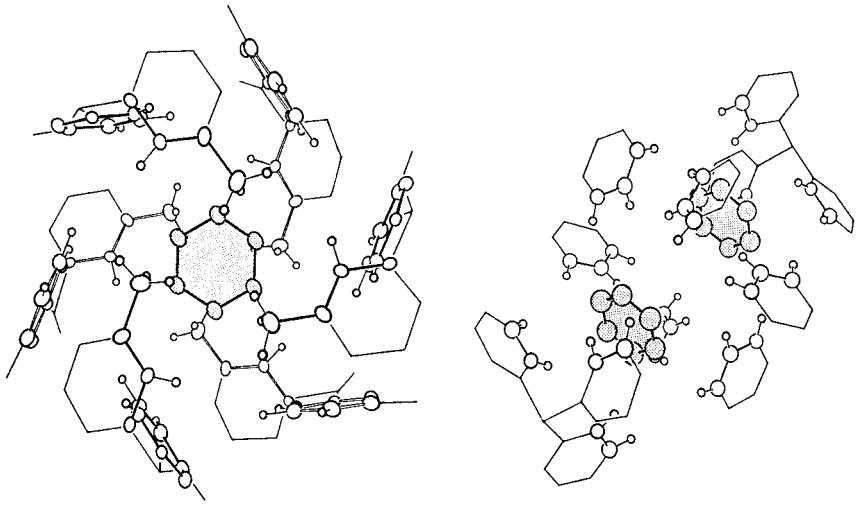

(a) (b)

Figure 1-25. (a) The octahedral cavity in (*m*-Tol)$_3$PAuC≡CAuP(*m*-Tol)$_3{\cdot}C_6H_6$, viewed perpendicular to the C_6H_6 plane. (b) The elongated cavity in $Ph_3PAuC{\equiv}CAuPPh_3{\cdot}2C_6H_6$. In this case, the included C_6H_6 molecules are hatched.

Further syntheses and structurally characterized examples were reported by Mingos, Yam *et al.* in 1994 for the (μ-ethyne)bis(phosphine-gold(I)) complexes involving bulky phosphines as ligands, $NpPh_2PAuC{\equiv}CAuPNpPh_2{\cdot}2CHCl_3$ (**Figure 1-26**), $Np_2PhPAuC{\equiv}CAuPPhNp_2{\cdot}6CHCl_3$ (**Figure 1-27**) and $Fc_2PhPAuC{\equiv}CAuPPhFc_2{\cdot}4EtOH$ (**Figure 1-28**).[108]

None of the compounds have short Au--Au contacts, but compounds $NpPh_2PAuC{\equiv}CAuPNpPh_2{\cdot}2CHCl_3$ and $Np_2PhPAuC{\equiv}CAuPPhNp_2{\cdot}6CHCl_3$ do show novel C-H···π interactions between the proton of $CHCl_3$ and the π-electron system of the C≡C bond.

In $NpPh_2PAuC{\equiv}CAuPNpPh_2{\cdot}2CHCl_3$ the pairs of $CHCl_3$ molecules are located with their protons 2.4 Å from the center of the C≡C bond and directed orthogonally towards the ethyne bond (**Figure 1-26**).

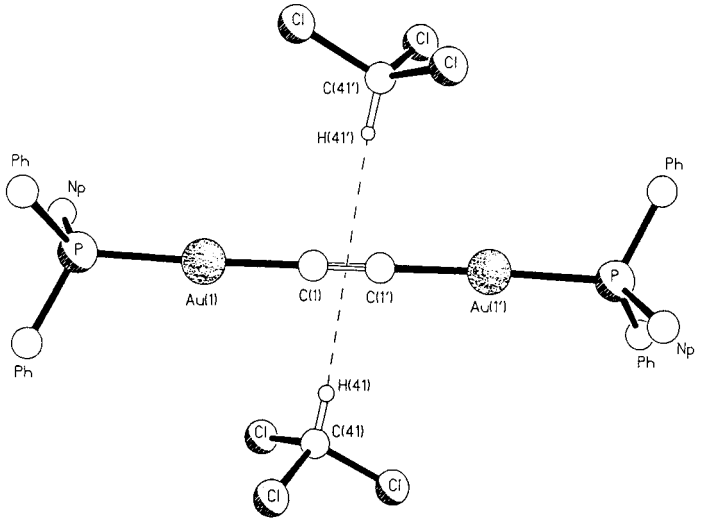

Figure 1-26. Molecular structure of $NpPh_2PAuC{\equiv}CAuPNpPh_2{\cdot}2CHCl_3$ with C-H···π interaction.

In $Np_2PhPAuC{\equiv}CAuPPhNp_2{\cdot}6CHCl_3$ two pairs of $CHCl_3$ molecules are located around the C≡C bond, with 2.5 Å between the proton and the center of the triple C≡C bond, resulting in a pseudo-octahedral arrangement around the C≡C bond, directed orthogonally towards the ethyne bond (**Figure 1-27**). In addition to the C-H···π interactions, both structures show a range of intermolecular arene-arene interactions.

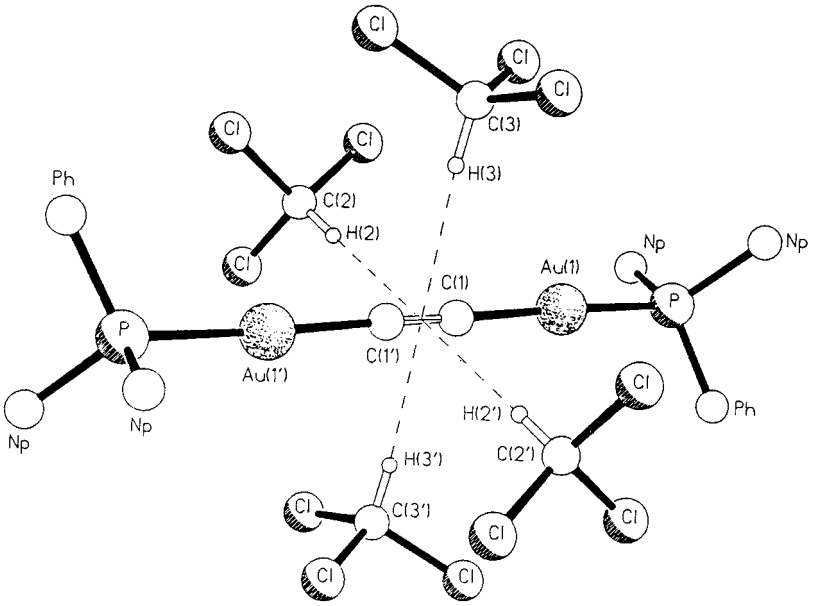

Figure 1-27. Molecular structure of $Np_2PhPAuC{\equiv}CAuPPhNp_2{\cdot}6CHCl_3$ with C-H···π interaction.

Contrary to the structures of the compounds $NpPh_2PAuC{\equiv}CAuPNpPh_2{\cdot}2CHCl_3$ and $Np_2PhPAuC{\equiv}CAuPPhNp_2{\cdot}6CHCl_3$, the positions of the OH hydrogen atoms could not be located in the compound $Fc_2PhPAuC{\equiv}CAuPPhFc_2{\cdot}4EtOH$ (**Figure 1-28**). Pairs of ethanol molecules have their oxygen atoms positioned 3.10 Å from the center of the ethyne bond. The O-O vector is inclined orthogonally to the C(1)-C(1') bond. Analogous O-H···π interactions directed towards the ethyne π system have been detected in the structure of cis-$[Me_2C(OH)C{\equiv}C]_2Pt(PPh_3){\cdot}2H_2O$.[117,118]

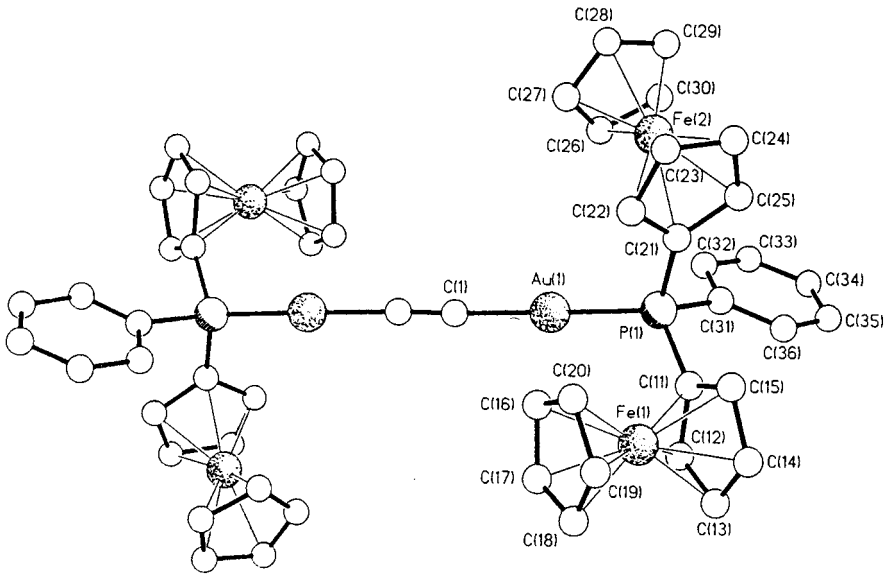

Figure 1-28. Molecular structure of $Fc_2PhPAuC{\equiv}CAuPPhFc_2$.

[117] Rzepa, H. S., Smith, M. H., Webb, M. L., J. Chem. Soc., Perkin Trans. **1994**, 2, 703.

[118] Furlani, A., Licoccia, S., Russo, M. V., Villa, A. C., Guastino, C., J. Chem. Soc., Dalton Trans., **1984**, 2197.

2 Structural and Spectroscopic Studies of Bis(triphenylphosphoranylidene)ammonium dicyanoaurate(I)

2.1 Introduction

Alkali di(cyano)aurate(I) salts are key intermediates in the recovery and processing of gold. Oxidative gold extraction from ores with aqueous alkali cyanide (NaCN or KCN) is followed by adsorption of the produced complexes $Na[Au(CN)_2]$ or $K[Au(CN)_2]$ on the surface of carbonaceous or resinous materials, for which the linear five-atomic anions $[NC\text{-}Au\text{-}CN]^-$ appear to exhibit a specific affinity.[119,120] Although the details of this adsorption and desorption processes are still not perfectly understood on the molecular level, there is convincing evidence for anion aggregation both in solution, on the substrate surface, and in salts with small cations.[121-123] During the investigations[124-126] into the supramolecular chemistry of neutral [L-Au-X], cationic $[L\text{-}Au\text{-}L]^+$ or anionic gold(I) complexes $[X\text{-}Au\text{-}X]^-$ it has been observed that anion aggregation to give oligomers or one-dimensional arrays is observed only in very special cases, and this is also true for the di(cyano)aurate(I) anion.[127]

With few exceptions,[128,129] most structural studies were carried out for compounds featuring

---

[119] a) Adams, M. D., Johns, M. W., Dew, D. W., in Schmidbaur, H. (ed.): Gold, Progress in Chemistry, Biochemistry and Technology, p.65 ff., Wiley & Sons, Chichester, **1999**. b) Raubenheimer, H. G., Cronje, S., ibid. p.557 ff.

[120] Marsden, J., House, I., The Chemistry of Gold Extraction, Ellis Horwood, New York, **1992**.

[121] Adams, M. D., Flöming, C. A., Metal. Trans. **1989**, 20B, 315.

[122] Gmelin Handbook of Inorganic and Organometallic Chemistry, Gold, Suppl. Vol. B2, p.320 ff., Springer, Berlin, **1994**.

[123] a) Rawashdeh-Omary, M. A., Omary, M. A., Patterson, H. H., J. Am. Chem. Soc. **2000**, 122, 10371. b) Fischer, P., Mesot, J., Lucas, B., Ludi, A., Patterson, H. H., Hewat, A., Inorg. Chem. **1997**, 36, 2791.

[124] Schmidbaur, H., Gold Bull. **1990**, 23, 11.

[125] Schmidbaur, H., Gold Bull. **2000**, 33, 3.

[126] Schmidbaur, H., Chem. Soc. Rev. **1995**, 24, 391.

[127] a) Leznoff, D. B., Xue, B.-Y., Batchelor, R. J., Einstein, F. W. B., Patrick, B. O., Inorg. Chem. **2001**, 40, 6026. b) Yeung, W.-F., Wong, W.-T., Zuo, J.-L., Lau, T.-C., Chem. Soc., Dalton Trans. **2000**, 629.

[128] a) Jones, P. G., Clegg, W., Sheldrick, G. M., Acta Crystallogr. **1980**, B 36, 160. b) Khan, M. N. I., King, C., Heinrich, D. D., Fackler (Jr.), J. P., Porter. L. C., Inorg. Chem. **1989**, 28, 2150.

the rod-like $[Au(CN)_2]^-$ anion highly oriented between stacks of flat, plate-like cations.[127b,130-142] For several years these materials have been of considerable interest owing to their electrical conductor or semi-conductor properties.

---

[129] a) Schubert, R. J., Range, K.-J., Z. Naturforsch. **1990**, 45b, 1118. b) Blom, N., Ludi, A., Bürgi, H.-B., Ticky, K., Acta Crystallogr. **1984**, C 40, 1767. c) Blom, N., Ludi, A. Bürgi, H.-B., ibid. **1984**, C 40, 1770. d) Cramer, R. E., Smith, D. W., Van-Doorne, W., Inorg. Chem. **1998**, 37, 5895.

[130] a) Krasnova, N. F., Simonov, Yu. A., Bel'skii, V. K., Abashkin, V. M.,Yakshin. V. V., Malinovskii, T. I., Laskorin, B. N., Dokl. Akad. Nauk SSSR **1984**, 276, 607. b) Fu, W.-F., Chan, K.-Ch. Miskowski, V. M., Che, Ch.-M., Angew. Chem. Int. Ed. Engl. **1999**, 28, 2783.

[131] McCleskey, T. M., Henling, L. M., Flanagan, K. A., Gray, H. B., Acta Crystallogr. **1993**, C 49, 1467.

[132] Balch, A. L., Olmstead, M. M., Reedy (Jr.), P. E., Rowley, S. P., Inorg. Chem. **1988**, 27, 4289.

[133] Schwellnus, A. H., Denner, L. Boeyens, J. C. A., Polyhedron, **1990**, 9, 975.

[134] Fournique, M., Meziere, C., Canadell, E., Zitoun, D., Bechgaard, K. Auban-Senzier, P., Advanced Materials, **1999**, 11, 766.

[135] Beon, M. A., Firestone, M. A., Leung, P. C. W., Sowa, L. M., Wang, H. H., Williams, J. M., Whangbo, M.-H., Solid State Commun. **1986**, 57, 735.

[136] a) Amberger, E., Polborn, K., Fuchs, H., Angew. Chem. Int. Ed. Engl. **1986**, 25, 729. b) Amberger, E., Fuchs, H., Polborn, K., Synth. Metals **1987**, 19, 605.

[137] Kurnoo, M., Day, P., Mitani, T., Kitagawa, H., Shimoda, H., Yoshkin, D., Guionneau, P., Barrans, Y., Chasseau, D. Ducasse, L., Bull. Chem. Soc, Jpn. **1996**, 69, 1233.

[138] a) Nigrey, P. J., Morosin, B., Kwak, J. F., Venturini, E. I., Baughman, R. J., Synth. Metals **1986**, 15, 1. b) Nigrey, P. J., Morosin, B., Kwak, J. F., Venturini, E. L., Schirber, J. E., Beno, M. A., Synth. Metals **1987**, 19, 617.

[139] a) Kikuchi, K., Ishikawa, Y., Saito, K., Ikernoto, I., Kobayashi, K., Acta Crystallogr. **1988**, C 44, 466. b) Kikuchi, K., Ishikawa, Y., Saito, K., Ikernoto, I., Kobayashi, K., Synth. Metals **1988**, 27, B391. c) Kato, R., Kobayashi, H., Kobayashi, A., Chem. Lett. **1989**, 781. d) Fujiwara, H., Kobayashi, H., Chem. Commun. **1999**, 2417. e) Arai, E., Fujiwara, H., Kobayashi, H., Kobayashi, A., Takimiya, K., Otsubo, T., Ogura, F., Inorg. Chem. **1996**, 37, 2850. f) Naito, T., Tateno, A., Udagawa, T., Kobayashi, H., Kato, R., Kobayashi, A., Nogami, T., J. Chem. Soc. Farad. Trans. **1994**, 90, 763.

[140] Yamashita, Y., Tornura, M., Zaman, M. B., Imeada, K., Chem. Commun. **1998**, 1657.

[141] a) Takimiya, K., Oharuda, A., Morikami, A., Aso, Y., Otsubo, T., J. Org. Chem. **2000**, 3013. b) Kawamoto, A., Tanaka, J., Oda, A., Mizumura, H., Murata, I., Nakasuji, N., Bull. Chem. Soc. Jpn. **1990**, 63, 2137. c) Okano, Y., Sawa, H., Aonuma, S., Kato, R., Synth. Metals **1995**, 70, 1161. d) Mori, T., Inokuchi, H., Misaki, Y., Nishikawa, H., Yamabe, T., Tanaka, S., Chem. Lett. **1993**, 2085. e) Mori, T., Misaki, Y., Yamabe, T., Bull. Chem. Soc. Jpn. **1994**, 67, 3187. f) Misaki, Y., Higuchi, N., Fujiwara, H., Yamabe, T., Mori, T., Mori, H., Tanaka, S., Angew. Chem. Int. Ed. Engl. **1995**, 34, 1222. g) Mori, H., Hirabayashi, I., Tanaka, S., Mori, T., Muruyama, Y., Inokuchi, H., Solid State Commun. **1993**, 88, 411. h) Ashizawa, M., Aragaki, M., Mori, T., Misaki, Y., Yamabe, T., Chem. Lett. **1997**, 649.

[142] Chu, I. K., Shek. I. P. Y., Siu, K. W. M., Wong, W.-T., Zuo, J.-L., Lau, T.-C., New J. Chem. **2000**, 24, 765.

In the present study it was attempted to prepare and isolate a di(cyano)aurate(I) salt with a very bulky "innocent" cation with high flexibility and no directional influence to allow a spectroscopic and structural characterization of anion association through aurophilic d^{10}-d^{10} interactions in an unperturbing environment both in solution and in the solid state.

For precise NMR measurements, ^{13}C-enriched cyanide was used in the preparations. ^{13}C-labeled gold pseudohalides were investigated in the course of several earlier studies which provided fundamental data.[143,144] Previous spectroscopic and structural studies of simple di(cyano)aurates(I) are also summarized in the comprehensive Gmelin Handbook compilation.[122]

2.2 Preparative Studies

For the present investigation, the bis(triphenylphosphoranylidene)ammonium cation $[PPN]^+$ was chosen as the bulky and highly flexible counterion for $[Au(CN)_2]^-$. Treatment of (tetrahydrothiophene)gold(I) chloride with an equimolar quantity of $[PPN]^+Cl^-$ afforded high yields (84 %) of the corresponding di(chloro)aurate(I) $[Ph_3PNPPh_3]^+[AuCl_2]^-(CH_2Cl_2)$ (**1**) (**Figure 2-1**).[145,146] This product could be readily converted into the di(cyano)aurate(I) (**2**) by reaction with two equivalents of KCN in a dichloromethane / water two-phase system. $[PPN]^+[Au(CN)_2]^-$ (**2**) was obtained in 87 % yield as a colorless crystalline product. Compound **2** was also prepared with ^{13}C-labeled cyanide (99 % enriched):

$$[(Ph_3P)_2N]^+Cl^- + (C_4H_8S)AuCl \longrightarrow C_4H_8S + [(Ph_3P)_2N]^+[AuCl_2]^- \quad \textbf{(1)}$$

$$[(Ph_3P)_2N]^+[AuCl_2]^- + 2\,K^{13}CN \longrightarrow 2\,KCl + [(Ph_3P)_2N]^+[Au(^{13}CN)_2]^- \quad \textbf{(2)}$$

For comparative purposes, ^{13}C-labeled $K[Au(CN)_2]$ was prepared (in 89 % yield) from unlabeled AuCN and $K^{13}CN$ (99 % enriched) to give a product which was approximately 50 %

---

[143] Pesek. J. S., Mason, W. R., Inorg. Chem. **1979**, 18, 924.

[144] a) Isab, A. A., Ghazi, I., Al-Arfaj, A. R., J. Chem. Soc., Dalton Trans. **1993**, 841. b) Isab, A. A., Hussain, M. S., Akhtar, M. N., Wazeer, M. I. M., Polyhedron, **1999**, 18, 1401.

[145] Jones, P. G., Z. Kristallogr. **1995**, 210, 375.

[146] Vicente, J., Chicoto, M.-T., Gonzales-Herrero, P., Jones, P. G., Ahrens, B., Angew. Chem. Int. Ed. Engl. **1994**, 33, 1852.

enriched in ^{13}C:

$$AuCN + K^{13}CN \longrightarrow K[Au(CN)(^{13}CN)]$$

For this product, ligand scrambling of labeled and unlabeled cyanide leads to a statistical mixture of three complex anions: $[Au(^{12}CN)_2]^-$, $[Au(^{12}CN)(^{13}CN)]^-$ and $[Au(^{13}CN)_2]^-$.

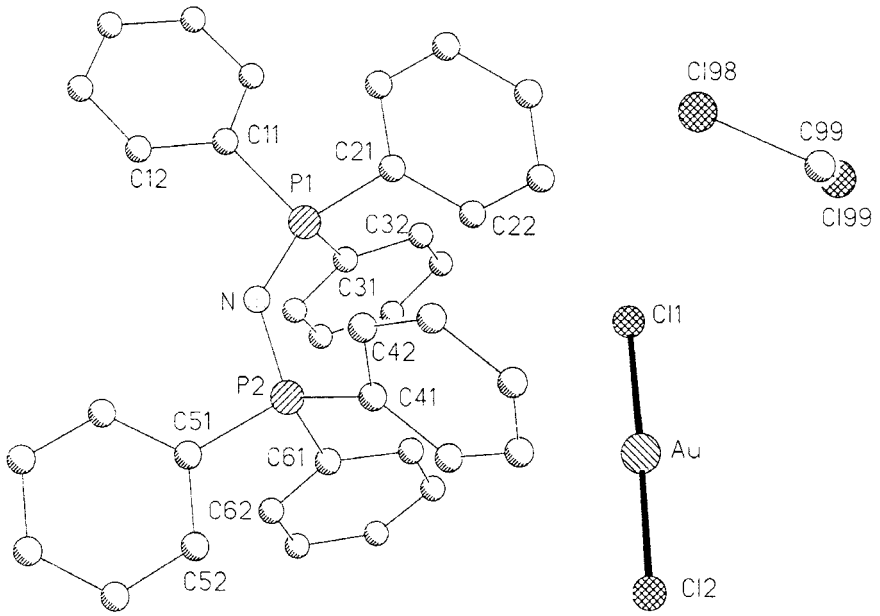

Figure 2-1. The structure of $[Ph_3PNPPh_3]^+[AuCl_2]^-(CH_2Cl_2)$.

2.3 Spectroscopic Studies

In an attempt to detect anion association equilibria in water, the complexes were investigated by solution infrared and NMR spectroscopy. Aqueous solutions (ca. 3 molar) of $K^{12}CN$ and $K^{13}CN$ show ν(CN) stretching frequencies at 2078.6 and 2035 cm^{-1}, respectively. Upon complexation to gold(I) in $[Au(CN)_2]^-$, these bands are shifted and split into bands with maxima at 2145.2 / 2105.0 and 2076.9 / 2034.2 cm^{-1}, respectively. The concentration dependence (between 0.35 and 6.53 molar solutions) is very small and within the standard deviation of the experiment (±1 cm^{-1}). The corresponding data for complex (**2**) (in dichloromethane) are 2140.1 / 2098.3 cm^{-1}, again with no significant concentration dependence at ambient temperature.

The ^{13}C NMR resonances of aqueous KCN and $K[Au(CN)_2]$ are known to appear at 164.6 and 154.2 ppm,[25] respectively. The ^1H, ^{13}C and ^{31}P NMR spectra of compound **2** in CD_2Cl_2 show the multiplets of the phenyl protons / carbons in the range 7.2 – 7.6 / 126.9 – 132.6 ppm and

the phosphorus signal as a singlet at 22.3 ppm for the cation. The ^{13}C resonance of the anion appears at 151.3 ppm and is neither concentration nor temperature dependent to any significant extent: for concentrations between 0.040 and 0.200 mole/L the shift displacement is only 0.15 ppm (**Table 2-1**), and for the temperature range 170-300 K only 0.2 ppm (**Table 2-2**).

It therefore appears that (using standard equipment) neither vibrational nor NMR spectroscopy are sensitive enough to detect any small effects that could be attributed to aggregation of $[Au(CN)_2]^-$ anions in solution. By contrast, through UV/Vis absorption and luminescence measurements[123] it was possible for the first time to obtain data on the formation constants of anion dimers in aqueous and methanol solutions of $K[Au(CN)_2]$. UV/Vis spectroscopy is clearly more sensitive to even small changes in the environment of the cyanoaurate anions e.g. as caused by metal-metal contacts.

Table 2-1: The concentration-dependent ^{13}C-NMR chemical shifts of $[PPN]^+[Au(\underline{C}N)_2]^-$ (**2**) in dichloromethane at RT.

$[PPN]^+[Au(CN)_2]^-$				
M (molar)	0.043	0.097	0.146	0.197
$\delta(^{13}C)$ / ppm	150.578	150.529	150.500	150.451

Table 2-2: The temperature-dependent ^{13}C-NMR chemical shifts of 0.197 M $[PPN]^+[Au(\underline{C}N)_2]^-$ (**2**) in dichloromethane.

$[PPN]^+[Au(CN)_2]^-$	0.197 M					
Temp. / K	299.0	273.0	253.0	233.0	213.0	193.0
$\delta(^{13}C)$ / ppm	150.451	150.451	150.455	150.426	150.381	150.324

The result prompted studies of the crystal structure of the $[PPN]^+[Au(CN)_2]^-$ salt, because the large and highly flexible $[(Ph_3P)_2N]^+$ cations should provide enough space for the anions to aggregate if the energy associated with the oligomerization is high enough to compensate for deficits in Coulomb energy of cation/anion contacts or other weak packing forces.

2.4 Crystal Structure Determination

Crystals of $[(Ph_3P)_2N]^+[Au(CN)_2]^-(CH_2Cl_2)_{0.5}$ (**2**) (from dichloromethane at -20 °C) are monoclinic, space group $P2_1/n$, with Z = 4 formula units and two molecules of dichloromethane in the unit cell (**Figure 2-2**). Cations and anions are well separated and show no sub-

van-der-Waals contacts. The cation has a structure which agrees well with the plethora of literature data for salts with the $[PPN]^+$ unit.[147] The P-N distances of 1.519(3) and 1.584(3) Å and the P-N-P angle of 136.3(2)° are comparable to the data found for $[(Ph_3P)_2N]^+(BF_4)^-(CH_2Cl_2)$ (**3**): 1.579(2) / 1.583(2) Å, 138.5(1)°.

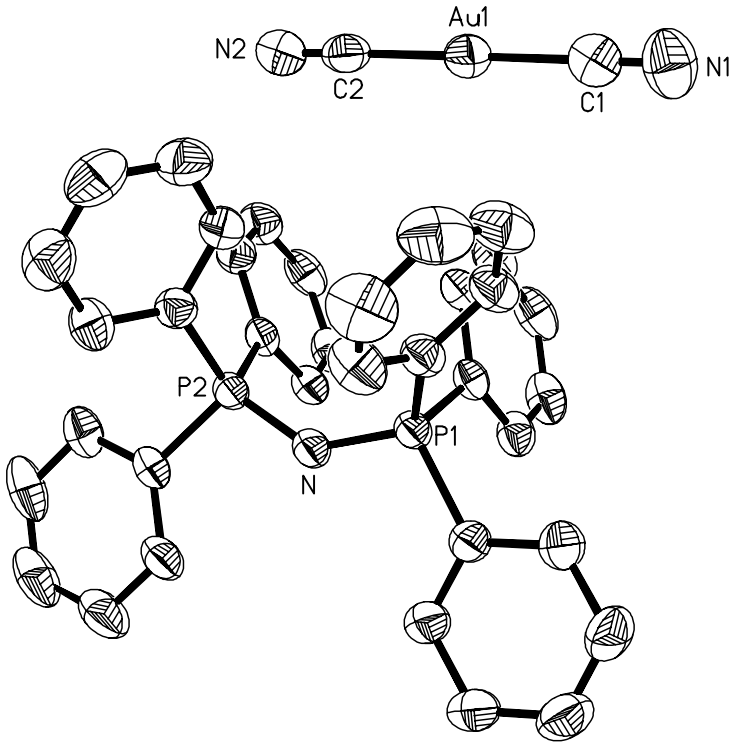

Figure 2-2. The structure of $[Ph_3PNPPh_3]^+[Au(CN)_2]^-(CH_2Cl_2)_{0.5}$ (**2**) (ORTEP drawing with 50% probability ellipsoids, H-atoms omitted for clarity).

The $[PPN]^+$ salt with the "innocent" $(BF_4)^-$ anion and the same interstitial solvent (CH_2Cl_2) was prepared and investigated in this work to have a suitable reference material. The crystals are triclinic, space group *P*1 with *Z* = 2 formula units and two dichloromethane molecules in the unit cell. For details see Experimental Section.

The results show that the anion $[Au(CN)_2]^-$ has no specific influence on the structure of the cation, which is known to be very flexible and hence "sensitive" to the presence of sterically unusual or functional anions.

---

[147] Corbridge, D. E. C., The Structural Chemistry of Phosphorus, p. 360, Elsevier, Amsterdam, **1974**.

The $[NC\text{-}Au\text{-}CN]^-$ anion has no crystallographically imposed symmetry, but its axis of five atoms is almost linear with N-C-Au angles of 178.4(5) / 178.7(6) and a C-Au-C angle of 179.1(2)°. The Au-C distances are similar at 1.929(6) and 1.937(5) Å, as are the C-N distances at 1.084(7) and 1.089(6) Å. The data suggest a completely unperturbed anion geometry which approaches very closely the maximum attainable symmetry of point group $D_{\infty h}$.

There is no evidence for interionic association. The crystal structure of $[PPN]^+[Au(CN)_2]^-$ (**2**) is closely related to that of the dichloroaurate(I) salt $[PPN]^+[AuCl_2]^-(CH_2Cl_2)$ the crystals of which have very similar cell constants and the same space group (**Figure 2-1**). The $[AuCl_2]^-$ anions also exhibitl no tendency to aggregate in the crystal lattice.[145,146] However, in the crystals of $[PPN]^+[Au(CN)_2]^-$ there is a Cl--Au contact between anions and solvent molecules which may compete (**Figure 2-3**) and be preferred over anion-anion interactions. No solvate-free crystals could be obtained to rule out this alternative.

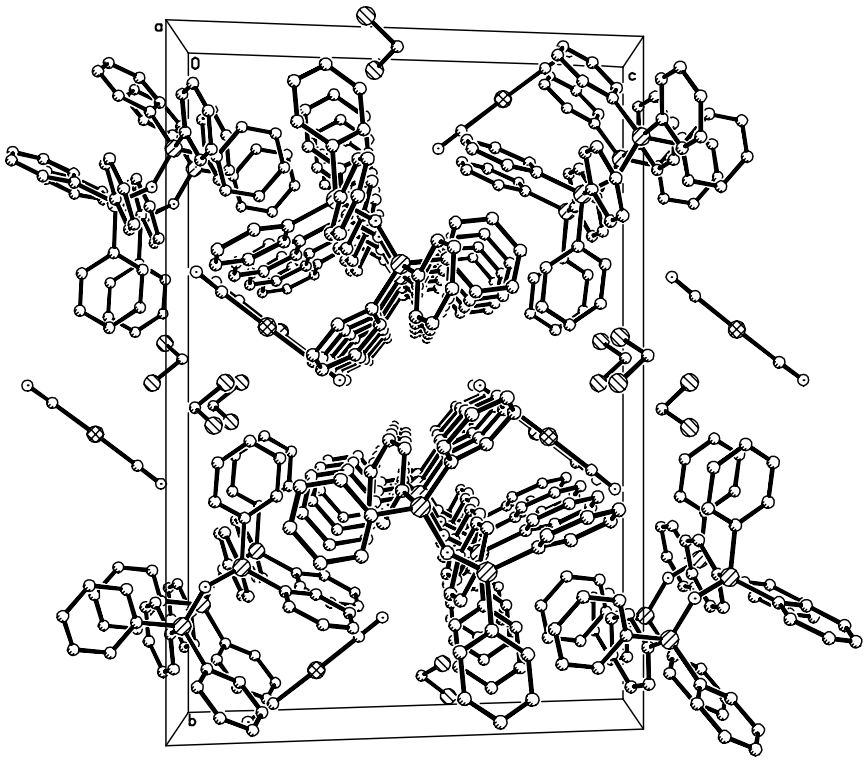

Figure 2-3. Projection of the unit cell of $[Ph_3PNPPh_3]^+[Au(CN)_2]^-(CH_2Cl_2)_{0.5}$ (**2**) onto the bc-plane showing the stacking of the cations and the contacts of the anions and the solvent molecules.

2.5 Discussion and Summary

The present study has demonstrated that the anion association in aqueous solutions of $M[Au(CN)_2]$ salts is very weak and not manifested in concentration-dependent IR and NMR spectra with standard resolution. The anions are also not associated in the crystal, where very large and flexible $[PPN]^+$ cations could give room for oligomerization.

From very detailed theoretical and luminescence studies, Patterson *et al.*[123] have estimated the free energy of dimerization (through Au--Au contacts) to give dianions $[Au(CN)_2]_2^{2-}$ as less than -2 kcal/mol (for the potassium salt in aqueous solution at room temperature). This small gain in energy is obviously not enough to induce rearrangements in an ionic structure against Coulomb forces, and to detect significant changes in NMR chemical shift [(δ(CN)] or vibrational frequencies of strong covalent bonds [ν(CN)] in solution.

In summary, the present work has shown that aurophilic interactions between anions $[Au(CN)_2]^-$ can be maintained only in structures where there is additional support from contacts with counterions or interstitial solvent molecules. Coordinative or hydrogen bonds provide an ideal combination, as demonstrated in several previous studies.[124,127] Bulky substitutents with the cationic centers shielded by organic groups as in $[Ph_3PNPPh_3]^+$ do not provide such support and therefore the anions remain separated with a preference for contacts to solvate molecules (**2**).

3 Structural, Spectroscopic and Theoretical Studies of (ᵗButyl-isocyanide)gold(I) Iodide

3.1 Introduction

Two-coordinate gold(I) complexes of the type L-Au-X are known to show association phenomena in the solid state[148] and under favorable conditions in solution.[149] In the crystal this association leads to short intermolecular, sub-van-der-Waals contacts between the gold atoms in the range of d(Au-Au) 2.90 - 3.50 Å. This distance is dependent on a number of factors with main contributions from steric and electronic effects of the substituents (the neutral ligand L and the anionic ligand X).[150] The geometry of the aggregates may vary from parallel (A) and antiparallel (B) to crossed / perpendicular dimers (C) (see **Figure 1-4**), and the energy associated with the aggregation has been measured[151] and calculated[152] to be in the order of 5 - 10 kcal/mol for a dimeric unit. However, the association can also be extended to give larger oligomers and one- or two-dimensional polymers.[153] The aggregation not only leads to interesting structures, but also to intriguing photophysical phenomena (absorption and luminescence spectra).[154] In general terms, "aurophilic" bonding of this type is now widely accepted as the most prominent example of a more general phenomenon "metallophilicity"[153] and recognized as a major force determining supramolecular structures and properties.[155]

While the effect is most obvious for most gold(I) complexes wih tertiary amine, phosphine and arsine, as well as sulfide and selenide ligands (R_3N, R_3P, R_3As, R_2S, R_2Se etc.), the iso-

---

[148] Schmidbaur, H., Gold. Bull. **1990**, 23, 11.

[149] Hyashi, A., Olmstead, M. M., Attar, S., Baldi, A. L., J. Am. Chem. Soc. ASAP, **2002**.

[150] Pyykkö, P., Li, J., Runeberg, N., Chem. Phys. Lett. **1994**, 218, 133.

[151] Müller, G., Graf, W., Schmidbaur, H., Angew. Chem. Int. Ed. Eng. **1988**, 27, 417.

[152] Pyykkö, P., Chem. Rev. **1997**, 97, 597.

[153] Schmidbaur, H., Gold. Bull. **2000**, 33, 3.

[154] a) Yam, V. W. W., Lai, T. F., Che. C.-M. J. Chem. Soc., Dalton Trans., **1990**, 3747. b) Vickery, J. C., Olmstead, M. M., Fung, E. Y., Balch, A. L., Angew. Chem. Int. Ed. Engl. **1997**, 36, 1179. c) Assefa, Z., McBurnett, B. G., Staples, R. J., Fackler Jr., J. P., Assmann, B., Angermaier, K., Schmidbaur, H., Inorg. Chem. **1995**, 34, 75.

[155] a) Schmidbaur, H., Chem. Soc. Rev. **1995**, 391. b) Braga, D., Grepioni, F., Desiraju, G. R., Chem. Rev. **1998**, 98, 1357.

cyanide ligands RNC appear to weaken aurophilic bonding as witnessed by exceedingly long intermolecular Au--Au contacts in crystals of compounds of the type (RNC)AuX.[156] Previous studies in this laboratory showed erratic results as the substituents R and X were changed from alkyl to aryl and ester, or from Cl to Br, I, NO_3 etc., respectively.[157-161] Contrary to expectations based on previously proposed rules,[150,152] the combination isocyanide / iodide - both extremely soft donors - seemed to lead to particularly poor interactions.

In order to clarify this point, the iodine compound was investigated in detail in the current study, following work on the corresponding chloro and bromo analogues. (ᵗBuNC)AuCl and (ᵗBuNC)AuBr are isomorphous and form chain structures with rather long Au--Au distances of 3.695(1) and 3.689(1) Å, respectively.[157] Along these chains, neighboring molecules are arranged antiparallel head-to-tail, but the molecules are shifted against each other in such a way that the Au--Au contacts are not the minimum distance between the molecules. These shifts also indicate very weak – if any – Au--Au bonding.

3.2 Preparation

(ᵗButyl-isocyanide)gold(I) iodide (**4**) was prepared from the corresponding chloride[157] by metathesis reaction with potassium iodide in a dichloromethane / water two-phase system. The product was isolated from the organic phase as a colorless microcrystalline material in 70 % yield. Protection of the reaction vessel against incandescent light is required to avoid decomposition. Single crystals of (ᵗBuNC)AuI (**4**) were grown from dichloromethane / pentane.

$$(CH_3)_3CNC + (tht)AuCl \longrightarrow (CH_3)_3CNCAuCl + tht$$

$$(CH_3)_3CNCAuCl \xrightarrow[(H_2O)]{KI} (CH_3)_3CNCAuI + KCl$$

(**4**)

[156] Mathieson, T., Schier, A., Schmidbaur, H., J. Chem. Soc., Dalton Trans., **2001**, 1196.

[157] Schneider, W., Angermaier, K., Sladek, A., Schmidbaur, H., Z. Naturforsch. **1996**, 51b, 790.

[158] Wilton-Ely, J. D. E. T., Ehlich, H., Schier, A., Schmidbaur, H., Helv. Chim. Acta **2001**, 84, 3216.

[159] Mathieson, T., Langdon, A. G., Milestone, N. B., Nicholson, B. K., J. Chem. Soc., Dalton Trans. **1999**, 201.

[160] Xiao, H., Cheung, K.-K., Che, C.-M., J. Chem. Soc., Dalton Trans. **1996**, 3699.

[161] Ahrland, S., Dreisch K., Norén, B., Oscarsson, Å., Mater. Chem. Phys. **1971**, 276, 281.

For the spectroscopic studies, the compound with ^{13}C-enrichment at the isocyanide function was also synthesized. For this purpose, $^{t}BuN^{13}C$ was generated from $^{13}CHCl_3$ / $^{12}CHCl_3$ (7 % ^{13}C), $^{t}BuNH_2$ and NaOH in the presence of $[Et_3NBz]Cl$ in a dichloromethane / water two-phase system at reflux temperature. The product was isolated as a colorless liquid by fractional distillation in 66 % yield.

From this carbon-labeled isocyanide the AuCl complex was prepared using (tetrahydrothiophene)gold chloride as the substrate. The resulting labeled chloride (7 % ^{13}C, 80 % yield) was then converted into the labeled iodide (7 % ^{13}C, 70 % yield) following the above procedure.

3.3 Crystal Structure

Crystals of (^{t}BuNC)AuI (**4**) are monoclinic, space group *C*2/*c*, with Z = 8 formula units in the unit cell. The molecules are arranged in pairs with the components related by a twofold axis (**Figure 3-1**). The shortest distance between the monomers is between the two gold atoms, but the Au--Au' distance of 4.162 Å indicates that this is at best a weak van-der-Waals contact. The structure of the monomer is a linear array of five atoms (I-Au-C-N-C) with standard distances and angles. Au-Cl 1.95(1), Au-I 2.513(1), C1-N1 1.13(1), C2-N1 1.47(2) Å; I-Au-C1 178.7(4)°, N1-C1-Au 179(1)°, C1-N1-C2 177(1)°. The monomers are in a crossed orientations with a dihedral angle I-Au-Au'-I' = 108.8° (**Figure 3-1**).

Projections of the unit cell along its axes show that there are no conspicuously short contacts between the iodine atoms of the molecules. (**Figure 3-2** shows a projection onto the bc plane). In fact all intermolecular I--I distances are well beyond 4.50 Å. The crystal structure thus can be considered to be a space-filling array of monomers with no indication for discrete aurophilic (Au--Au) or other closed-shell interactions (I--I, Au--I).

3.4 Spectroscopic Studies

Solutions of ($^{t}BuN^{13}C$)AuI (**4**) in dichloromethane-d_2 show three ^{13}C-NMR signals at 29.8 ppm (s, $\underline{C}H_3$), 59.4 ppm (s, $Me_3\underline{C}$) and 143.2 ppm [t, $^{1}J^{14}_{N}\text{-}^{13}_{C}$ = 21.9 Hz, N$\underline{C}$]. The corresponding data for ($^{t}BuN^{13}C$)AuCl are 29.83 ppm (s, $\underline{C}H_3$), 59.60 ppm [t, $^{1}J^{14}_{N}\text{-}^{13}_{C}$ = 4.1 Hz, $Me_3\underline{C}$] and 132.49 ppm [t, $^{1}J^{14}_{N}\text{-}^{13}_{C}$ = 24.2 Hz, N$\underline{C}$]. Both spectra are largely independent of concentration (0.20 - 0.65 mole/L for the chloride, 0.3 - 1.0 mole/L for the iodide) and temperature (-80 to +20 °C). The small shifts with concentration and temperature are all close to

the standard deviations of the experiments. The resonances of (ᵗBuNC)AuI become broad at low temperature (-60 °C) and the ^{14}N-^{13}C coupling is lost. This result may be ascribed to a ligand redistribution involving ionic isomers or to a reduced fluctuation in the solvation which generates a change in the electric field gradient at the quadrupolar nuclei (^{14}N, ^{197}Au) and a change in relaxation times. Therefore there is no indication for oligomerization of (ᵗbutyliso-cyanide)gold(I) iodide in solution.

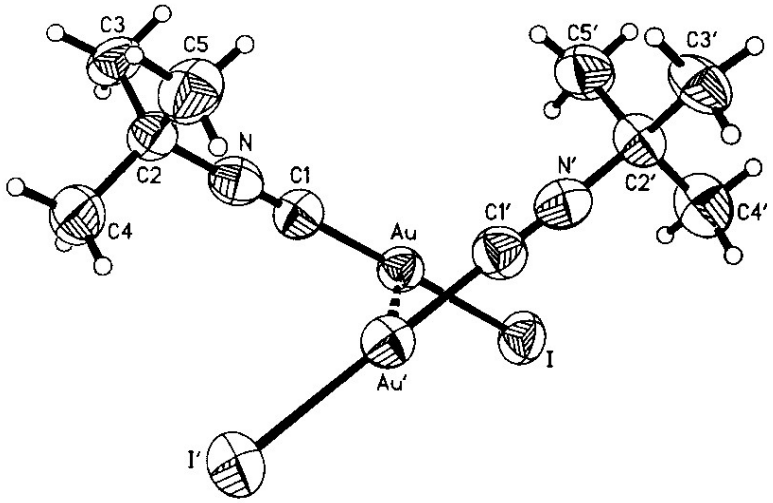

Figure 3-1. X-ray structure of the dimeric subunits in (Me_3CNC)AuI (**4**) (ORTEP drawing, ellipsoids at the 50 % probability level). The monomers are in a crossed orientation with a dihedral angle I-Au-Au'-I' = 108.8° and an Au--Au' distance of 4.612(3) Å. Selected monomer parameters: Cl-Au = 1.95(1), Au-I = 2.513(1) Å and C(1)-Au-I = 177(1)°.

3.5 Computational Section

The solid state structure of ᵗBuNCAuI (**4**) (**Figure 3-1**) shows exceedingly long intermolecular Au--Au distances (4.16 Å). It is therefore a particularly striking example of the general trend that solid state structures of Au(I) isocyanide complexes show very long intermolecular Au--Au contacts. The result prompts the question: "Is this an intrinsic electronic effect induced by the isonitrile ligand?" In an attempt to answer this question, (methylisonitrile)gold(I) chloride and iodide dimers {$[MeNCAuX]_2$, X = (Cl, I)} were studied by quantum-chemical methods in the gas phase as model systems and the results of these calculations compared with previous computational data on the analogous phosphine systems {$[H_3PAuX]_2$, X = (H, F, Cl, Br, I, -CN, CH_3, $-SCH_3$)]}.[150]

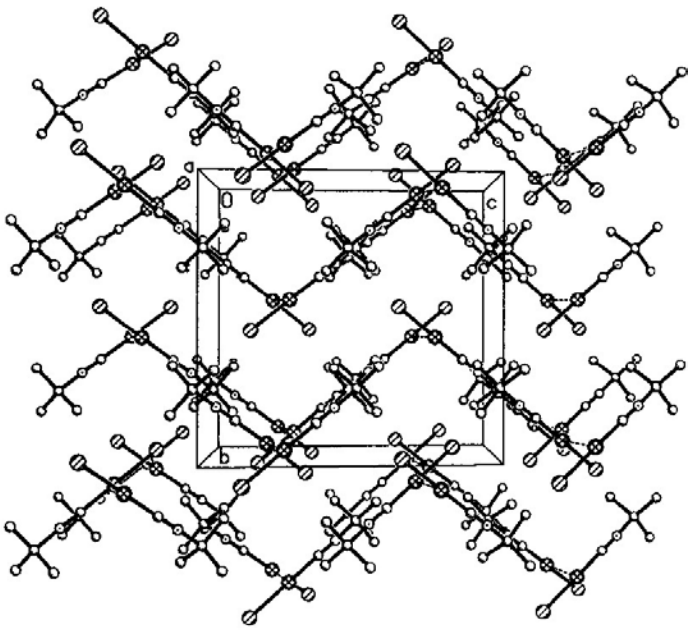

Figure 3-2. Projection onto the bc plane of the crystal of (Me_3CNC)AuI (**4**). All I-I distances are well beyond 4.50 Å. The structure can be considered to be a space-filling array of monomers with no indication for discrete aurophilic (Au--Au) or other closed-shell interactions (I--I, Au--I).

In calculations of the dimers the monomers were aligned to produce X-Au-Au angles of 90°. The optimized monomer structures and the dihedral angle [Θ = 90° (perpendicular arrangement)] were frozen and only the Au--Au distance was changed (see **Figure 3-3**).

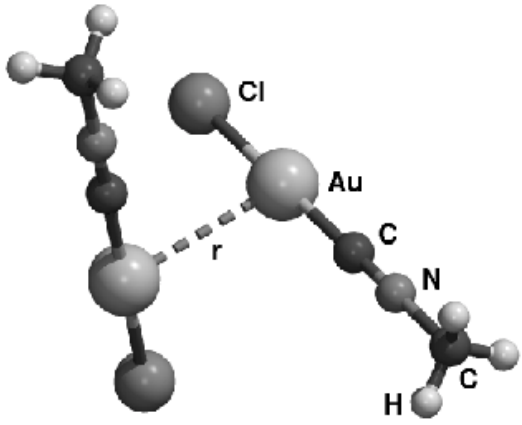

Figure 3-3. The structure of the $(H_3CNCAuX)_2$ model dimer.

At LMP2 level (local-MP2, see Computational Details) the Au--Au equilibrium distance of the $(MeNCAuCl)_2$ dimer is found to be 3.230 Å, and the corresponding interaction energy is 19 kJ/mol (see **Figure 3-4**, perpendicular arrangement).

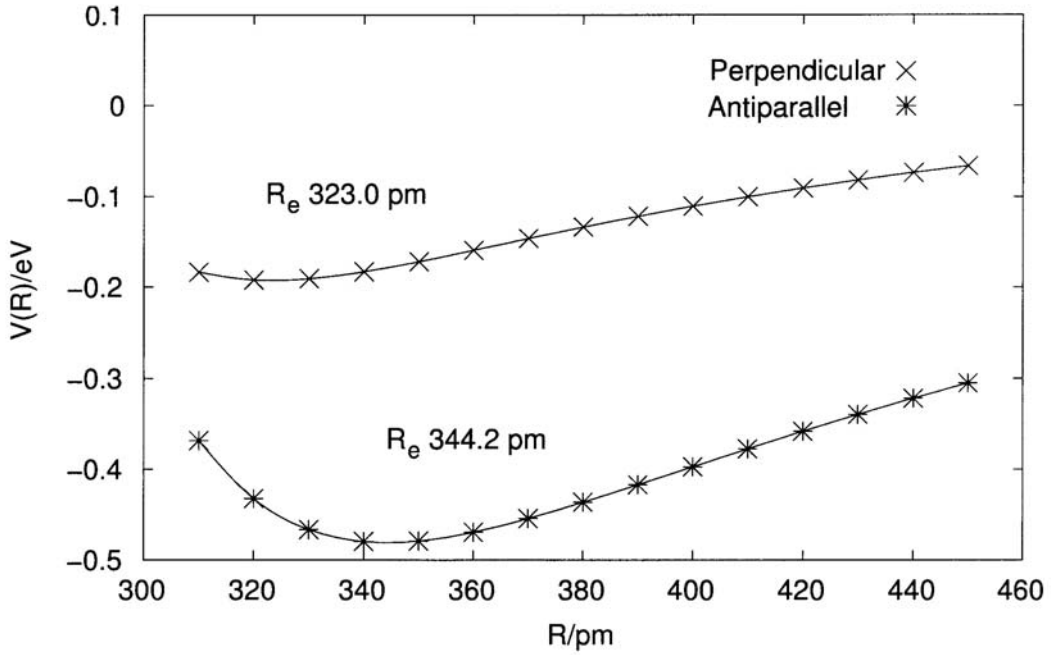

Figure 3-4. The calculated interaction energy of the $(MeNCAuCl)_2$ dimer in perpendicular (Θ = 90°) and antiparallel (Θ = 180°) arrangement at LMP2/AVDZ level of theory.

At SCF level the intermolecular potential appears to be purely repulsive (see **Figure 3-5**, perpendicular arrangement), which is as expected, since aurophilic attractions are basically dispersion interactions, which can only be described in terms of electronic correlation.

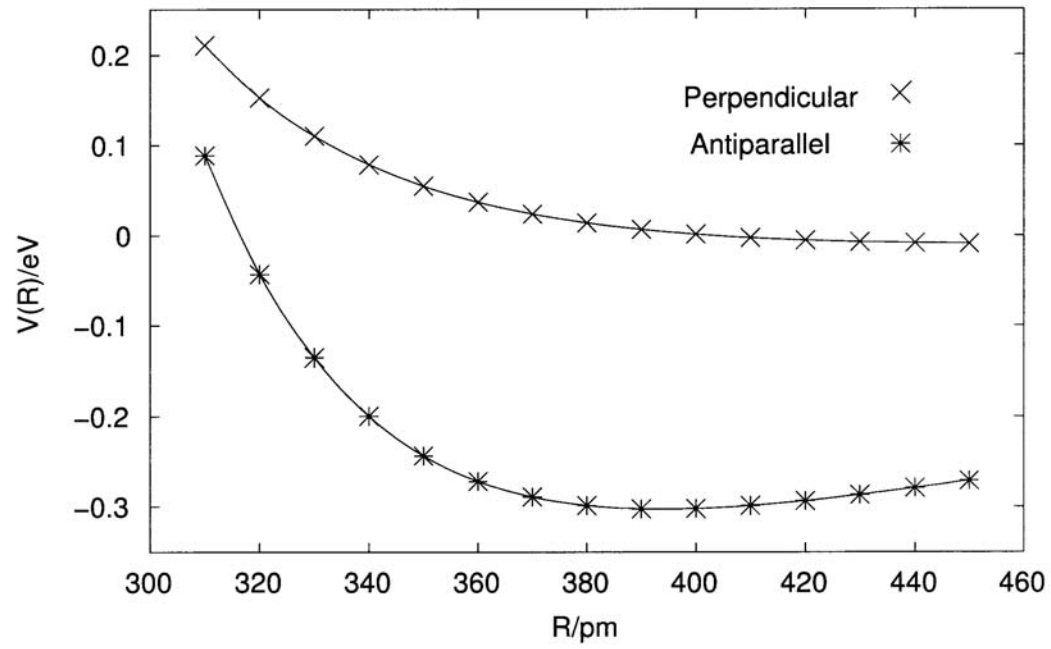

Figure 3-5. The calculated interaction energy of the $(MeNCAuCl)_2$ dimer in perpendicular (Θ = 90°) and antiparallel (Θ = 180°) arrangement at SCF/AVDZ level of theory.

For the $(MeNCAuI)_2$ dimer the Au--Au equilibrium distance is 3.180 Å and the interaction energy is 25 kJ/mol at LMP2 level (see **Figure 3-6**, perpendicular arrangement). SCF methods again yield a repulsive potential without any local minima for the $(MeNCAuI)_2$ dimer (see **Figure 3-7**).

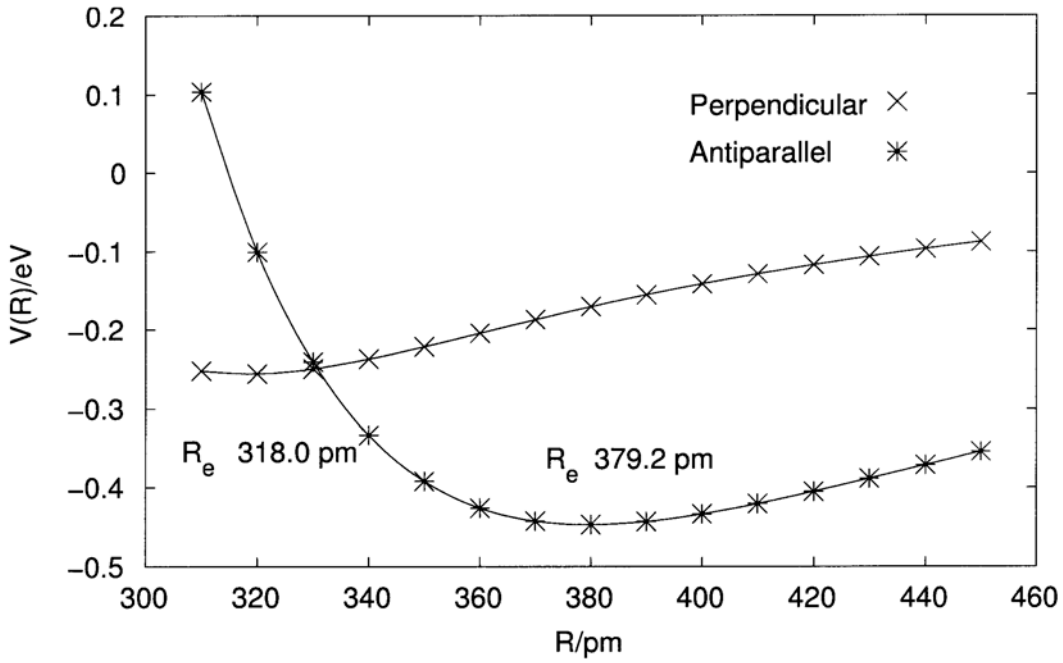

Figure 3-6. The calculated interaction energy of the $(MeNCAuI)_2$ dimer in perpendicular (Θ = 90°) and antiparallel (Θ = 180°) arrangement at LMP2/AVDZ level of theory.

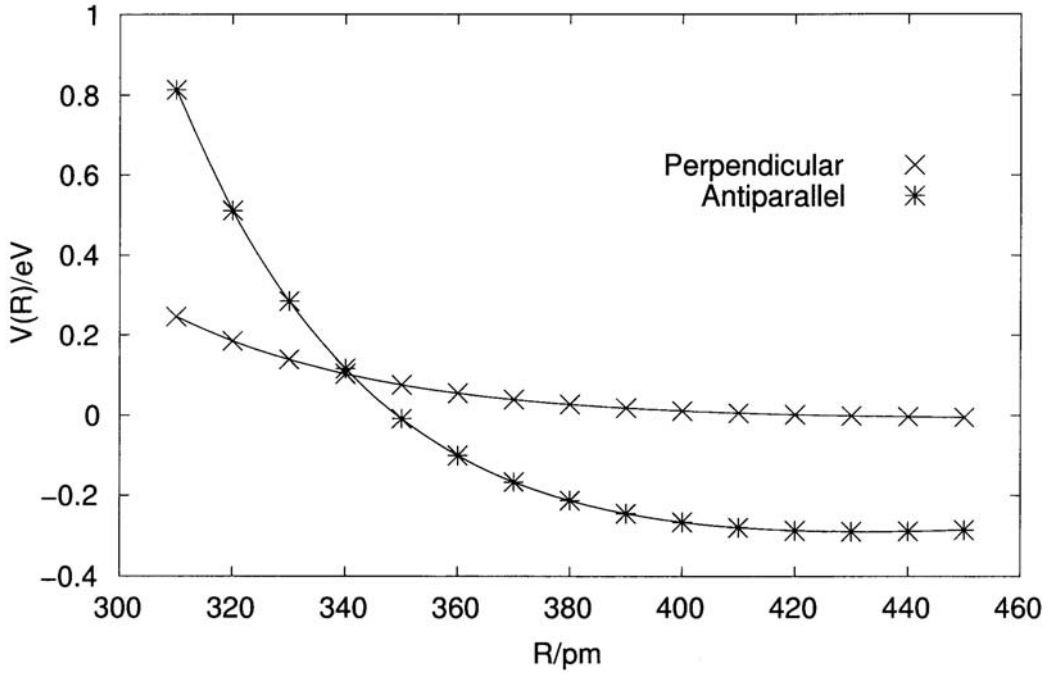

Figure 3-7. The calculated interaction energy of the $(MeNCAuI)_2$ dimer in perpendicular (Θ = 90°) and antiparallel (Θ = 180°) arrangement at SCF/AVDZ level of theory.

Table 3-1 shows the results together with the corresponding values calculated for the phosphine complexes.[150] Firstly, the comparison suggests that there is no principal difference in interaction energies between isonitrile and phosphine complexes within computational accuracy (at least ± 5 kJ/mol). Secondly, the interaction energy on changing from the harder chloride to the softer iodide increases not only in the case of the phosphine ligand[150] but also for the isonitrile ligand. Thirdly and most surprisingly, the isonitrile complexes have shorter Au--Au contacts than the phosphines complexes in these model systems. Since this is clearly in contrast to the experimental observations, attempts were made to refine the model.

Table 3-1. Equilibrium distances and interaction energies of $(LAuX)_2$ (L = MeNC, H_3P; X = Cl, I) dimers in perpendicular arrangement (Θ = 90°) calculated at second-order-perturbation-theory levels.

Molecule	R_c [Å]	Δ E [kJ/mol]
$(H_3PAuCl)_2$[3]	3.366	17
$(MeNCAuCl)_2$	3.230	19
$(H_3PAuI)_2$[3]	3.315	23
$(MeNCAuI)_2$	3.180	25

Loosening the restraint of a 90° torsion angle Θ yields an Au-Au distance of 3.442 Å for the chloride and of 3.792 Å for the iodide, with a torsion angle at equilibrium of 180° (= antiparallel configuration) in both cases (see **Figure 3-8**). The dimerization energies for these configurations are 47 kJ/mol and 41 kJ/mol for the chloride and iodide, respectively (**Table 3-2**, **Figure 3-6, Figure 3-8**). Surprisingly, the SCF potential for the antiparallel $(MeNCAuCl)_2$ dimer is no more repulsive and shows a local minimum at about 3.95 Å, while for $(MeNCAuI)_2$ it is flat for all R values larger than 4.20 Å. The result is a much higher total (LMP2) dimer stabilization energy at an antiparallel arrangement, but at a longer intermolecular distance.

Table 3-2. Equilibrium distances and interaction energies of $(MeNCAuX)_2$ (X = Cl, I) dimers in antiparallel arrangement (Θ = 180°) calculated at LMP2/AVDZ level of theory.

Molecule	R_c [Å]	Δ E [kJ/mol]
$(MeNCAuCl)_2$	3.442	47
$(MeNCAuI)_2$	3.792	41

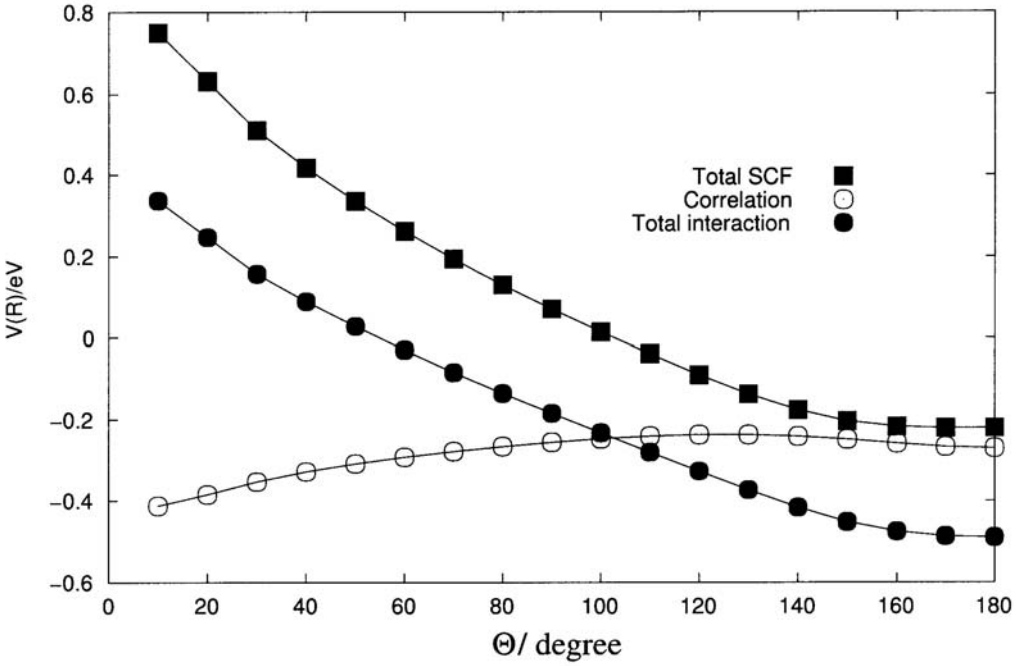

Figure 3-8. The calculated interaction energy of the $(MeNCAuCl)_2$ dimer at a fixed Au-Au distance of 3.442 Å and different torsion angles Θ (LMP2/AVDZ level of theory).

To make the situation more transparent, an energy contribution analysis in terms of classical electrostatic potentials (see Computational Details) was carried out for the perpendicular and the antiparallel equilibrium geometry of the $(MeNCAuCl)_2$ dimer (see **Figure 3-9** and **Figure 3-10**). The major repulsive contribution in the antiparallel case is the short range "Pauli" repulsion, followed by a quadrupole-quadrupole interaction, while the major attractive contribution is represented by the dipole-dipole interactions, followed by dipoleinduced-dipole interactions. In summary, these contributions yield a slightly repulsive (SCF) potential.

In contrast to the antiparallel case, the major repulsive contribution in the perpendicular configuration is no longer the very short range "Pauli" repulsion but rather the somewhat more long ranging quadrupole-quadrupole interaction, and the major attractive contribution in this case is the dipoleinduced-dipole interaction. In classical electrostatic terms again a repulsive SCF potential is obtained.

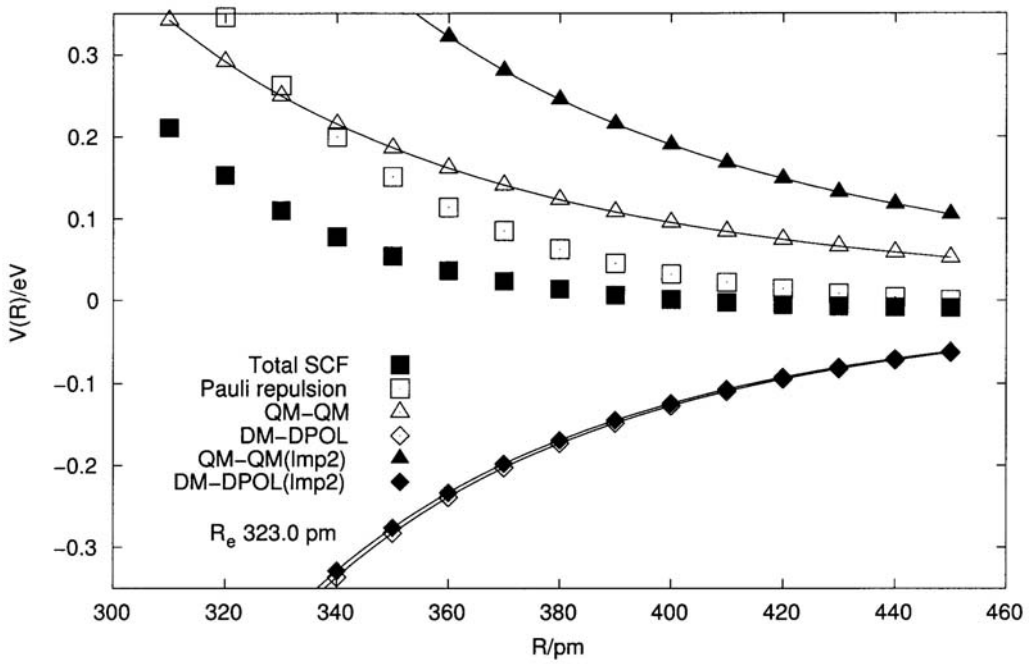

Figure 3-9. The calculated LMP2/AVDZ interaction potential contributions of the perpendicular $(MeNCAuCl)_2$ dimer partitioned according to equations 1-3. The (LMP2) labels correspond to results obtained by using the LMP2 values.

It is the correlation energy which is responsible for the main part of the aurophilic interaction and leads in both cases (parallel and antiparallel configuration) to a potential curve with a distinct local minimum. Since the correlation energy contribution is largely the same for the antiparallel and the perpendicular case (see **Figure 3-9**), the difference in the potential curves between the parallel and the perpendicular configuration is only determined by the classical electrostatic contributions. In other words: Aurophilic attraction is a necessary but not commensurate condition for the structure of the dimers.

Electron correlation energies are the smallest contributions to the total energy of the dimers for antiparallel arrangement and are of the same order of magnitude as the dipoleinduced-dipole interaction energies for the perpendicular arrangement (see **Figure 3-11**).

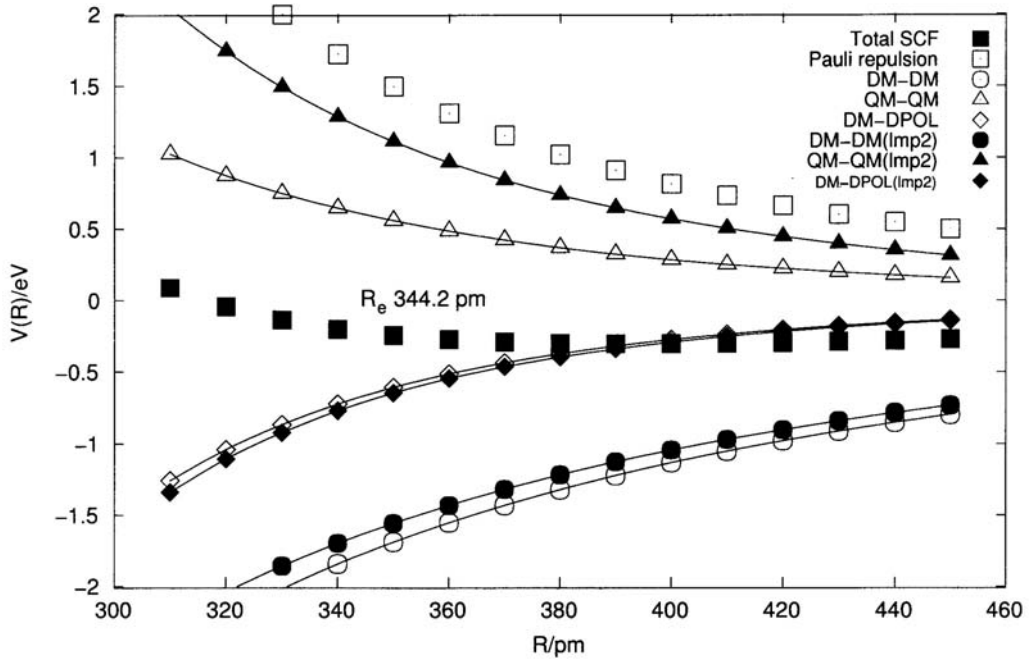

Figure 3-10. The calculated LMP2/AVDZ interaction energy of the antiparallel $(MeNCAuCl)_2$ dimer partitioned according to equations 1-3. The (LMP2) labels correspond to results obtained by using the LMP2 values for the properties.

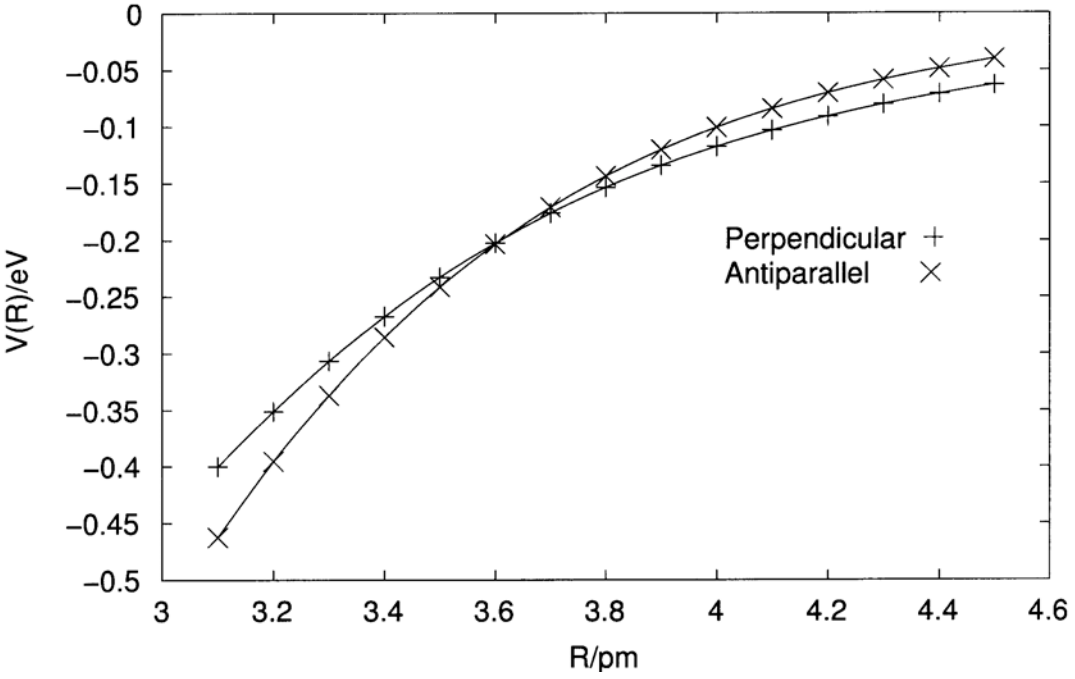

Figure 3-11. The calculated LMP2/AVDZ correlation energy of the $(MeNCAuCl)_2$ dimer in parallel and antiparallel orientation.

3.6 Summary

The strong monomer-monomer interaction at a relatively large distance in (RNC)AuX dimers with antiparallel orientation of monomers is mainly a result of the dominating long-range dipole-dipole attraction and the short-range steric ("Pauli") repulsion. The short but only weak monomer-monomer interaction in the perpendicular case is a result of the less dominating steric repulsion and the dipoleinduced dipole attraction, which is weaker than the dipole-dipole attraction of the antiparallel case. The necessary condition to make these effects experimentally observable is an aurophilic correlation attraction, which is not significantly influenced by the type of ligands present (methylisonitrile and phosphine).

3.7 Computational Details

In the present work the interaction energies of the $(MeNCAuX)_2$ (X = Cl, I) dimers were studied for various structural combinations of the monomers. All calculations were performed at the local MP2 (LMP2) level, as implemented in the MOLPRO program package.[162] The basis sets are of polarized valence double-zeta (VOZP) quality, comprising an energy-consistent 19 valence-electron (VE) quasirelativistic pseudopotential (QRPP) with an (8s7p6d2f) / [7s6p3d2f] valence basis set on gold,[163,164] a 8-VE QRPP with a (4s4p1d) basis on I,[165, 166] and all-electron basis sets for H, C, N and Cl.[167,168]

The LMP2 method introduces some conceptual advantages for studying intermolecular interactions, such as a drastically reduced basis-set superposition error (BSSE) and the possibility to decompose the correlation energy into physically meaningful contributions.[162]

The Au 5s5p, the Cl 1s2s2p as well as the 1s electrons on C and N were excluded from the

---

[162] *MOLPRO*, a package of ab initio programs written by Werner, H.-J. and Knowles, P. J., with contributions from Amos, R. D., Berning, A., Cooper, D. L., Deegan, M. J. O., Dobbyn, A. J., Eckert, F., Hampel, C., Leininger, T., Lindh, R., Llyod, A. W., Meyer, W., Mura, M. E., Nicklass, A., Palmieri, P., Peterson, K., Pitzer, R., Pulay, P., Rauhut, G., Schütz, M., Stoll, H., Stone, A. J. and Thorsteinsson, T., **1999**.

[163] Andrae, D., Häusserman, U., Dolg, M., Stoll, H., Preuss, H., Theor. Chim. Acta **1990**, 77, 123.

[164] Runeberg, N., Schütz, M., Werner, H.-J., J. Chem. Phys. **1999**, 110, 7210.

[165] Bergner, A., Dolg, M., Kuechle, W., Stoll, H., Preuss, H., Mol. Phys. **1993**, 80, 1431.

[166] Huzinaga, S., Gaussian Basis Sets for Molecular Calculation Amsterdam: Elsevier, **1984**.

[167] Dunning Jr., T. H., J. Chem. Phys. **1989**, 90, 1007.

[168] Woon, D., Dunning Jr., T. H., J. Chem. Phys. **1993**, 98, 1358.

correlational treatment. The optimized structural parameters of the monomers are given in **Table 3-3**. Some important physical properties are compiled in **Table 3-4**.

The energy of the two interacting linear polar molecules is dominated by the following non-vanishing components: The short range "Pauli" repulsion (V_{short}), dipole-dipole interaction ($V_{dm\text{-}dm}$), quadrupole-quadrupole interaction ($V_{qm\text{-}qm}$), inductive dipole-polarizability interaction ($V_{dm\text{-}pol}$), and the dispersion due to interaction between the dipole polarizabilities (V_{disp}). The classical expressions for $V_{dm\text{-}dm}$, $V_{qm\text{-}qm}$ and $V_{dm\text{-}pol}$ of two identical, linear polar molecules are

$$V_{dm-dm} = \frac{u}{R^3}\cos(\Theta), \qquad \text{(Eq. 3-1)}$$

$$V_{qm-qm} = \frac{3\omega^2}{4R^5}(1+2\cos(\Theta)), \qquad \text{(Eq. 3-2)}$$

$$V_{dm-pol} = \frac{\alpha u^2}{R^6} + \frac{(\alpha_{II}-\alpha_{\perp})\mu^2}{R^6}(3\cos^2(\Theta)-1). \qquad \text{(Eq. 3-3)}$$

Table 3-3. At LMP2/AVDZ level optimized parameters of the MeNCAuX (X=Cl, I) monomers. Bond lengths in Å, angles in degree.

	MeNCAuX			MeNCAuX	
	X = Cl	X =I		X = Cl	X =I
X-Au	2.26	2.56	Au-C	1.90	1.93
C-N	1.18	1.18	N-C	1.43	1.43
C-H	1.09	1.09			
X-Au-C	180	180	Au-C-N	180	180
C-N-C	180	180	N-C-H	109	109

Table 3-4. Calculated dipole moment (μ), quadrupole moment (ω) and dipole polarizability [parallel ($\alpha_{\parallel}$) and perpendicular ($\alpha_{\perp}$)] components of the MeNCAuX (X=Cl, I) monomers in au.

Method	μ	ω	$\alpha_{\parallel}$	$\alpha_{\perp}$
MeNCAuCl:				
SCF	4.24	10.75	103.99	48.40
LMP2	4.07	15.16	120.13	51.31
MeNCAuI:				
SCF	4.41	22.21	144.60	63.91
LMP2	4.18	26.42	162.83	65.33

4 Studies of Mono- and Digoldacetylide Complexes (LAuC≡CH and LAuC≡CAuL, L=PR_3)

4.1 Introduction

The gold acetylide Au_2C_2 ("explosive gold") was first discovered by Berthelot[169] in 1866. Early work on this gold-carbon binary compound marked the start of extensive research in organogold chemistry which still continues to attract great interest.[170] While there has been steady growth in organogold chemistry in recent years, research into gold alkynyl compounds has become a particularly active field. The special position of gold acetylides is based on a set of interesting chemical and physical properties which suggest extensive applications in a variety of modern technologies including non-linear optics, mesogenic phases, sensors (photoluminescence), crystal engineering etc. The specific properties encompass a) the thermal and chemical stability of gold acetylide derivatives, e.g. towards oxidation and hydrolysis, which is quite remarkable considering the lability of ligand-free Au_2C_2; b) their rod-like structures which can be modified extensively both by substituents at the alkyne unit or in the auxiliary ligands attached to the gold atoms; and finally c) the ready formation of intermolecular aurophilic interactions which can influence greatly the configuration, conformation and HOMO-LUMO characteristics of the monomers. Recent literature reflects this potential in a series of highly successful experimental studies.[170]

Regarding the specific area of our research, alkynyl gold complexes of the type LAuC≡CAuL (**A**) and LAuC≡CH (**B**, L = PR_3), the following investigation made fundamental contributions to the literature: Initial preparative studies by Cross *et al.* led to the characterization of the first complexes, **A** and **B,** obtained from the corresponding R_3PAuCl complexes, acetylene

---

[169] Berthelot, M. P., Liebigs Ann. Chem. **1866**, 139, 150.

[170] a) Schmidbaur, H. "Organogold Compounds", in Gmelin Handbuch der Anorganischen Chemie, Slawisch, A., editor, 8. edition, Springer-Verlag, Berlin **1980**. b) Schmidbaur, H., Grohmann, A., Olmos, M. E., "Organogold Chemistry", in Gold: Progress in Chemistry, Biochemistry and Technology, Schmidbaur, H., editor, Wiley & Sons Ltd., Chichester, **1999**. c) Yam, V. W.-W., Choi, S. W.-K., J. Chem. Soc., Dalton Trans. **1996**, 4227. d) Chao, H.-Y., Lu, W. L., Chan, M. C. W., Che, C.-M., Cheung, K.-K., Zhu, N., J. Am. Chem. Soc. **2002**, 124, 14696.

gas and a strong base in alcohol.[171] This work was paralleled by studies of Bruce *et al.*[172] on these and other substituted acetylides $R_3PAuC{\equiv}CR'$ (**C**) which followed up previous investigations by Coates[170,173] and Puddephatt.[174] In the mid-90's the photophysical properties of this type of complex was investigated by Mingos, Yam *et al.* using a set of specific substituents for the phosphine ligands.[175] Vicente, Chicote *et al.* developed a new strategy for the synthesis of pure monoaurated acetylenes **B**[176] and gold acetylide complexes with ylidic components.[177]

Structural studies on compounds of types **A** and **C** are limited, and few prototypes have been investigated: bis[(triphenylphosphine)gold]acetylene, bis[tri(*m*-tolyl)phosphine-gold]acetylene (**Figure 1-24**);[172] bis[(diphenyl-1-naphthyl)phosphine)gold]acetylene (**Figure 1-26**), bis[(phenyl-di-1-naphthylphosphine)gold]acetylene (**Figure 1-27**), bis[(diferrocenyl-phenylphosphine)gold]acetylene (**Figure 1-28**) (all type **A**);[175] [(triphenylphosphine)gold-]phenylacetylene (**Figure 1-22**),[172] [(diferrocenyl-phenylphosphine)gold]phenylacetylene (**Figure 1-23**) and [(triphenylphosphine)gold]pentafluorophenylacetylene (**Figure 1-21**) (all type **C**).[175] No structure of a representative example from the type **B** series has been reported.

An inspection of these structures shows that all molecules of types **A** and **C** are monomeric in the crystal except for $[(Ph_3P)Au]C{\equiv}CPh$ (type **C**), which is a dimer with a relatively long Au--Au contact [3.379(1) Å] (see Ch.1.2.3).[172] For the other examples the monomeric nature is of no surprise since in all cases very bulky ligands and substituents were employed which rule out any close intermolecular gold-gold contacts.

Extensive experimental and theoretical studies related to the aurophilicity concept[178] have clearly demonstrated that this type of bonding should be and actually is ubiquitous in gold(I)

---

[171] a) Cross, R. J., Davidson, M. F., McLennan, A. J., J. Organomet. Chem. **1984**, 265, C37. b) Cross, R. J., Davidson, M. F., J. Chem. Soc., Dalton Trans. **1986**, 411.

[172] a) Bruce, M. I., Horn, E., Matisons, J. G., Snow, M. R., Aust. J. Chem. **1984**, 37, 1163. b) Bruce, M. I., Duffy, D. N., Aust. J. Chem. **1986**, 39, 1697. c) Bruce, M. I., Grundy, K. R., Lidell, M. J., Snow, M. R., Tiekink, R. T., J. Organomet. Chem. **1988**, 344, C49.

[173] Coates, G. E., Parkin, C., J. Chem. Soc. **1962**, 3220.

[174] Johnson, A., Puddephatt, R. J., J. Chem. Soc., Dalton Trans. **1977**, 1384.

[175] Müller, T. E., Choi, S. W.-K., Mingos, D. M. P., Murphy, D., Williams, D. J., Yam, V. W.-W., J. Organomet. Chem. **1994**, 484, 209.

[176] Vicente, J., Chicote, M.-T., Abrisqueta, M.-D., J. Chem. Soc., Dalton trans. **1995**, 497.

[177] Vicente, J., Singhal, A. R., Jones, P. G., Organometallics **2002**, 21, 5887.

[178] a) Schmidbaur, H., Gold Bull. **1990**, 23, 11. b) Schmidbaur, H., Chem. Soc. Rev. **1995**, 24, 391. c) Schmidbaur, H., Gold Bull. **2000**, 33, 3.

chemistry provided that the coordination sphere of the metal atoms is sufficiently open such that aggregation of neighboring molecules is not impeded.[179] It therefore appears that Au_2C_2 complexes should have a rich supramolecular chemistry. The potential for aggregation is even particularly great due to the α,ω-difunctionality which should give rise to extended oligomerization. The current work presents evidence to verify this prediction.

4.2 Preparation

To ensure free access to the linearly two-coordinate gold atoms in molecules of the types **A** and **B** the smallest tertiary phosphines were chosen in this work. The preparative work followed the published procedures employing the corresponding R_3PAuCl complexes (R_3P = Me_3P, Et_3P, Me_2PhP, $MePh_2P$ and $(p\text{-Tol})_3P$).[171-174] These were dissolved or suspended in ethanol and a stream of gaseous acetylene was passed into the solutions which also contained slightly more than one equivalent of sodium ethanolate as a base. NMR and Raman spectroscopic investigations of the products showed that in most cases (except for R = Et almost only **A** and for R = (*p*-Tol) only **B**) mixtures of the products **A** and **B** were obtained. Generally the complexes of type **B** were obtained as first precipitates separating from the reaction mixture. The diaurated complexes of type **A** were suspended as very fine particles in the mother liquor. They were collected, dried in a vacuum and then washed with water, redissolved in dichloromethane and dried again in a vacuum. Work-up of the products by fractional crystallization generally gave pure crystals of the least soluble complex.

$$(R_3P)AuCl + C_2H_2 + EtONa \longrightarrow NaCl + EtOH + (R_3P)AuC{\equiv}CH \quad (\mathbf{B})$$

$$(R_3P)AuC{\equiv}CH + EtONa + (R_3P)AuCl \longrightarrow NaCl + EtOH + (R_3P)AuC{\equiv}CAu(PR_3) \quad (\mathbf{A})$$

With the phosphines Me_3P, Et_3P and Me_2PhP only the symmetrical dinuclear compounds (**A**) were crystallized, while for $MePh_2P$ and $(p\text{-Tol})_3P$ the unsymmetrical mononuclear complex of type (**B**) was isolated. Single crystals could be grown of all five complexes. It should be noted that several symmetrical triarylphosphine complexes (**A**) have already been reported which also include the $(Ph_3P)AuC{\equiv}CAu(PPh_3)$ prototype.[172]

---

[179] Recent examples: a) Schmidbaur, H., Hamel, A., Mitzel, N. W., Schier, A., Nogai, S., Proc. Natl. Acad. Sci. (Washington) **2002**, 99, 4916. b) Ehlich, H., Schier, A., Schmidbaur, H., Inorg. Chem. **2002**, 41, 3721.

4.3 Spectroscopic Studies and Structures

Analytical and spectroscopic identification of the products was not always straightforward. It has been observed previously, for example, that the mass spectroscopic characteristics show a surprising variety of multinuclear species which indicate the presence of oligomers undergoing multibranch fragmentation.[172c] The expected molecular ions represent only a small minority in the list of ions. Note that this result suggests association of the compounds in the solid state and in solution.

Infrared and Raman spectroscopic data were not always unambiguous. While the C≡C stretching vibration for the symmetrical compounds (**A**, point group C_i) is expected to be Raman-active and IR-silent, for the unsymmetrical species of type **B** (point group C_3) this vibration should also be IR-active. The complexes of type **A** described in this work did not exhibitl C≡C stretching bands in the IR spectra and the complexes of type **B** described in this work did exhibit generally very weak C≡C and CH stretching bands for C≡CH in the IR spectra [1971.1 cm^{-1}, *v*(C≡C) and 3272.2 cm^{-1}, 3258.8 cm^{-1} *v*(CH) for (Me_3P)AuC≡CH (**5**); 1974.0 cm^{-1}, *v*(C≡C) for (Et_3P)AuC≡CH (**7**); 1978.5 cm^{-1} *v*(C≡C), 3279.6 cm^{-1} *v*(CH) for (Ph_2MeP)AuC≡CH (**11**) and 3275.5 cm^{-1} *v*(CH) for (*p*-tol)$_3$PAuC≡CH (**13**)]. In the C≡C triple bond range of the Raman spectra, there were not only very strong C≡C stretching bands for every diaurated complexes of type **A** [except (*p*-tol)$_3$PAuC≡CAuP(*p*-tol)$_3$) (**14**)], but also strong C≡C stretching bands for the complexes of unsymmetrical type **B** [except (Me_2PhP)-AuC≡CH (**9**)] (**see Table 4-1**). The differences between the frequencies of two authentic samples (**A** and **B**) are about 20 ~ 35 cm^{-1}. For complexes of type **B**, this is novel compared with those reported in the literature.[170c,171,172,175,176]

Table 4-1. IR and Raman bands for LAuC≡CAuL (**A**) and LAuC≡CH (**B**).

	Raman/ ν(C≡C) (cm^{-1})	IR / ν(C≡C) (cm^{-1})	IR / ν(CH) (cm^{-1}) (C≡CH)
(Me_3P)AuC≡CH (**5**)	1973.8	1971.1	3272.2 3258.8
(Me_3P)AuC≡CAu(PMe_3) (**6**)	1999.3		
(Et_3P)AuC≡CH (**7**)	1974.0		
(Et_3P)AuC≡CAu(PEt_3) (**8**)	2009.1 1921.9		
(Me_2PhP)AuC≡CH, (**9**)		1963.6 1973.8	3274.6
(Me_2PhP)AuC≡CAu($PPhMe_2$) (**10**)	1998.3		
(Ph_2MeP)AuC≡CH (**11**)	1981.8	1978.5	3279.6

$(Ph_2MeP)AuC{\equiv}CAu(PMePh_2)$ (**12**)	2001.6 1918.1		
$(p\text{-Tol})_3PAuC{\equiv}CH$ (**13**)	1981.8		3275.5
$(p\text{-Tol})_3PAuC{\equiv}CAuP(p\text{-Tol})_3$ (**14**)	2025[106]		
$(Vi_3P)AuC{\equiv}CAu(PVi_3)$	1995.3 1920.8		

NMR spectroscopy was elusive in all cases because it was found that the resonances of the acetylene carbon atoms of the symmetrical compounds of type **A** are difficult to detect even at low temperatures, and this is also true for the carbon atom of the unsymmetrical species **B** which carries no hydrogen atom. Previous tentative assignments[176] of the C-H resonance in the range 85 - 95 ppm were finally confirmed by the proton-coupled ^{13}C spectrum of $(Ph_2MeP)AuC{\equiv}CH$ (**11**) which showed the expected doublet splitting $^1J(^{13}C\text{-}^1H) = 228.6$ Hz. The range for the resonances of the other acetylene carbon atoms spreads over a large region from 120 ppm to as much as 210 ppm, where quite generally only very weak signals (if any) are detectable. There is also an overlap of this region with the low-field part of the range for aryl resonances which may mask the low-intensity acetylene resonances. Assignments are therefore most unambiguous for the fully alkylated complexes (with Me_3P and Et_3P ligands).

Another general difference between the mono- and di-aurated complexes of types **A** and **B** was found in the mass spectra. The peaks of oligomerization species $[2M - PR_3 + Au]^+$ and $[2M - PR_3 + H]^+$ were found as characteristic signals for diaurated complexes of type **A** {except only $[2M - PR_3 + H]^+$ for (**5**) and (**14**)} in comparison to **B**.

4.3.1 Characterization of Mono- and Bis(trimethylphosphinegold)acetylene

$$(Me_3P)AuCl + C_2H_2 + EtONa \longrightarrow NaCl + EtOH + (Me_3P)AuC{\equiv}CH \quad (\mathbf{5})$$

$$(Me_3P)AuC{\equiv}CH + EtONa + (Me_3P)AuCl \longrightarrow NaCl + EtOH + (Me_3P)AuC{\equiv}CAu(PMe_3) \quad (\mathbf{6})$$

From the reaction of $(Me_3P)AuCl$ and C_2H_2, the monosubstituted compound $(Me_3P)AuC{\equiv}CH$ (**5**) was isolated in addition to the disubstituted compound $(Me_3P)AuC{\equiv}CAu(PMe_3)$ (**6**) (**Figure 4-3**) whose crystal structure has been determined. The yellow disubstituted compound (**6**) readily decomposes at ambient temperature on contact with light. A comparison is

drawn between the mono- and di-substituted complexes in **Table 4-2**.

Table 4-2. Characterization of $(Me_3P)AuC{\equiv}CH$ (5) and $(Me_3P)AuC{\equiv}CAu(PMe_3)$ (6).

		$(Me_3P)AuC{\equiv}CH$ (**5**)	$(Me_3P)AuC{\equiv}CAu(PMe_3)$ (**6**)
Molecular weight (g/mol)		298.07	570.10
Substance			pale yellow solid
mp (°C)		111-112	206-207
MS (FAB) [m/z]	$[M+H]^+$		571.5
El.-anal. (cal. / found)	C	20.15/20.12	16.85/16.77
	H	3.38/3.37	3.18/3.21
	P	10.39/10.01	10.87/9.98
IR (Nujol) (cm^{-1})	ν(C≡C)	1971.1	
	ν(CH) (AuC≡CH)	3272.2 3258.8	
Raman (cm^{-1})	ν(C≡C)	1973.8, s	1999.3, s 1921.9, w
^{1}H-NMR (ppm)	$C\underline{H}_3$	1.48, d, 9H $^2J_{HP}$ = 9.9 Hz	1.49, d $^2J_{HP}$ = 9.9 Hz
	AuC≡C$\underline{H}$	2.09, s, 1H	
^{13}C(^{1}H-coupled)-NMR (ppm)	$\underline{C}H_3$	31.0, dq $^1J_{CP}$ = 35 Hz, $^1J_{CH}$ = 128.2 Hz	15.81 dq $^1J_{CP}$ = 35.9 Hz, $^1J_{CH}$ = 130.9 Hz
	C≡$\underline{C}$H	90.4, dd $^1J_{CH}$ = 227.3 Hz, $^3J_{CP}$ = 12.9 Hz	
	Au$\underline{C}$≡CH	128.3, dd $^2J_{CH}$ = 38.7 Hz, $^2J_{CP}$ = 143.4 Hz	
	Au$\underline{C}$≡$\underline{C}$Au		206.7, dd $^2J_{CP}$ = 12.0 Hz, $^3J_{CP}$ = 5.5 Hz
^{31}P{^{1}H}-NMR (ppm)		1.03, s	1.03, s
Crystal structure			zig-zag chain polymer
Au--Au (Å)			3.0747(8)

The IR spectrum of $(Me_3P)AuC{\equiv}CH$ (**5**) exhibited bands characteristic of ν(C≡C) (1971.1 cm^{-1}), ν(CH) and -AuC≡CH (3272.2 and 3258.8 cm^{-1}). The Raman spectrum showed one peak at 1973.8 (s) cm^{-1} for ν(C≡C) (**Figure 4-1**).

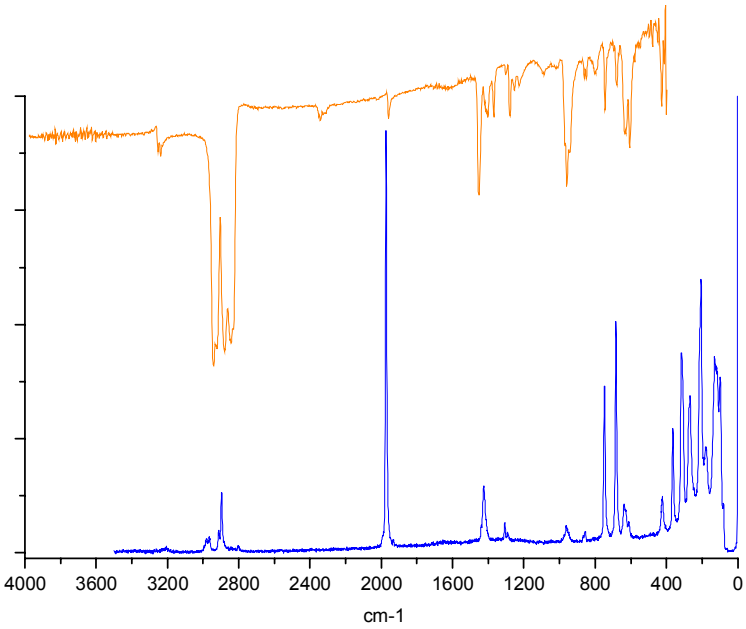

Figure 4-1: IR and Raman spectra (above and below, respectively) of [(trimethylphosphine)gold]acetylene, [(Me_3P)AuC≡CH] (**5**).

Complex (Me_3P)AuC≡CAu(PMe_3) (**6**) exhibited a characteristic band at 1999.3 (s) cm^{-1} for the expected symmetric ν(C≡C) in the Raman spectrum (**Figure 4-2**).

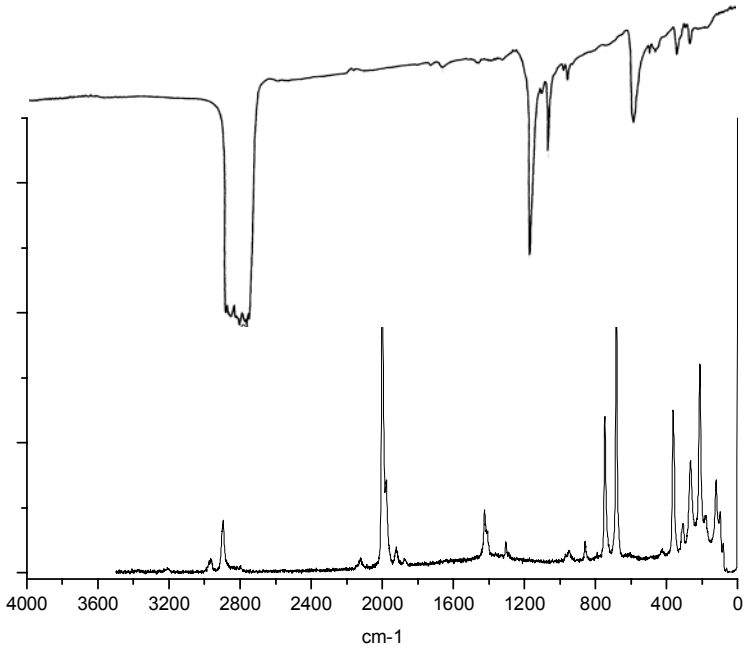

Figure 4-2. IR and Raman spectra (above and below, respectively) of bis[(trimethylphosphine)gold]acetylene, [(Me_3P)AuC≡CAu(PMe_3)] (**6**).

Crystals of bis[(trimethylphosphine)gold]acetylene, [(Me_3P)AuC≡CAu(PMe_3)] (**6**), are tetragonal, space group *P*4/*ncc*, with Z = 8 molecules in the unit cell. The individual dinuclear complex has point group C_i symmetry with C≡C, C-Au and Au-P distances of 1.21(2), 2.010(10) and 2.277(3) Å, respectively, very similar to those of the PEt_3 analogue. The angles P-Au-C1 [176.0(3)°] and C1'-C1-Au [177(1)°] show small deviations from linearity.

Contrary to the findings for the PEt_3 complex, the monomers of the PMe_3 complex are clearly associated into zig-zag chain oligomers via aurophilic bonding [Au--Au' 3.0747(8) Å] (**Figure 4-3**). The head-to-tail connectivity follows a pattern which relates neighboring molecules by a twofold axis passing through the mid-point of the Au--Au linkage. The folding of the zig-zag chain is determined by a dihedral angle P-Au-Au'-P' of 118.2° at either end of the molecule. Required by the C_i symmetry, for each molecule the α,ω-connections occur at opposite sides of the molecular axis. Together with the dihedral angle relation this leads to a non-parallel orientation of the molecular axis of neighboring molecules which is obvious from a view down the c-axis of the unit cell (**Figure 4-4**).

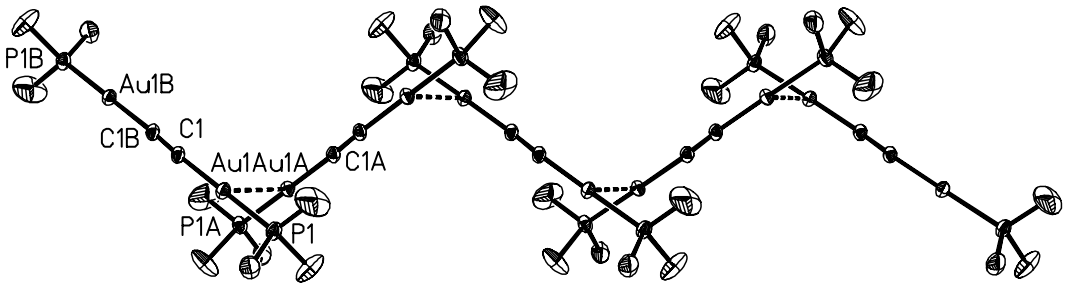

Figure 4-3. Zig-zag chain association of molecules [(Me_3P)AuC≡CAu(PMe_3)] (**6**) (ORTEP drawing with 50% probability ellipsoids, H-atoms omitted for clarity). Selected bond lengths [Å] and angles [°]: Au1-P1 2.277(3), Au1-C1 2.01(1), C1-C1B 1.21(2); Au1···Au1A 3.0747(8) ; P1-Au1-C1 176.0(3), Au1-C1-C1B 177(1), P1-Au1-Au1A-P1A 118.2(3).

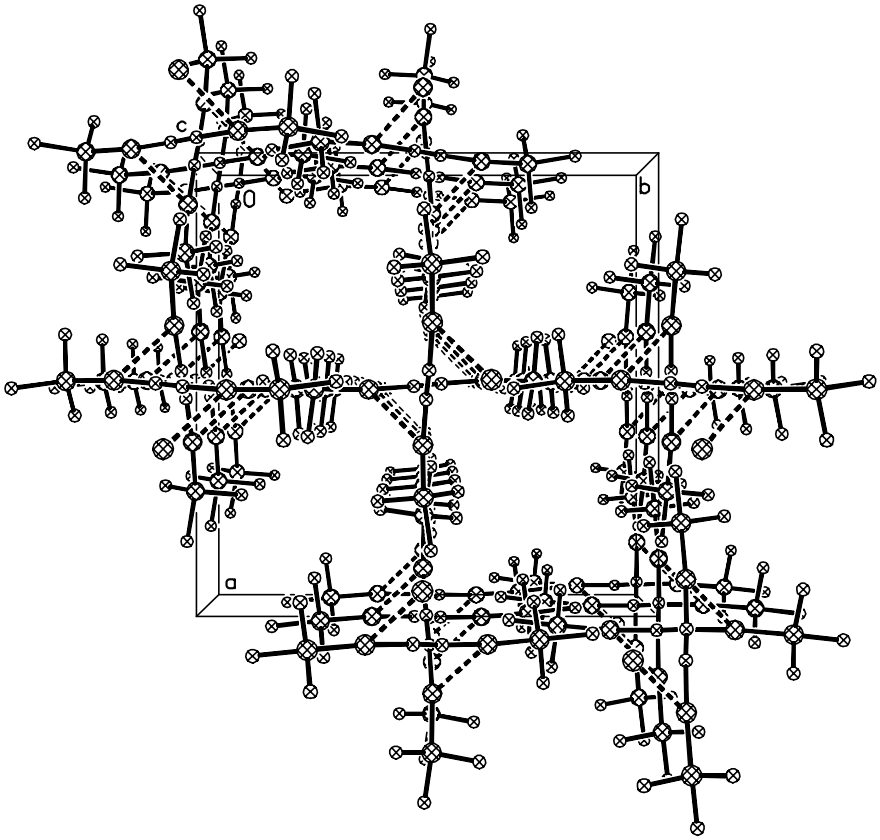

Figure 4-4. Packing of [(Me_3P)AuC≡CAu(PMe_3)] (**6**), viewed down the c-axis of the tetragonal cell.

4.3.2 Characterization of Mono- and Bis(triethylphosphinegold)acetylene

$$(Et_3P)AuCl + C_2H_2 + EtONa \longrightarrow NaCl + EtOH + (Et_3P)AuC{\equiv}CH \quad (\mathbf{7})$$

$$(Et_3P)AuC{\equiv}CH + EtONa + (Et_3P)AuCl \longrightarrow NaCl + EtOH + (Et_3P)AuC{\equiv}CAu(PEt_3) \quad (\mathbf{8})$$

Because (**7**) was present only in minor quantities, a Raman line at 1974.0 for ν(C≡C) (**Figure 4-5**), which corresponds in the ^{13}C-NMR signale at δ = 88.755 ppm of C≡CH (**Table 4-3**) is the only evidence for this by-product. The disubstituted complex (**8**) was spectroscopically fully identified and its crystal structure determined.

Table 4-3. Characterization of $(Et_3P)AuC{\equiv}CH$ (7) and $(Et_3P)AuC{\equiv}CAu(PEt_3)$ (8).

		$(Et_3P)AuC{\equiv}CH$ (**7**)	$(Et_3P)AuC{\equiv}CAu(PEt_3)$ (**8**)
Molecular weight (g/mol)		340.16	654.25
Substance			white solid
mp (°C)			180-181
MS (FAB) [m/z]	$[M+H]^+$		655.7
El.-anal. (cal. / found)	C		25.7/25.25
	H		4.62/4.38
	P		9.47/8.87
Raman (cm^{-1})	ν(C≡C)	1974.0, vw	2009.1, s 1921.6
^{1}H-NMR (ppm)	$C\underline{H}_3$		1.05, dt $^3J_{HP}$ = 18 Hz $^3J_{HH}$ = 7.6 Hz
	$-C\underline{H}_2-$		1.70, dq $^2J_{HP}$ = 8.1 Hz $^3J_{HH}$ = 7.5 Hz
	$AuC{\equiv}C\underline{H}$	2.09, s, 1H	
^{13}C(^{1}H-coupled)-NMR (ppm)	$\underline{C}H_3$		8.90, qt $^1J_{CH}$ = 128.2 Hz $^2J_{CH}$ = 4.6 Hz
	$-\underline{C}H_2-$		18.04, td $^1J_{CH}$ = 130 Hz $^1J_{CP}$ = 32.3 Hz
	$C{\equiv}\underline{C}H$	88.755, vw	
	$Au\underline{C}{\equiv}\underline{C}Au$		150.0, br., s
$^1P\{^1H\}$-NMR (ppm)			39.20, s
Crystal structure			monomer

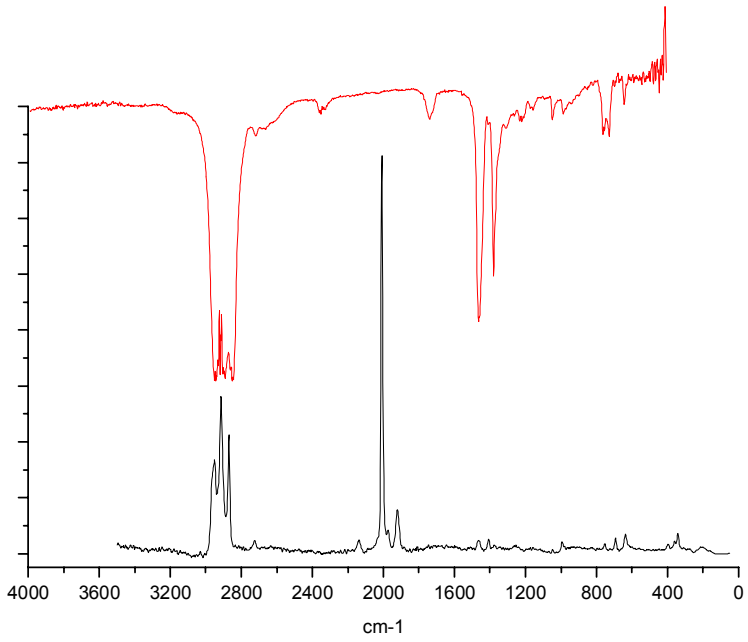

Figure 4-5: IR and Raman spectra (above and below, respectively) of bis[(triethylphosphine)gold]acetylene, [(Et_3P)AuC≡CAu(PEt_3)] (**8**).

Symmetrical compounds of the type **A** with triarylphosphine ligands have been shown to have "wheel-and axle" type structures where the rigid digold acetylene rod connects the two three-fold phosphine rotors.[172] Even more extended "weight-lift gear" (dumb-bell) structures have been found for the anionic bis-isocyanide gold complexes $[(RNC)_2Au]^-$ and related combinations of isocyanide and other ligands with linear geometry.[180]

The same structural type has now been confirmed for bis[(triethylphosphine)gold]acetylene, [(Et_3P)AuC≡CAu(PEt_3)] (**8**). The compound crystallizes in the rare cubic space group $Pa\bar{3}$ with Z = 4 molecules in the unit cell. The individual molecule has D_3 point group symmetry as shown in **Figure 4-6**. The crystals are free of solvent and have an efficient packing of the molecules (**Figure 4-7**), but there is no evidence for any aurophilic interactions. The shortest intermolecular Au--Au distance is 6.959 Å. It should be noted that the packing of the triphenylphosphine and tri(*m*-tolyl)phosphine complexes is significantly less dense and leaves room for solvent inclusion.[172]

[180] Ehlich, H., Schier, A., Schmidbaur, H., Z. Naturforsch. **2002**, 57b, 890.

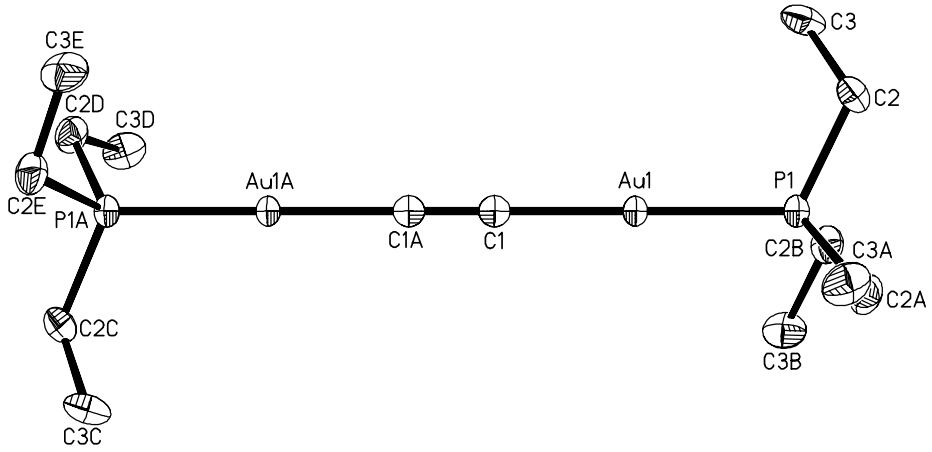

Figure 4-6. Molecular structure of [(Et_3P)AuC≡CAu(PEt_3)] (**8**) (ORTEP drawing with 50% probability ellipsoids, H-atoms omitted for clarity). Selected bond lengths [Å] and angles [°]: Au1-P1 2.283(2), Au1-C1 1.994(8), C1-C1A 1.21(2); P1-Au1-C1 180, Au1-C1-C1A 180.

The molecular axis comprising six atoms is linear with C≡C, C-Au and Au-P distances of 1.211(17), 1.994(8) and 2.283(2) Å, respectively. The Au-P-C angles are larger, the C-P-C angles smaller than the tetrahedral standard as observed for most metal complexes of tertiary phosphines.

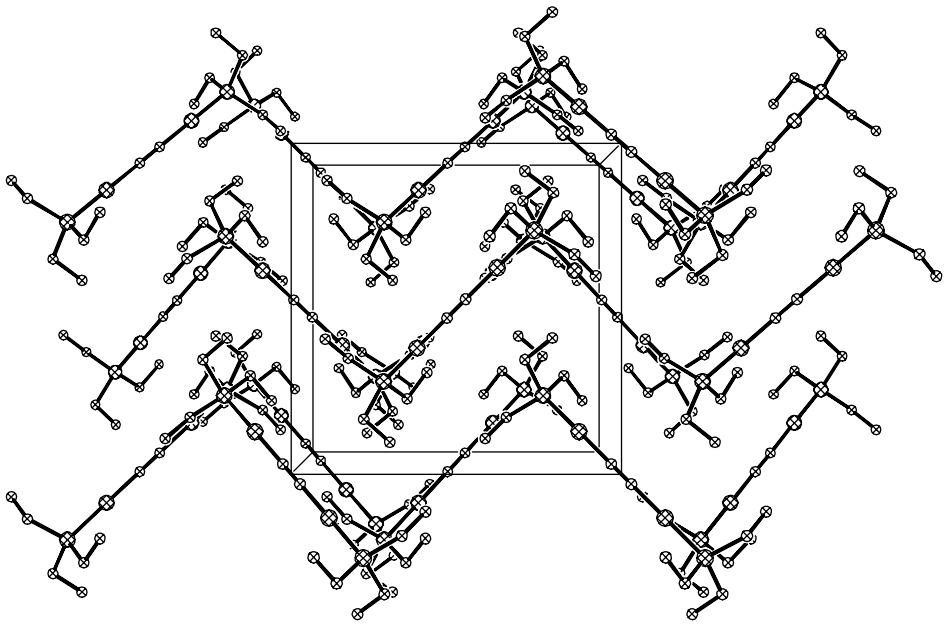

Figure 4-7. Packing of [(Et_3P)AuC≡CAu(PEt_3)] (**8**) in the cubic cell.

4.3.3 Characterization of Mono- and Bis(dimethylphenylphosphine)gold]-acetylene

$$(Me_2PhP)AuCl + C_2H_2 + EtONa \longrightarrow NaCl + EtOH + (Me_2PhP)AuC{\equiv}CH \quad (\mathbf{9})$$

$$(Me_2PhP)AuC{\equiv}CH + EtONa + (Me_2PhP)AuCl \longrightarrow NaCl + EtOH + (Me_2PhP)AuC{\equiv}CAu(PMe_2Ph) \quad (\mathbf{10})$$

For the reaction of $(Me_2PhP)AuCl$ and C_2H_2, both $(Me_2PhP)AuC{\equiv}CAu(PMe_2Ph)$ (**10**) (**Figure 4-9**) and the monosubstituted complex $(Me_2PhP)AuC{\equiv}CH$ (**9**) were identified and characterized. This is represented in **Table 4-4**.

Table 4-4. Characterization of $(Me_2PhP)AuC{\equiv}CH$ (9) and $(Me_2PhP)AuC{\equiv}CAu(PMe_2Ph)$ (10).

		$(Me_2PhP)AuC{\equiv}CH$ (**9**)	$(Me_2PhP)AuC{\equiv}CAu(PPhMe_2)$ (**10**)
Molecular weight (g/mol)		360.03	694.23
Substance		white solid	white solid
mp (°C)		157	181-182
MS (FAB) [m/z]	$[M+H]^+$	361.2	695.3
El.-anal. (cal. / found)	C		31.14/31.16
	H		3.19/3.27
	P		8.92/8.77
IR (Nujol) (cm^{-1})	ν(C≡C)	1963.6 1973.8	
	ν(CH) (AuC≡CH)	3274.6	
Raman (cm^{-1})	ν(C≡C)		1998.3
^{1}H-NMR (ppm)	$C\underline{H}_3$	1.73, d $^2J_{HP}$ = 7.6 Hz, 6H	1.73, d $^2J_{HP}$ = 7.6 Hz, 6H
	ArH	7.46-7.75, m 5H	7.46-7.75, m 5H
^{13}C(^{1}H-coupled)-NMR (ppm)	$\underline{C}H_3$	15.70, qdq $^1J_{CH}$ = 131.0 Hz $^1J_{CP}$ = 34.6 Hz $^3J_{CH}$ = 3.1 Hz	15.70, qdq $^1J_{CH}$ = 131.0 Hz $^1J_{CP}$ = 34.6 Hz $^3J_{CH}$ = 3.1 Hz
	C≡$\underline{C}$H	90.47,d $^1J_{CH}$ = 228.4 Hz	

	m-$C_{3/5}$	129.5, dd $^3J_{CP}$ = 10.8 Hz	129.5, dd $^3J_{CP}$ = 10.8 Hz
	p-C_4	131.7,dd $^4J_{CP}$ = 2.3 Hz	131.7, dd $^4J_{CP}$ = 2.3 Hz
	o-$C_{2/6}$	132.5, dd $^2J_{CP}$ = 13.1 Hz	132.5, dd $^2J_{CP}$ = 13.1 Hz
	i-C_1	134.2, d $^1J_{CP}$ = 53.0 Hz	134.2, d $^1J_{CP}$ = 53.0 Hz
	Au<u>C</u>≡CH	128.6, dd $^2J_{CH}$ = 143.4 Hz $^2J_{CP}$ = 38.7 Hz	
	Au<u>C</u>≡<u>C</u>Au		148.3, s
$^{31}P\{^1H\}$-NMR (ppm)		12.9, s	33.21, s
Crystal structure			zig-zag string

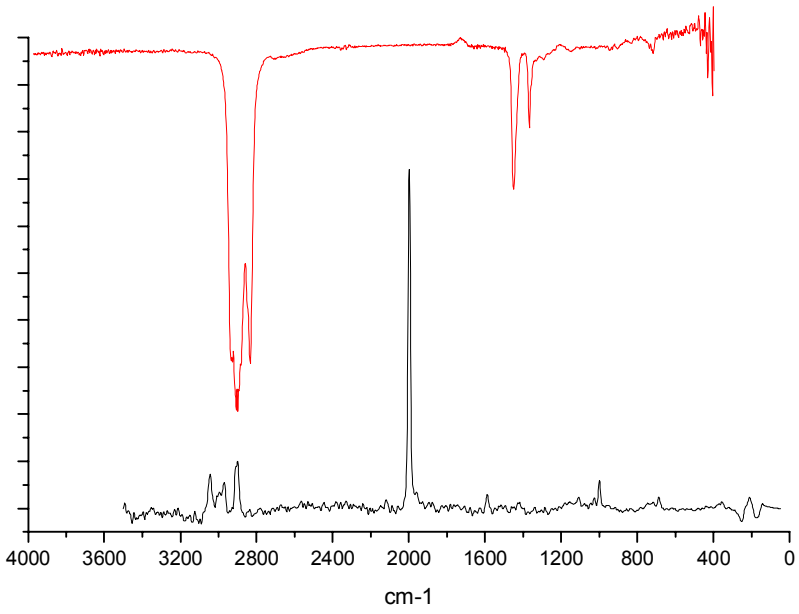

Figure 4-8: IR and Raman spectra (above and below, respectively) of bis[(dimethylphenylphosphine)gold]acetylene, [($PhMe_2P$)AuC≡CAuPMe_2Ph] (**10**).

Crystals of bis[(dimethylphenylphosphine)gold]acetylene, [(Me_2PhP)AuC≡CAu$P(PhMe_2)$], are orthorhombic, space group *Pbca*, with Z = 8 molecules in the unit cell. The individual molecule has no crystallographically imposed symmetry but approaches quite closely the requirements of point group C_2 (**Figure 4-9**). Its axis is puckered quite significantly with all its angles C1-C2-Au2 176.4(4), C2-C1-Au1 175.6(4), P1-Au1-C1 176.5(2), and P2-Au2-C2

173.0(1)° deviating markedly from 180°. The distances C1≡C2 1.216(7), Au1-C1 2.001(5), Au2-C2 2.011(5), Au1-P1 2.284(1), and Au2-P2 2.285(1) Å show no anomalies.

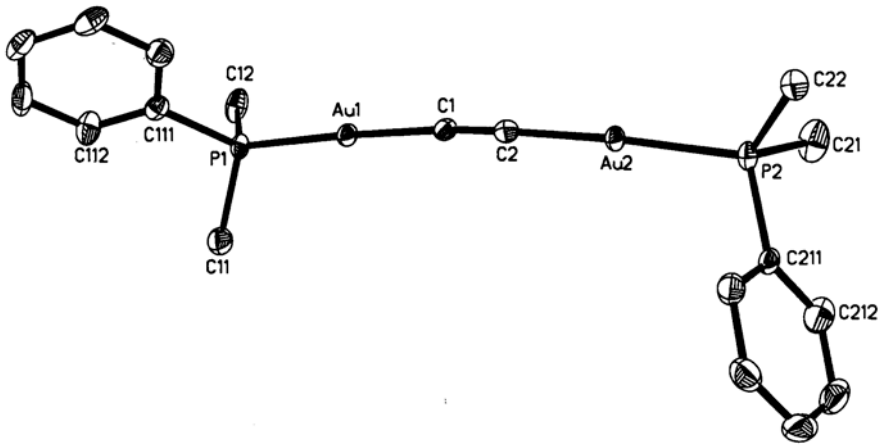

Figure 4-9. Molecular structure of compound [(Me_2PhP)AuC≡CAu($PPhMe_2$)] (**10**) (ORTEP drawing with 50% probability ellipsoids, H-atoms omitted for clarity). Selected bond lengths [Å] and angles [°]: Au1-P1 2.284(1), Au1-C1 2.001(5), C1-C2 1.216(7); Au2-P2 2.2849(1), Au2-C2 2.011(5); P1-Au1-C1 176.5(2), Au1-C1-C2 175.6(4), C1-C2-Au2 176.4(4), C2-Au2-P2 173.0(1).

Like the [(Me_3P)Au]$_2C_2$ molecules, the monomers of the Me_2PhP complex are also associated into zig-zag strings through head-to-tail aurophilic interactions [Au1--Au2' 3.1680(3) Å] (**Figure 4-10**). The projection of the chain along the b-axis of the crystal reveals a connectivity pattern very similar to that of the Me_3P analogue (**Figure 4-11**). The dihedral angle P1-Au1--Au2'-P2' is 112.0°.

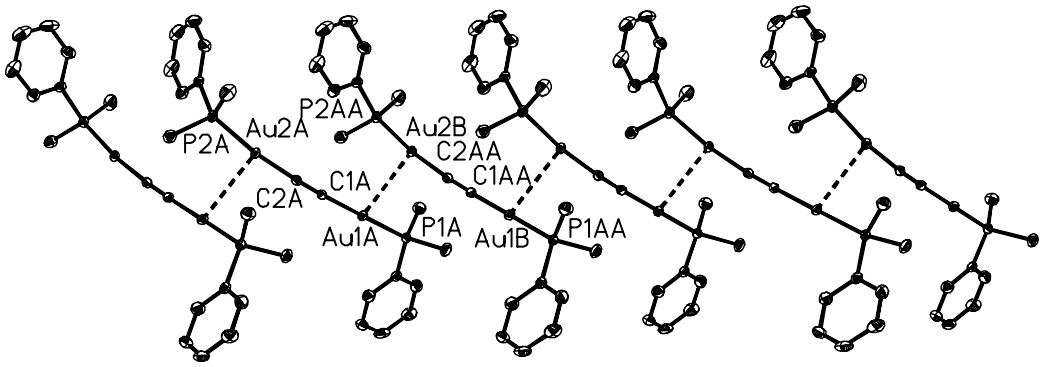

Figure 4-10. Zig-zag chain formation through head-to-tail aurophilic interaction between molecules [(Me_2PhP)AuC≡CAu($PPhMe_2$)] (**10**) [Au1···Au2 3.1680(3) Å].

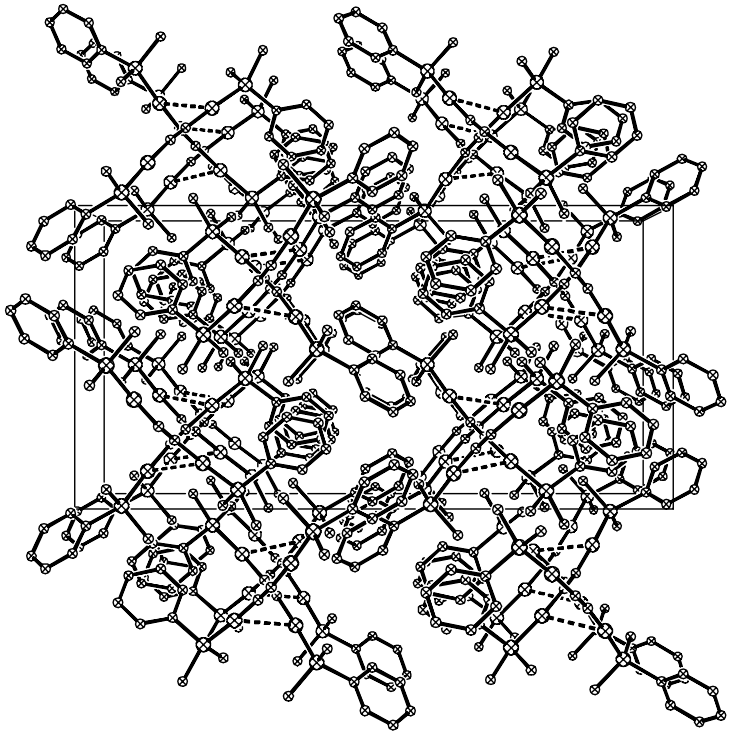

Figure 4-11. Projection of the chains of molecules [(Me_2PhP)AuC≡CAu($PPhMe_2$)] (**10**) along the b-axis of the orthorhombic cell.

4.3.4 Characterization of Mono- and Bis[(diphenylmethylphosphine)gold]-acetylene

$$(Ph_2MeP)AuCl + C_2H_2 + EtONa \longrightarrow NaCl + EtOH + (Ph_2MeP)AuC{\equiv}CH$$

(**11**)

$$(Ph_2MeP)AuC{\equiv}CH + EtONa + (Ph_2MeP)AuCl \longrightarrow$$

$$NaCl + EtOH + (Ph_2MeP)AuC{\equiv}CAu(PMePh_2)$$

(**12**)

For the reaction of (Ph_2MeP)AuCl and C_2H_2, both (Ph_2MeP)AuC≡CH (**11**) (**Figure 4-14**), and (Ph_2MeP)AuC≡CAu($PMePh_2$) (**12**) have been isolated and characterized. A comparison is drawn between the mono- and di-substituted complexes in **Table 4-5**.

Table 4-5. Characterization of $(Ph_2MeP)AuC{\equiv}CH$ (11) and $(Ph_2MeP)AuC{\equiv}CAu(PMePh_2)$ (12).

		$(Ph_2MeP)AuC{\equiv}CH$ (**11**)	$(Ph_2MeP)AuC{\equiv}CAu(PMePh_2)$ (**12**)
Molecular weight (g/mol)		422.20	818.39
Substance		white solid	white solid
mp (°C)		215	
MS (FAB) [m/z]	$[M+H]^+$	423.4	819.2
El.-anal. (cal. / found)	C	42.67/42.50	41.09/39.60
	H	3.34/3.32	3.20/3.18
	P	7.34/7.06	7.57/7.50
IR (Nujol) (cm^{-1})	ν(C≡C)	1978.5, w	
	ν(CH) (AuC≡CH)	3279.6, w	
Raman (cm^{-1})	ν(C≡C)	1981.8, s	2001.6, s; 1918.1
^{1}H-NMR (ppm)	AuC≡C<u>H</u>	1.62, s, 1H	
	C<u>H</u>$_3$	2.06, d $^2J_{HP}$ = 8.8 Hz, 3H	2.06, d $^2J_{HP}$ = 8.8 Hz
	Ph	7.45-7.63, m, 10H	7.45-7.63, m
^{13}C(^{1}H-coupled)-NMR (ppm)	<u>C</u>H$_3$	14.07, dq $^1J_{CH}$ = 132.8 Hz $^1J_{CP}$ = 34.5 Hz	15.70, qdq $^1J_{CH}$ = 131.0 Hz $^1J_{CP}$ = 34.6 Hz $^3J_{CH}$ = 3.1 Hz
	C≡<u>C</u>H	90.06, dd $^1J_{CH}$ = 228.6 Hz $^3J_{CP}$ = 2.3 Hz	
	m-$C_{3/5}$	129.34, dm $^1J_{CH}$ = 164 Hz	129.3, dm $^1J_{CH}$ = 164 Hz
	p-C_4	131.49, dt $^1J_{CH}$ = 138 Hz $^4J_{CP}$ = 7.0 Hz	131.5, dt $^1J_{CH}$ = 138 Hz $^4J_{CP}$ = 7.0 Hz
	i-C_1	132.16, d $^1J_{CP}$ = 54.6 Hz	132.2, d $^1J_{CP}$ = 54.6 Hz
	o-$C_{2/6}$	133.11 dm $^1J_{CH}$ = 153 Hz	133.1 dm $^1J_{CH}$ = 153 Hz
	Au<u>C</u>≡CH	127.85, d $^2J_{CP}$ = 39.7 Hz	147.4, br. s
^{31}P{^{1}H}-NMR (ppm)		26.08, s	27.53, s
Crystal structure		dimer	
Au--Au (Å)		3.0316(3)	

The IR spectrum of $(Ph_2MeP)AuC{\equiv}CH$ (**11**) exhibits characteristic bands at 1978.5 (w) cm^{-1}

ν(C≡C) and 3279.6 cm^{-1} for ν(CH) of -AuC≡CH. The Raman spectrum shows one peak at 1981.8 (s) cm^{-1} for ν(C≡C) (**Figure 4-12**).

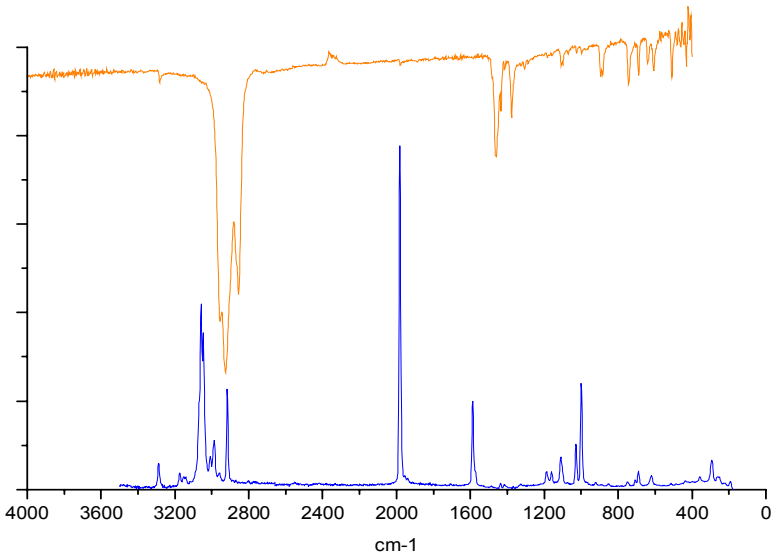

Figure 4-12. IR and Raman spectra (above and below, respectively) of [(methyldiphenyl-phosphine)gold]acetylene, [(Ph_2MeP)AuC≡CH] (**11**).

In comparison to the vibrational spectra of (Ph_2MeP)AuC≡CH (**11**), (Ph_2MeP)AuC≡CAu(P$MePh_2$) (**12**) exhibits only symmetric vibrational bands at 2001.6 (s) cm^{-1} and 1918.1 (w) cm^{-1} ν(C≡C) in the Raman spectrum (**Figure 4-13).**

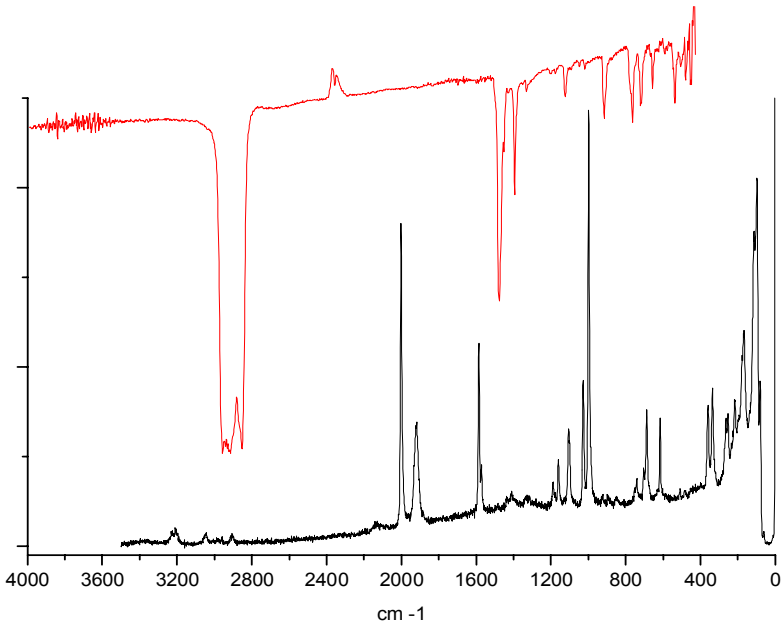

Figure 4-13. IR and Raman spectra (above and below, respectively) of bis[(methyldiphenylphosphine)gold]acetylene, [(Ph_2MeP)AuC≡CAu(P$MePh_2$)] (**12**).

Although analytical and spectroscopic data have shown that type **A** and **B** molecules are obtained in the reaction of $(MePh_2P)AuCl$ with acetylene in EtOH/EtONa, only [(methyldiphenylphosphine)gold]acetylene, $[(MePh_2P)Au]C{\equiv}CH$ (**11**), could be crystallized (monoclinic, space group *C*2/*c*, Z = 8). The asymmetric unit contains one molecule which is part of a dimer with the second molecule related by a two fold axis (**Figure 4-14**). The dimer features an aurophilic contact Au1--Au1' of 3.0316(3) Å and a dihedral angle P1-Au1--Au1'-P1' of 112.0(3)°. The packing of these dimers in the crystal shows no further sub-van-der-Waals contacts (**Figure 4-15**). The molecular axis P1-Au1-C1 is slightly bent [174.77(12)°]. The position of the acetylene hydrogen atom H1 was localized and its position refined with fixed isotropic parameters. The C≡C, Au-C and Au-P distances [1.187(6), 2.008(4) and 2.2812(9) Å, respectively] are all similar to those in the three compounds of type **A** (above) indicating that the structure of a $(R_3P)AuC{\equiv}CH$ unit is not influenced significantly by H/Au substitution at the other end of the acetylene group.

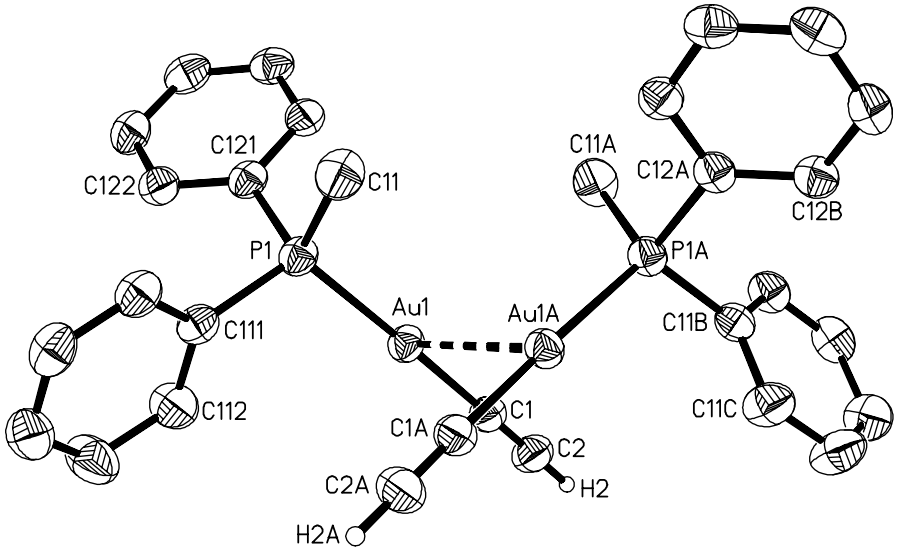

Figure 4-14. Dimeric units of $[(MePh_2P)AuC{\equiv}CH]$ (**11**) (ORTEP drawing with 50% probability ellipsoids, H-atoms omitted for clarity). Selected bond lengths [Å] and angles [°]: Au1-P1 2.2812(9), Au1-C1 2.008(4), C1-C2 1.187(6); Au1···Au1A 3.0316(3); P1-Au1-C1 174.8(1), Au1-C1-C2 178.9(4), P1-Au1-Au1A-P1A 112.0(3).

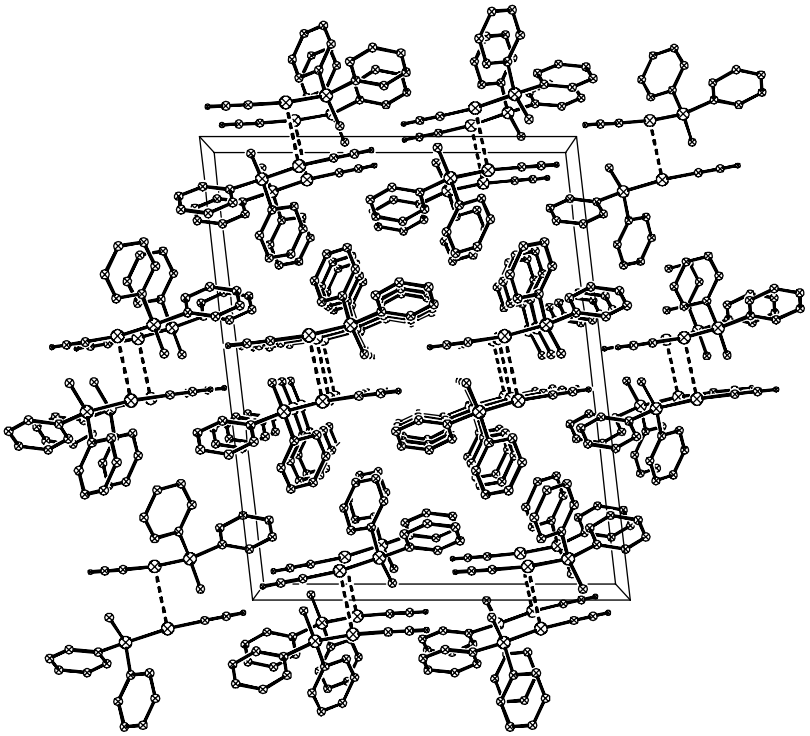

Figure 4-15. Projection along the chains of molecules [($MePh_2P$)AuC≡CH] (**11**) in the crystal.

4.3.5 Characterization of Mono- and Bis[(tri(*p*-tolyl)phosphinegold]acetylene

$$(p\text{-Tol})_3PAuCl + C_2H_2 + EtONa \longrightarrow NaCl + EtOH + (p\text{-Tol})_3PAuC{\equiv}CH \quad (\mathbf{13})$$

$$(p\text{-Tol})_3PAuC{\equiv}CH + EtONa + (p\text{-Tol})_3PAuCl \longrightarrow NaCl + EtOH + [(p\text{-Tol})_3PAuC{\equiv}CAuP(p\text{-Tol})_3] \quad (\mathbf{14})$$

Cross *et al.* first reported the above reaction in 1984 with a reaction time of 45 min at room temperature.[106] They detected no intermediate (p-Tol)$_3$PAuC≡CH (**13**). The diaurated [(p-Tol)$_3$PAuC≡CAuP(p-Tol)$_3$] (**14**) was characterized by elemental analysis and Raman spectroscopy. When the reaction was repeated in this work under similar conditions at room temperature, the resultant white compound was mixed with a black substance (colloidal gold). Therefore the reaction was carried out at low temperature (ca -60 °C) and following the addition the reaction mixture was allowed to warm to room temperature.

In contrast to the report of Cross *et al.* the major product of the reaction was the monoaurated complex (*p*-Tol)$_3$PAuC≡CH (**13**). The only evidence for the diaurated complex (**14**) was a very weak characteristic trace signal detected at δ_C = 147.86 ppm in the $^{13}C\{^1H\}$-NMR. The symmetric C≡C stretching vibration reported in Cross's work was not observed in the Raman spectrum of (**13**). A comparison is drawn between the mono- and di-substituted complexes in **Table 4-6**.

The IR spectrum of (*p*-Tol)$_3$PAuC≡CH (**13**) exhibits characteristic bands at 1978.5 (w) cm^{-1} for *ν*(C≡C) and 3279.6 cm^{-1} for *ν*(CH) of -AuC≡CH. The Raman spectrum shows one peak at 1981.8 (s) cm^{-1} for *ν*(C≡C) pertaining to -AuC≡CH (**Figure 4-16**).

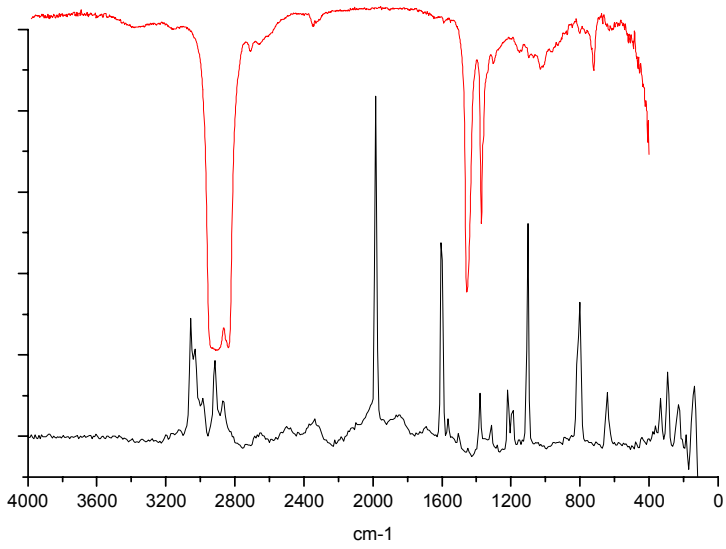

Figure 4-16. IR and Raman spectra (above and below, respectively) of [(tri(*p*-tolyl)phosphinephosphine)gold]acetylene, [(*p*-Tol)$_3$PAuC≡CH] (**13**).

The $^{31}P\{^1H\}$-NMR spectrum of the complex (**13**) shows a singlet signal at δ_P 40.45 at room temperature which shifts to δ_P 39.43 ppm (s) at -90 °C (**Figure 4-17**).

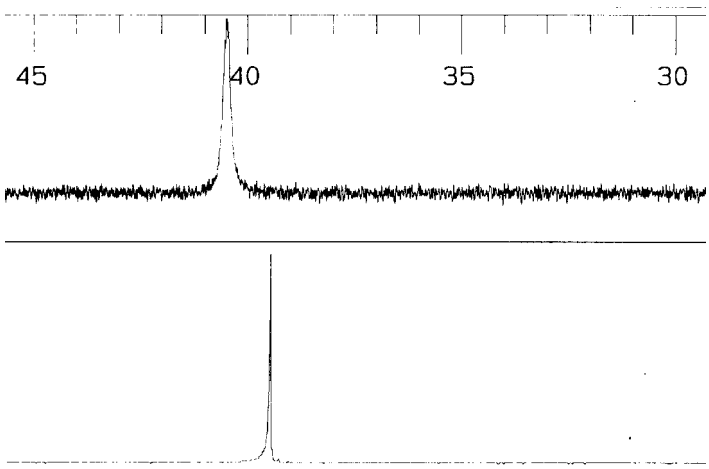

Figure 4-17. $^{31}P\{^{1}H\}$-NMR spectrum of [(*p*-Tol)$_3$P AuC≡CH] (**13**) measured at different temperatures (above: 20 ° C, δ_P 40.450 (s); below: -90 °C, δ_P 39.433 (s) in CD_2Cl_2).

The aromatic region of the $^{13}C\{^{1}H\}$-NMR shows only one group of signals both at room temperature and at low temperature (-90 °C) (**Figure 4-18, Figure 4-19**). At -90 °C the doublet signal for the carbon atoms of the monoaurated Au<u>C</u>≡CH unit was found at δ = 127.08 (d) with a characteristic coupling constant $^{2}J_{CP}$ = 139.0 Hz.

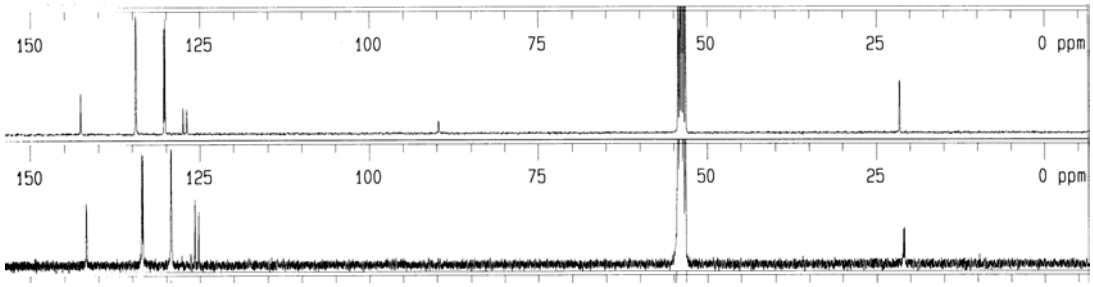

Figure 4-18. $^{13}C\{^{1}H\}$-NMR spectrum of [(*p*-Tol)$_3$PAuC≡CH] (**13**) measured at different temperatures (above: 23.9 ° C; below: -90 °C in CD_2Cl_2).

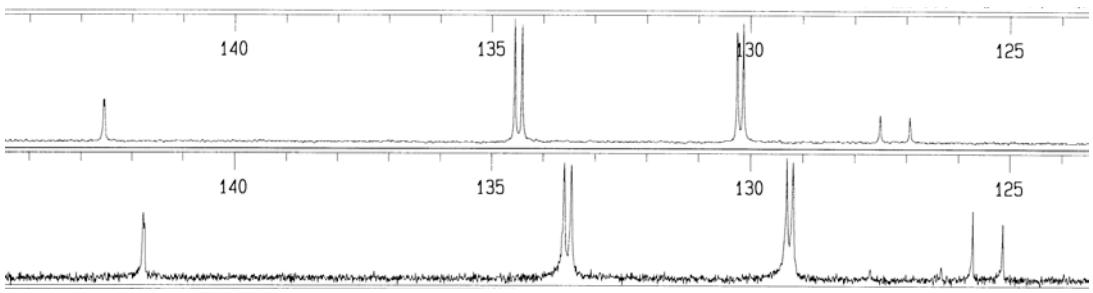

Figure 4-19. $^{13}C\{^{1}H\}$-NMR spectrum (aromatic region) of [(*p*-Tol)$_3$PAuC≡CH] (**13**) measured at different temperatures (above: 23.9 ° C; below: -90 °C in CD_2Cl_2).

In addition to the previous observation the signals of AuC≡CH (δ 89.747) and CH_3 (δ 21.541) were observed at -90 °C, AuC≡CH (δ = 89.7 ppm) and CH_3 (δ = 21.541 ppm, d, J = 20.9 Hz) (**Figure 4-20**), respectively.

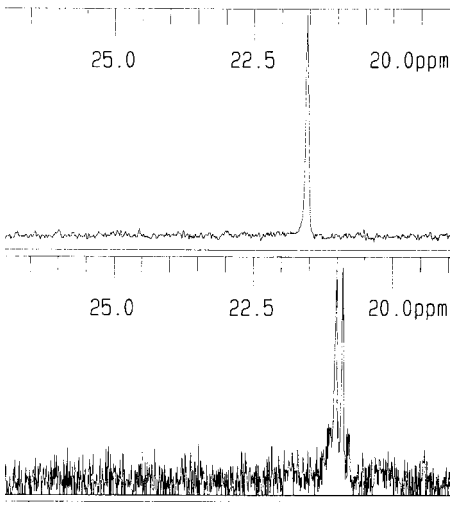

Figure 4-20. $^{13}C\{^1H\}$-NMR spectrum (-CH_3) of [(*p*-Tol)$_3$PAuC≡CH] (**13**) measured at different temperature (above: 23.9 ° C; below: -90 °C in CD_2Cl_2).

It was also observed in the proton NMR that there were two singlet resonances for the protons in the AuC≡CH unit at δ = 1.60 ppm (s) and 1.53 ppm (s) at RT with a difference of 27.4 Hz. At -90 °C two singlet resonances were observed at δ = 1.70 ppm (s) and 1.68 ppm (s) with a difference of 5.90 Hz. Because the splitting between the two signals varied according to temperature, these were not a doublet signal, which would have a fixed coupling constant. It was proposed that there were two different proton atoms in the AuC≡CH units with different chemical bonding environments.

Table 4-6. Characterization of (*p*-Tol)$_3$PAuC≡CH (13) and [(*p*-Tol)$_3$PAuC≡CAuP(*p*-Tol)$_3$] (14).

		(*p*-Tol)$_3$PAuC≡CH (**13**)	(*p*-Tol)$_3$PAuC≡CAuP(*p*-Tol)$_3$ (**14**)
Molecular weight (g/mol)		526.37	1026.70
Substance		white solid	
mp (°C)		145	
MS (FAB) [m/z]	$[M+H]^+$	527.4	1027.5
El.-anal. (cal. / found)	C	52.48/52.28	
	H	4.21/4.33	
	P	5.88/5.93	
IR (Nujol) (cm^{-1})	*ν*(CH) (AuC≡CH)	3275.5, vw	
Raman (cm^{-1})	*ν*(C≡C)	1981.8, s	2025[106]

^{1}H-NMR (ppm)	AuC≡C<u>H</u>	1.62, s, 1H	
	C<u>H</u>$_3$	2.36, s, 9H	
	m-<u>H</u>$_{3/5}$	7.25, dd $^{3}J_{HH}$= 8.1 $^{4}J_{HP}$= 1.8	
	o-<u>H</u>$_{2/6}$	7.42, dd $^{3}J_{HH}$= 8.1 $^{3}J_{HP}$= 13.3	
^{13}C(^{1}H-coupled)-NMR (ppm)	<u>C</u>H$_3$	21.52, qt $^{1}J_{CH}$= 127 Hz $^{3}J_{CH}$= 3.7 Hz	
	C≡<u>C</u>H	89.7, d $^{1}J_{CH}$ = 227 Hz	
	Au<u>C</u>	127.93	
	i-<u>C</u>$_1$	127.08, dt $^{1}J_{CP}$= 58.1 Hz $^{3}J_{CH}$= 8.30	
	m-<u>C</u>$_{3/5}$	130.06, ddq $^{1}J_{CH}$= 161.35 $^{3}J_{CP}$= 11.52 $^{3}J_{CH}$= 5.53	
	o-<u>C</u>$_{2/6}$	134.30, ddd $^{1}J_{CH}$= 163.19 $^{2}J_{CP}$=13.83 $^{3}J_{CH}$ = 6.45	
	p-<u>C</u>$_4$	142.3, s	
	Au<u>C</u>≡<u>C</u>Au		147.86
^{31}P{^{1}H}-NMR (ppm)		40.44	40.4 (in $CDCl_3$)[106]
Crystal structure		dimer	
Au--Au (Å)		3.0316(3)	

The complex [(tri(*p*-tolyl)phosphine)gold]acetylene, (*p*-Tol)$_3$PAuC≡CH (**13**), of type (**B**) crystallizes in the monoclinic space group $P2_1/c$, $Z = 8$ (**Figure 4-21**).

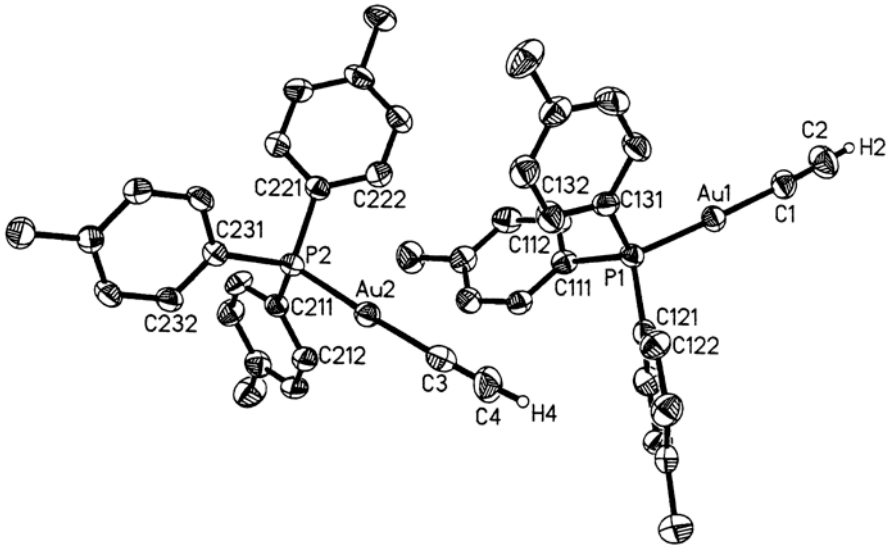

Figure 4-21. Dimeric units of [(*p*-Tol)$_3$PAuC≡CH] (**13**) (ORTEP drawing with 50% probability ellipsoids, H-atoms omitted for clarity). Selected bond lengths [Å] and angles [°]: Au1-P1 2.2812(9), Au1-C1 2.008(4), C1-C2 1.187(6); Au1···Au1A 3.0316(3); P1-Au1-C1 174.8(1), Au1-C1-C2 178.9(4), P1-Au1-Au1A-P1A 112.0(3).

The molecules are monomers in the crystal (**Figure 4-22**). The molecular axis P1-Au1-C1 has a angle of 176.91(17)°, which is closer to linearity compared to the slightly bent angle 174.8(1)° in complex (Ph$_2$MeP)AuC≡CH (**11**). Conversely the Au1-C1-C2 axis has an angle of 175.9(6)° in complex (**13**) and 178.9(4)° in complex (**11**). The C≡C, Au-C and Au-P distances are all similar to those of complex (**11**) of type **B** and those in the three compounds of type **A** (above). This indicates that the structure of a (R$_3$P)AuC≡CH unit is not influenced significantly by H/Au substitution at the other end of the acetylene group.

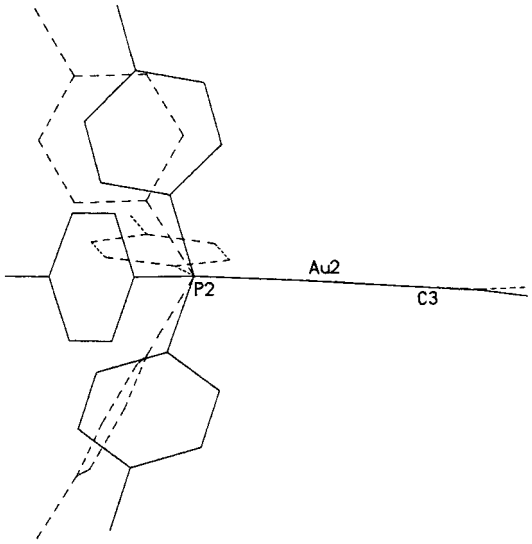

Figure 4-23. Superposition of the two monomers of [(*p*-Tol)$_3$PAuC≡CH] in the crystal (**13**).

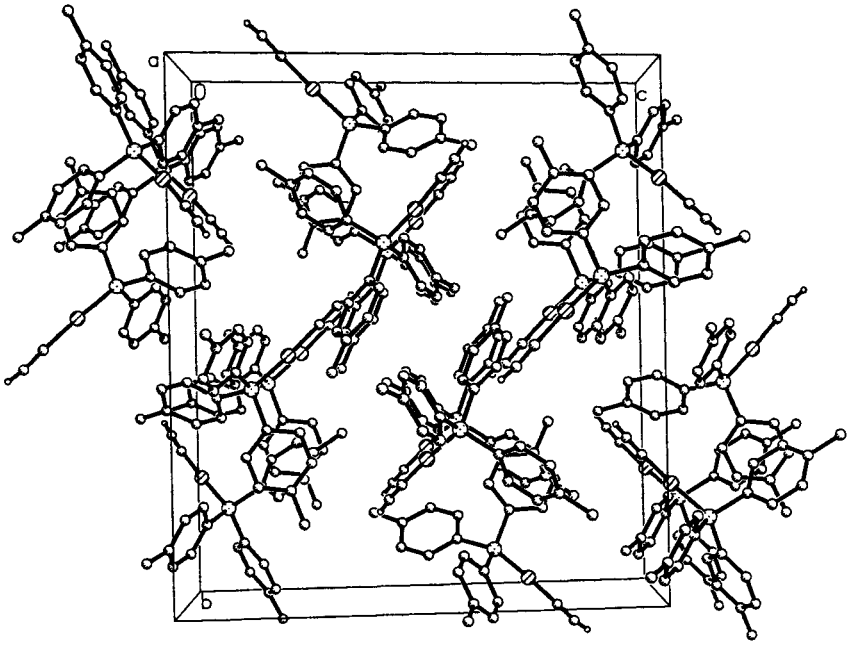

Figure 4-24. Projection of the unit cell of crystals of [(*p*-Tol)$_3$PAuC≡CH] (**13**).

4.4 Discussion and Summary

The aurophilic concept[178] suggests that mono- and dinuclear gold acetylide complexes LAuC≡CAuL (**A)** and LAuC≡CH (**B**, L = tertiary phosphine donor ligand) should have a rich supramolecular chemistry. The dinuclear species in particular are to be considered as rigid difunctional building blocks for the construction of oligo- or polymeric aggregates. All compounds of the type **A** reported in the literature were found to be monomers, however, probably owing to the presence of bulky ligands L. In the present works therefore complexes of gold acetylides with five different phosphine ligands featuring a variety of cone angles [PEt_3, PMe_3, PMe_2Ph, $PMePh_2$ and (*p*-Tol)$_3$P] were prepared and structurally characterized.

In this preparation product mixtures of types **A** and **B** were obtained and identified by the spectral data of the components. The prominent and least soluble complexes were isolated by fractional crystallization and their structures were determined.

The dinuclear complex with the larger phosphine (PEt_3) was found to be a monomer with a "weight-lifting gear" structure of D_3 symmetry. By contrast, the complex with the smallest phosphine (PMe_3) was shown to be a zig-zag chain polymer in which molecular units with inversion symmetries are linked in a head-to-tail pattern via aurophilic contacts [3.047(8) Å].

The folding of the chain arises from a dihedral angle P-Au--Au'-P' of 118.2° which minimizes steric interference of the PMe_3 ligands. A closely related structure has been found for the dimethylphenylphosphine complex (Me_2PhP) with the Au--Au contact slightly longer at 3.1680(3) Å and the dihedral angle P-Au--Au'-P' at 112.0°.

A similar angular unit is found for the complex [(Me_2PhP)AuC≡CH] of type **B** which forms dimers with an Au--Au' distance of 3.0316(3) Å and a dihedral angle of 111.7°. The dinuclear complex with PMe_2Ph ligands could not be crystallized. The observations made during the preparations suggest that efficient dimerization and/or low solubility of the mononuclear complexes (**B**) may retard the formation of the dinuclear complexes (**A**) quite considerably. This seems to be true for ($MePh_2$)AuC≡CH, which was obtained practically without any dinuclear by-product. By contrast, the reaction with [(Et_3P)Au]Cl under similar experimental conditions gave exclusively the dinuclear complex. The mononuclear complex (Et_3P)AuC≡CH is probably not associated into oligomers and therefore aurated further without steric hindrance. (*p*-Tol)$_3$PAuC≡CH (**13**) is a monomer in the crystal.

Generally, varying the phosphine did not influence the P-Au-C≡C unit. The Au-P and Au-C distances are found in the ranges 2.277(3) - 2.284(1) and 1.994(8)-2.011(5) Å, respectively, either for mono- and di-nuclear complexes. The C≡C distance was shown to be in the range 1.21(2) - 1.216(7) Å for dinuclear complexes of type **A** and 1.172(9) - 1.187(6) Å for mononuclear complexes of type **B**, respectively, and also within the range found previously for the types of **A** (see **Table 4-8**) and **C** (**Table 4-9**). The shortest C≡C bond length of type **A** was 1.13 (2) Å in (*m*-Tol)$_3$PAuC≡CAuP(*m*-Tol)$_3$ with no solvate molecules.[116] A comparison of the bond distances (Å) and angles (°) of LAuC≡CAuL (**A**) and LAuC≡CH (**B**) complexes of this work is shown in **Table 4-7**.

In summary it could be demonstrated that complexes of monogold and digold acetylide (AuC≡CH and AuC≡CAu) with small tertiary phosphine ligands undergo oligomerization to form dimers or polymers, respectively, through short-range aurophilic bonding. The compounds have a common structural pattern with very similar angular units in the dimers and in the zig-zag one-dimensional supramolecular aggregates. The energy associated with the aurophilic interactions is estimated to be of the order of 8 - 11 kcal,[178] comparable to the energy of hydrogen bonds. The Au--Au contacts are therefore significant in determining the solid state structure. The photophysical properties of the new compounds, under standard conditions and under pressure, are presently under investigation.

Table 4-7. Selected bond distances (Å) and angles (°) of LAuC≡CAuL (**A**) and LAuC≡CH (**B**) complexes of the present work.

	$Me_3PAuC{\equiv}CAuPMe_3$ (**6**)	$Et_3PAuC{\equiv}CAuPEt_3$ (**8**)	$Me_2PhPAuC{\equiv}CAuPPhMe_2$ (**10**)	$Ph_2MePAuC{\equiv}CH$ (**11**)	$(p\text{-Tol})_3PAuC{\equiv}CH$ (**13**)
Structure type	zig-zag chain	monomer	zig-zag chain	dimer	monomer
Au1--Au1'	3.0747(8)		3.1680(3)	3.0316(3)	
Au1-C1	2.010(10)	1.994(8)	2.001(5)	2.008(4)	2.006(6)
Au2-C2/Au2-C3			2.011(5)		2.006(6)
Au1-P1	2.277(3)	2.283(2)	2.284(1)	2.2812(9)	2.2804(14)
Au2-P2			2.285(1)		2.2856(14)
C1-C2	1.21(2)	1.21(2)	1.216(7)	1.187(6)	1.172(9)
C3-C4					1.171(9)
P1-Au1-C1	176.0(3)	180	176.5(2)	174.8(1)	176.91(17)
P2-Au2-C3					175.81(18)
Au1-C1-C2	177(1)	180	175,6(4)	178.9(4)	175.9(6)
Au2-C3-C4					176.3(6)
C1-C2-Au2			176.4(4)		
C2-Au2-P2			173.0(1)		
P1-Au1-Au2-P2	118.2(3)		112.0	112.0(3)	

Table 4-8. Selected bond distances (Å) from crystal structures of complexe of the type LAuC≡CAuL (**A**) in the literature.

	structure type		Au-C	Au-P	C1-C2	Ref.
$(m\text{-Tol})_3PAuC{\equiv}CAuP(m\text{-Tol})_3$	monomer		2.02(1)	2.270(4)	1.13(2)	Bruce 1988
$(m\text{-Tol})_3PAuC{\equiv}CAuP(m\text{-Tol})_3\cdot C_6H_6$	monomer		2.002(9)	2.284(3)	1.19(2)	Bruce 1988
$Ph_3PAuC{\equiv}CAuPPh_3\cdot 2C_6H_6$	monomer		2.00(1)	2.280(3)	1.19(2)	Bruce 1988
$NpPh_2PAuC{\equiv}CAuPPh_3Np\cdot 2CHCl_3$	monomer	C-H···π 2.41(2.42)	1.983(8)	2.277(2)	1.222(16)	Müller 1994
$Np_2PhPAuC{\equiv}CAuPPhNp_2\cdot 6CHCl_3$	monomer	C-H···π 2.50(2.58)	1.986(17)	2.289(5)	1.225(34)	Müller 1994
$Fc_2PhPAuC{\equiv}CAuPPhFc_2\cdot 4EtOH$	monomer	O-H···π 3.10	2.002(6)	2.276(2)	1.196(12)	Müller 1994

Table 4-9. Selected bond distances (Å) of crystal structures of compounds of the type LAuC≡CR' (**C**) in the literature.

	structure type	Au--Au	Au-C	Au-P	C1-C2	Ref.
$^{i}PrNH_2AuC{\equiv}CPh$	infinite zigzag chain	3.274 (3.722)	1.935(19)		1.210(28)	Cor-field 1967
$Ph_3PAuC{\equiv}CC_6F_5$	monomer	> 5.0	1.993 (14)	2.274(3)	1.197(16)	Bruce 1984
$Ph_3PAuC{\equiv}CPh$	dimer	3.379(1)	1.97(2) 2.02(2)	2.276(5) 2.282(4)	1.18(2) 1.16(2)	Bruce 1986
$Fc_2PhPAuC{\equiv}CPh$	monomer		2.011(15)	2.274(4)	1.172(21)	Müller 1994
$\{[Au(C{\equiv}C^{t}Bu)]_6\}_2$	interlocking rings	3.304 - 3.301				Mingos 1995

5 Studies of Addition Reactions of Gold Acetylide Complexes

5.1 Introduction

Alkyne complexes are coordination compounds which contain at least one alkyne function. Generally the coordination of an alkyne to a metal atom causes a change in hybridization at the alkyne carbon atoms from sp toward sp^2 hybridization.[181] Likewise it is proposed that alkynyl gold complexes could coordinate to gold(I) centers in one of the following ways.

(**I**): The gold alkynes can act as two-electron donors and bond to a gold atom side-on as a π-donor ligand.

(**II**): Alkynes can act as a ligand that accepts substantial electron density from the gold atom through back bonding to give a gold-cyclopropene type complex.

(**III**): If the gold atom is highly electron deficient, the alkyne ligands can act as four-electron donors.

(**IV**): Alkynes can also coordinate to two or more metals as a bridging ligand in a variety of coordination modes. The structure represents π coordination of an alkyne ligand to two metal fragments that are connected by a direct metal-metal bond.[181]

This present work focused on the coordination of mono- and digold-substituted alkynes with gold phosphine cations. The possible coordination types are shown in **Figure 5-1**.

As an example, the compound $[Au(C{\equiv}C^tBu)_6]_2$ was observed to show various coordination modes (η^1- η^1, η^1- η^2, η^2- η^2), which are stabilized by inter- and intramolecular Au--Au contacts at two interlocked rings (**Figure 1-18**).[182] The solvated digoldacetylide compounds e.g. $NpPh_2PAuC{\equiv}CAuPNpPh_2{\cdot}2CHCl_3$ (**Figure 1-26**) and $Np_2PhPAuC{\equiv}CAuPPhNp_2{\cdot}6CHCl_3$ (**Figure 1-27**) showed C-H···π interactions between the protons of the $CHCl_3$ molecules and the C≡C bond of the digoldacetylides.[108] In $NpPh_2PAuC{\equiv}CAuPNpPh_2{\cdot}2CHCl_3$ a pair of $CHCl_3$ molecules is located with their protons 2.4 Å from the center of the C≡C bond, and in $Np_2PhPAuC{\equiv}CAuPPhNp_2{\cdot}6CHCl_3$ two pairs of $CHCl_3$ molecules are located around the C≡C

[181] In Encyclopedia of inorganic chemistry, King, R. B., ed., John Willey & Sons Ltd., **1994**, 89.

[182] Mingos, D. M., Yau, J., Menzer, S., Williams, D. J., Angew. Chem. Int. Ed. Engl. **1995**, 64, 1894.

bond, with 2.5 Å between the proton and the center of the triple bond. A similar coordination of an external gold center toward the acetylene bond of the goldacetylide is expected in this investigation, referring to the isolobal relation between the H^+ and $[R_3PAu]^+$ cations.

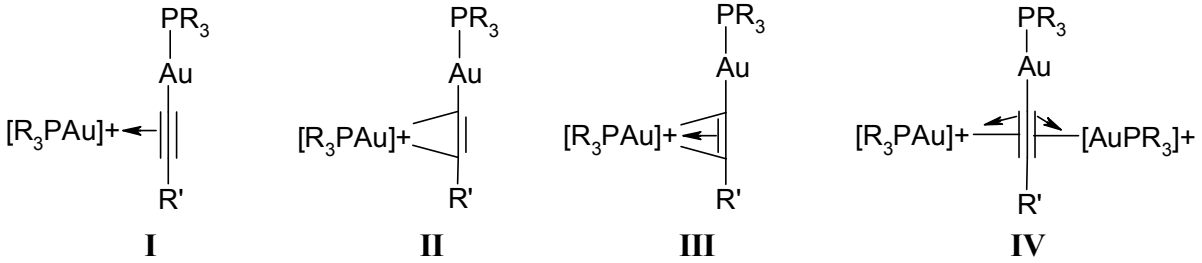

Figure 5-1. Possible coordination types of gold alkynes to gold acceptors $[R_3PAu]^+$. (R' = H for monoaurated alkyne, R' = $AuPR_3$ for diaurated alkyne)

5.2 Preparation

For the preparation of 1 : 1 adducts of types **I**, **II** or **III**, the mono- and digoldacetylide complexes, $(R_3P)AuC{\equiv}CAu(PR_3)$ (**A**) where R = Et and $(R_3P)AuC{\equiv}CH$ (**B**) where R = *p*-tol from Chapter 4 were treated with one equivalent of $[(R_3P)Au]X$ (X^- = BF_4^- or SbF_6^-). A 2 : 1 adduct of the type **IV** was prepared from the digoldacetylide complex $(R_3P)AuC{\equiv}CAu(PR_3)$ by treatment with two equivalents of $[(R_3P)Au]BF_4$, (R = Et) (Section 5.3.1.2).

The $[R_3PAu]X$ (X^- = BF_4^- or SbF_6^-) reagents were prepared by published procedures from the corresponding R_3PAuCl complexes. $[R_3PAu]Cl$ was reacted with $AgBF_4$ or $AgSbF_6$ in dichloromethane or tetrahydrofuran, respectively. Protection of the reaction vessel against incandescent light was required to avoid decomposition. The precipitated AgCl was separated from the reaction mixture by filtration and the clear filtrate was reacted with $(R_3P)AuC{\equiv}CAu(PR_3)$ (**A**) or $(R_3P)AuC{\equiv}CH$ (**B**) at -60 °C.

5.3 The reactions of $[(Et_3P)Au]BF_4$ with $(Et_3P)AuC{\equiv}CAu(PEt_3)$

5.3.1 Reaction conditions

The product obtained from the reaction described in Ch. 4.3.2, the dinuclear complex $(Et_3P)AuC{\equiv}CAu(PEt_3)$ (**8**), was chosen for further reaction with $[R_3PAu]X$ (X^- = BF_4^-).

A suspension of (triethylphosphine)gold chloride $[(Et_3P)Au]Cl$ was stirred with one equiva-

lent of $AgBF_4$ in THF at -60 °C. The reaction mixture was filtered into one equivalent $(Et_3P)AuC{\equiv}CAu(PEt_3)$ (**8**) in THF at -60 °C and the mixture stirred for a further 3 h. The solvent was evaporated under reduced pressure affording an orange solid (**15**) as illustrated in the following equations. Similarly a reaction in the ratio of 2 : 1 for $[(Et_3P)Au]Cl$ with $(Et_3P)AuC{\equiv}CAu(PEt_3)$ (**8**) was carried out to give the complex (**16**) as shown below.

$$(Et_3P)AuCl + AgBF_4 \longrightarrow [(Et_3P)Au]BF_4 + AgCl$$

$$(Et_3P)AuC{\equiv}CAu(PEt_3) + [(Et_3P)Au]BF_4 \longrightarrow$$

(**8**) $[(Et_3P)AuC{\equiv}CAu(PEt_3)]\cdot\{[(Et_3P)Au]BF_4\}$

(**15**)

$$(Et_3P)AuC{\equiv}CAu(PEt_3) + 2[(Et_3P)Au]BF_4 \longrightarrow$$

(**8**) $[(Et_3P)AuC{\equiv}CAu(PEt_3)]\cdot 2\{[(Et_3P)Au]BF_4\}$

(**16**)

5.3.1.1 Characterization of $[(Et_3P)AuC{\equiv}CAu(PEt_3)]\cdot[Et_3PAu]BF_4$ (15)

Elemental analysis and mass spectroscopy data of the compound resulting from the reaction of $(Et_3P)AuC{\equiv}CAu(PEt_3)$ (**8**) with one equivalent of $[(Et_3P)Au]BF_4$, were in good agreement with the calculated content of the complex $[(Et_3P)AuC{\equiv}CAu(PEt_3)]\cdot\{[(Et_3P)Au]BF_4\}$ (**15**). No asymmetric stretching frequencies of C≡C and CH (AuC≡CH) were detected in the IR spectrum, and in the Raman spectrum no ν(C≡C) line could be identified.

The $^{31}P\{^1H\}$-NMR spectrum of complex (**15**) showed two characteristic signals at shifts δ_P 34.525 and 47.615. This compares to one signal $\delta_P = 39.20$ in the $^{31}P\{^1H\}$-NMR spectrum of complex $(Et_3P)AuC{\equiv}CAu(PEt_3)$ (**8**) as shown in **Figure 5-2**.

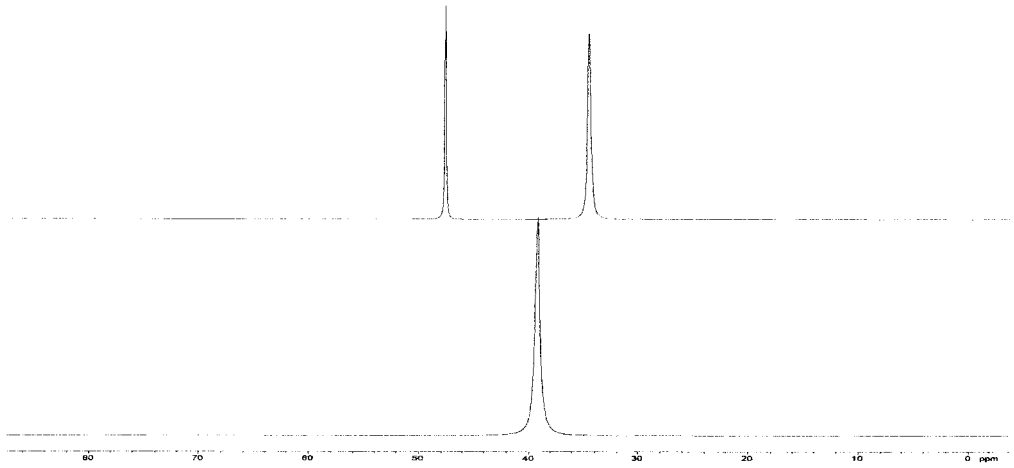

Figure 5-2. $^{31}P\{^{1}H\}$-NMR spectra of $[(Et_3P)AuC{\equiv}CAu(PEt_3)]\cdot[(Et_3P)Au]BF_4$ (**15**) (above) and $(Et_3P)AuC{\equiv}CAu(PEt_3)$ (**8**) (below) in CD_2Cl_2 at RT.

The ^{1}H signals for $C\underline{H}_2$ and $C\underline{H}_3$ of compound (**15**) were observed in the region (δ = 1.15 – 1.94 ppm) and were downfield shifted compared to the proton signals observed for $(Et_3P)AuC{\equiv}CAu(PEt_3)$ (**8**) (**Figure 5-3**). For the $C\underline{H}_2$-protons there were two groups of signals at different chemical shifts [1.883 ppm (dq) for the parent unit and 1.937 ppm (dq) for the ligand unit] with characteristic doublet of quartet coupling. This indicates two different environments for the ethyl groups, which is in agreement with the observations made in the $^{31}P\{^{1}H\}$-spectrum. The overlapping signals of the $C\underline{H}_3$-protons were observed at δ = 1.154 ppm (dt).

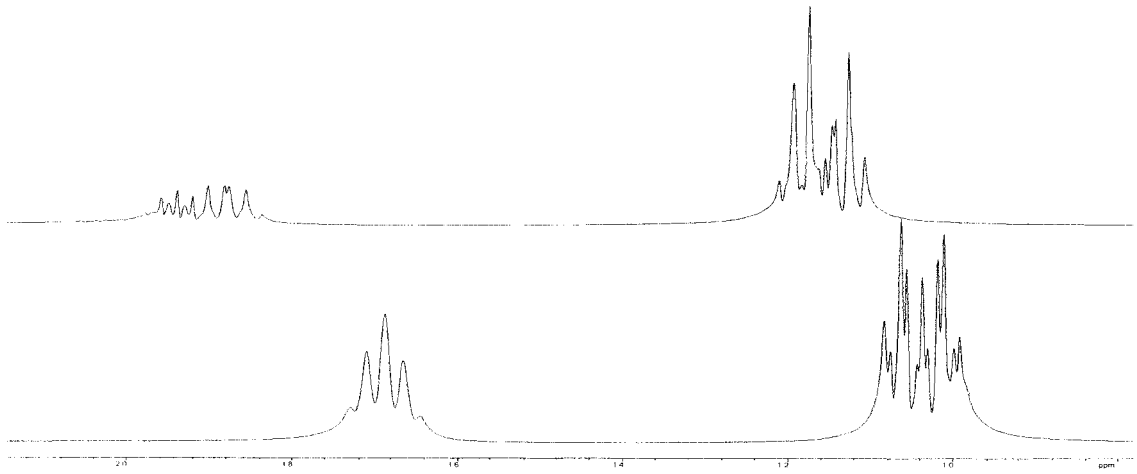

Figure 5-3. ^{1}H-NMR spectra of $[(Et_3P)AuC{\equiv}CAu(PEt_3)]\cdot[(Et_3P)Au]BF_4$ (**15**) (above) and $(Et_3P)AuC{\equiv}CAu(PEt_3)$ (**8**) (below) in CD_2Cl_2, RT.

Similarly two different groups of signals were observed for the $\underline{C}H_2$-and $\underline{C}H_3$-carbon atoms in

the $^{13}C(^{1}H$-coupled)-NMR, [8.969 ppm (qt) and 9.107 ppm (qt) for $\underline{C}H_3$; 17.210 ppm (tdq) and 17.788 ppm (tdq) for $\underline{C}H_2$-carbon atoms] (see **Figure 5-4**).

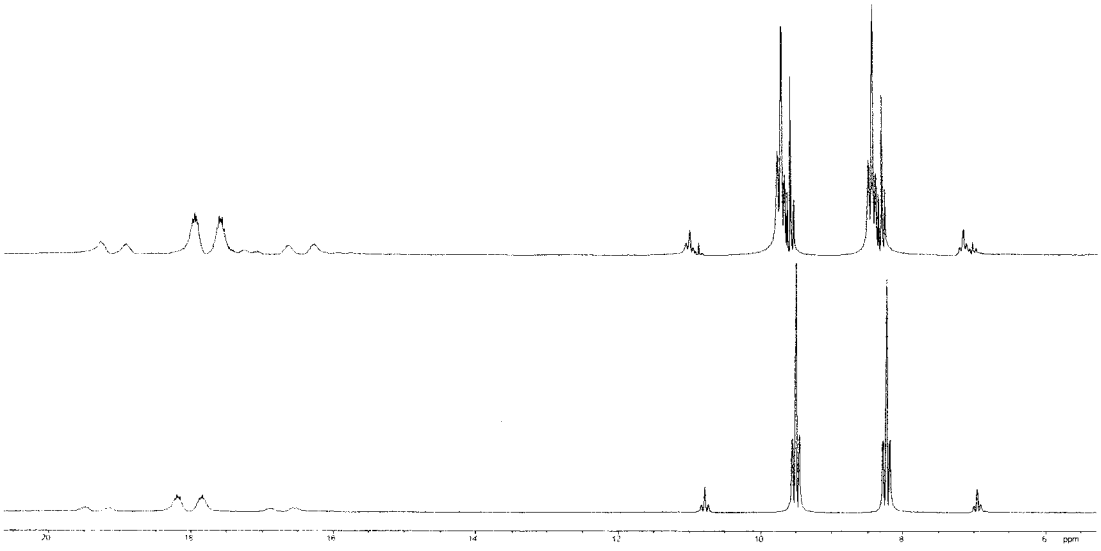

Figure 5-4. $^{13}C(^{1}H$-coupled)-NMR spectra (-$\underline{C}H_2$- and -$\underline{C}H_3$) of $[(Et_3P)AuC{\equiv}CAu(PEt_3)]\cdot[(Et_3P)Au]BF_4$ (**15**) (above) and $(Et_3P)AuC{\equiv}CAu(PEt_3)$ (**8**) (below) in CD_2Cl_2, RT.

For the carbon atoms of the $\underline{C}{\equiv}\underline{C}$ triple bond of complex (**15**) there was a strong signal identified at δ = 156.174 ppm, within the expected triple bond range for symmetrical diaurated alkynes (**Figure 5-5**). This signal is slightly shifted downfield in comparison to the chemical shift of the $\underline{C}{\equiv}\underline{C}$ resonance at δ = 150.0 ppm in the complex $(Et_3P)AuC{\equiv}CAu(PEt_3)$ (**8**). A very weak broad signal centered at δ = 149.516 ppm was observed as the residual signal of the starting material (**8**).

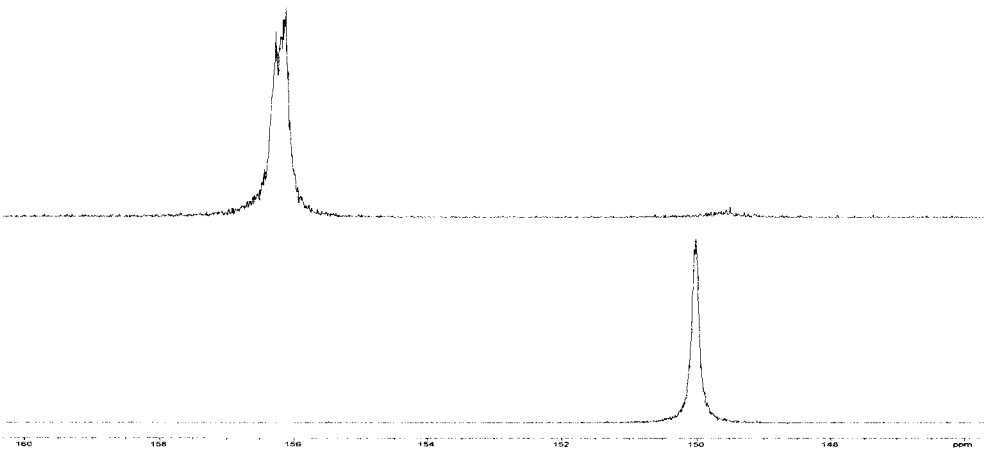

Figure 5-5. $^{13}C(^{1}H$-coupled)-NMR spectra (-Au$\underline{C}{\equiv}\underline{C}$Au-) of $[(Et_3P)AuC{\equiv}CAu(PEt_3)]\cdot[(Et_3P)Au]BF_4$ (**15**) (above) and $(Et_3P)AuC{\equiv}CAu(PEt_3)$ (**8**) (below) in CD_2Cl_2, RT.

The orange compound obtained from the reaction of diaurated $(Et_3P)AuC{\equiv}CAu(PEt_3)$ (**8**) with one equivalent of $[(Et_3P)Au]BF_4$ analyzed well for $[(Et_3P)AuC{\equiv}CAu(PEt_3)]{\cdot}\{[(Et_3P)Au]BF_4\}$ (**15**), but failed to give a suitable crystal for X-ray analysis. The following is a proposed structure for complex (**15**) (**Scheme 5-1**).

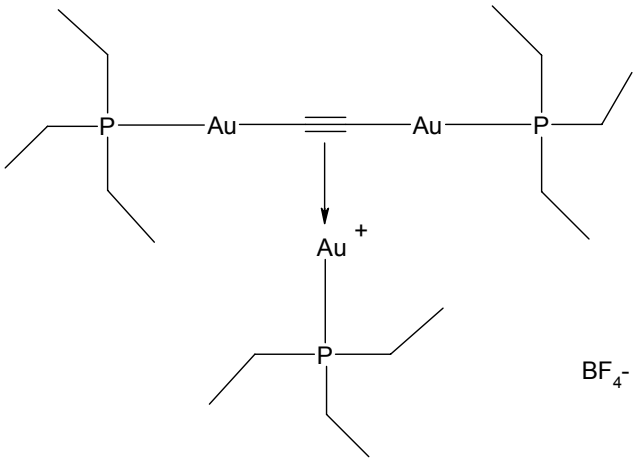

Scheme 5-1. Possible structure of $[(Et_3P)AuC{\equiv}CAu(PEt_3)]{\cdot}[(Et_3P)Au]BF_4$ (**15**).

5.3.1.2 Characterization of $[(Et_3P)AuC{\equiv}CAu(PEt_3)]{\cdot}2\{[Et_3PAu]BF_4\}$ (16)

The product of the reaction of $(Et_3P)AuC{\equiv}CAu(PEt_3)$ (**8**) with two equivalents of $[(Et_3P)Au]BF_4$ analyzed well for $[(Et_3P)AuC{\equiv}CAu(PEt_3)]{\cdot}2\{[(Et_3P)Au]BF_4\}$ (**16**). Comparison of the mass spectra of the complexes $(Et_3P)AuC{\equiv}CAu(PEt_3)$ (**8**) and $[(Et_3P)AuC{\equiv}CAu(PEt_3)]{\cdot}2\{[(Et_3P)Au]BF_4\}$ (**15**), showed significant differences, but the parent ion of (**15**) could not be detected. Likewise, C≡C stretching vibrations were not observed in the IR and Raman spectra.

The $^{31}P\{^1H\}$-NMR spectrum of complex (**16**) showed two characteristic peaks δ_P 36.098 ppm (s) and δ_P 47.468 ppm (s) in a ratio > 2 : 1, compared to the signals observed on complex (**8**) at δ_P = 39.20 and complex (**15**) at δ_P = 34.525 and 47.615. The integral ratio in (**15**) was ca. 2 : 1 for the signals at δ_P 34.525 and δ_P 47.615 (**Figure 5-6**). Accordingly, the chemical shift at δ_P 36.098 was assigned as the signal due to the phosphorus atom in the ligand unit $\{[(Et_3P)Au]BF_4\}$, and that at δ_P = 47.468 ppm was assigned as the contribution from the parent axle unit $[(Et_3P)AuC{\equiv}CAu(PEt_3)]$. Similarly, in the $^{31}P\{^1H\}$-NMR spectrum of the complex (**15**) the chemical shift at δ_P 34.525 (s) was assigned to the phosphorus atom in the ligand unit $\{[(Et_3P)Au]BF_4\}$, and that at δ_P = 47.615 ppm (s) to the parent axle unit $[(Et_3P)AuC{\equiv}CAu(PEt_3)]$.

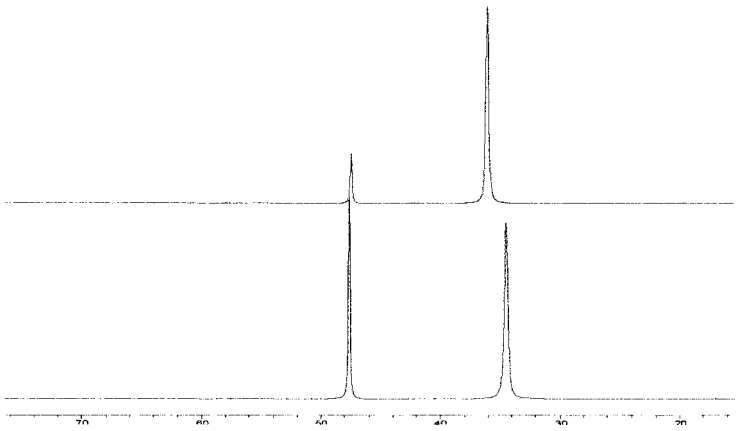

Figure 5-6. ^{31}P-NMR spectra of $[(Et_3P)AuC{\equiv}CAu(PEt_3)]\cdot 2\{[(Et_3P)Au]BF_4\}$ (**16**) (above) and $[(Et_3P)AuC{\equiv}CAu(PEt_3)]\cdot[(Et_3P)Au]BF_4$ (**15**) (below) in CD_2Cl_2, RT.

The signals in the proton NMR spectrum of compound (**16**) were observed to be only slightly downfield shifted compared to the corresponding signals of complex (**15**) (**Figure 5-7**). The C<u>H</u>$_3$-protons were observed in two groups of signals at different chemical shifts with characteristic doublet of quartet coupling at 1.192 ppm (dt) for the parent axle unit and at 1.203 ppm (dt) for the ligand unit, respectively. The signals of the C<u>H</u>$_2$-protons were observed overlapping at δ = 1.936 ppm (dq). This result was in agreement with the observations in the ^{31}P{^{1}H}-spectra.

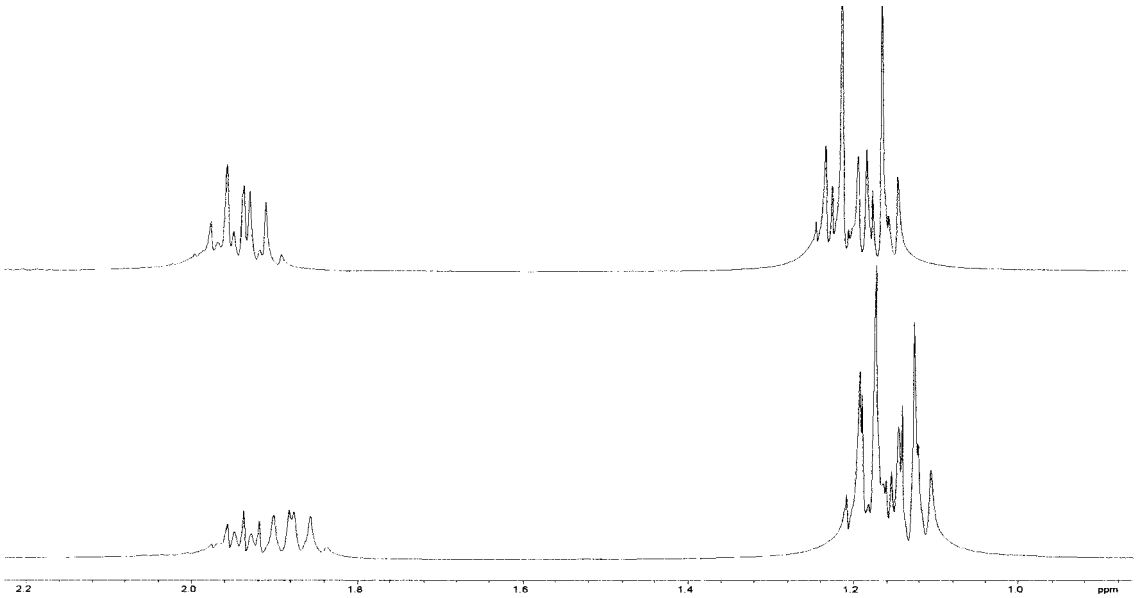

Figure 5-7. ^{1}H-NMR spectra (Et region) of $[(Et_3P)AuC{\equiv}CAu(PEt_3)]\cdot 2\{[(Et_3P)Au]BF_4\}$ (**16**) (above) and $[(Et_3P)AuC{\equiv}CAu(PEt_3)]\cdot[(Et_3P)Au]BF_4$ (**15**) (below) in CD_2Cl_2, RT.

Likewise two different signals were observed for each of the <u>C</u>H$_2$- and <u>C</u>H$_3$-carbon atoms in

the $^{13}C(^{1}H$-coupled)-NMR, [9.106 ppm (qt) and 9.391 ppm (qt) for $\underline{C}H_3$; 17.4 ppm (t) and 17.788 ppm (tdq) for $\underline{C}H_2$ (see **Figure 5-8** and **Figure 5-9**)].

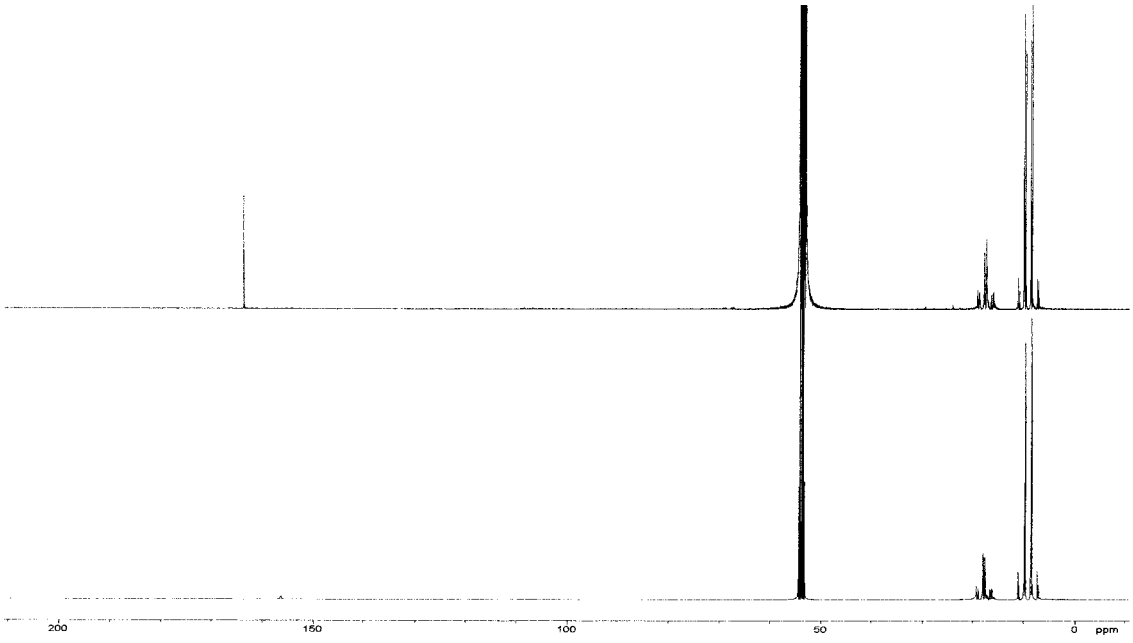

Figure 5-8. $^{13}C(^{1}H$-coupled)-NMR spectra of $[(Et_3P)AuC{\equiv}CAu(PEt_3)]\cdot 2\{[(Et_3P)Au]BF_4\}$ (**16**) (above) and $[(Et_3P)AuC{\equiv}CAu(PEt_3)]\cdot[(Et_3P)Au]BF_4$ (**15**) (below) in CD_2Cl_2, RT.

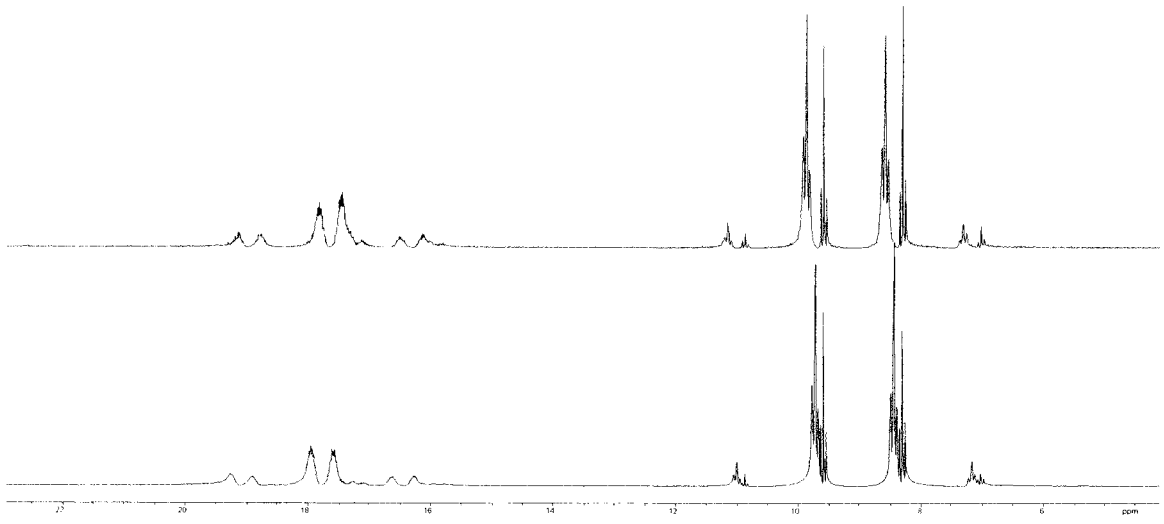

Figure 5-9. $^{13}C(^{1}H$-coupled)-NMR (-$\underline{C}H_2$- and -$\underline{C}H_3$) of $[(Et_3P)AuC{\equiv}CAu(PEt_3)]\cdot 2\{[(Et_3P)Au]BF_4\}$ (**16**) (above) and $[(Et_3P)AuC{\equiv}CAu(PEt_3)]\cdot[(Et_3P)Au]BF_4$ (**15**) (below) in CD_2Cl_2, RT.

A distinct single peak for the triple bond (C≡C) at δ = 163.970 ppm (s) was observed clearly downfield of the chemical shifts at δ = 156.174 ppm of the complex (**15**) and δ = 150.0 ppm of the complex (**8**).

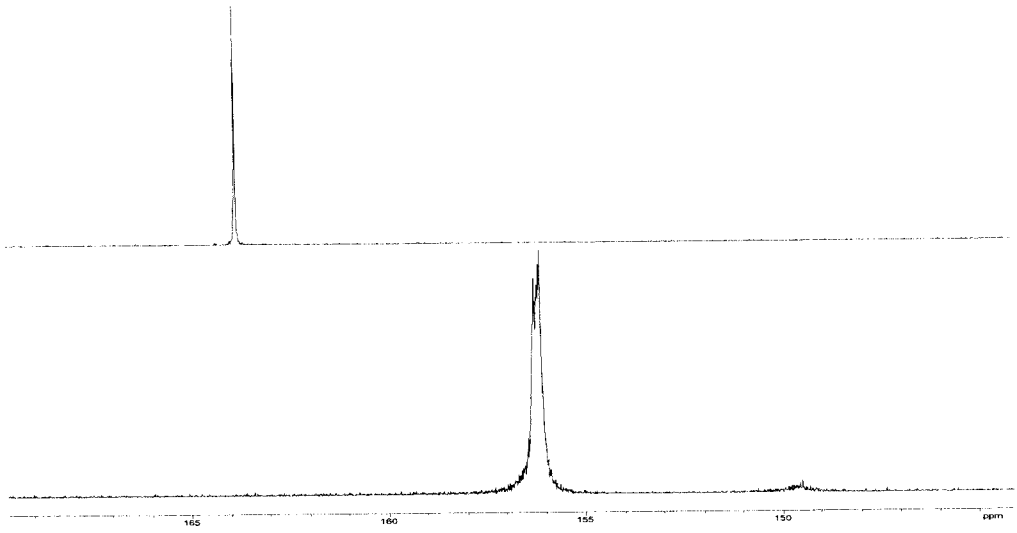

Figure 5-10. $^{13}C(^{1}H$-coupled)-NMR spectra (-AuC≡CAu-) of $[(Et_3P)AuC{\equiv}CAu(PEt_3)]\cdot 2\{[(Et_3P)Au]BF_4\}$ (**16**) (above) and $[(Et_3P)AuC{\equiv}CAu(PEt_3)]\cdot[(Et_3P)Au]BF_4$ (**15**) (below) in CD_2Cl_2, RT.

The orange compound obtained from the reaction of diaurated $(Et_3P)AuC{\equiv}CAu(PEt_3)$ (**8**) with two equivalents of $[(Et_3P)Au]BF_4$ analyzed well for $[(Et_3P)AuC{\equiv}CAu(PEt_3)]\cdot 2\{[(Et_3P)Au]BF_4\}$ (**16**), but failed to yield a suitable crystal for X-ray analysis. The following is a proposed structure for complex (**16**) (**Scheme 5-2**).

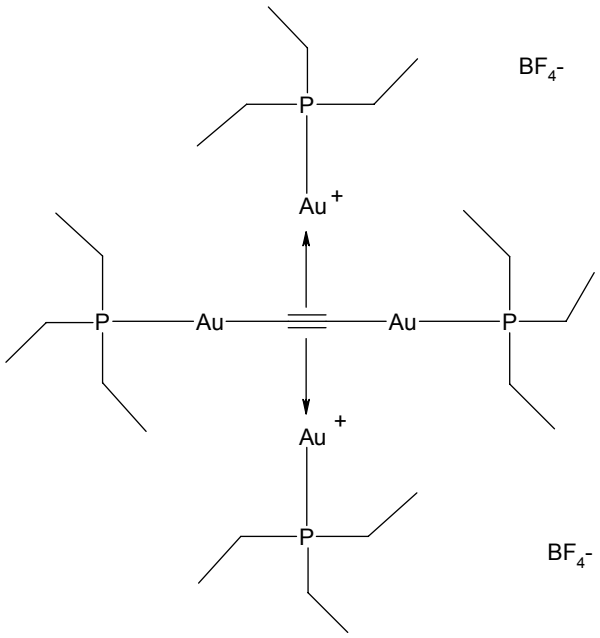

Scheme 5-2. Possible structure of $(Et_3P)AuC{\equiv}CAu(PEt_3)\cdot 2\{[(Et_3P)Au]BF_4\}$ (**16**).

5.4 Reaction of $(p\text{-Tol})_3PAuC{\equiv}CH$ and $[(p\text{-Tol})_3PAu]BF_4$

The product obtained from the reaction described in Ch. 4.3.5 was the mononuclear complex $(p\text{-Tol})_3PAuC{\equiv}CH$ (**13**). This complex was chosen for further reaction with $[(p\text{-Tol})_3PAu]X$ ($X^- = BF_4^-$ and SbF_6^-).

A suspension of [(tri(*p*-tolyl)phosphine]gold chloride $[(p\text{-Tol})_3PAu]Cl$ was reacted with one equivalent of $AgBF_4$ in dichloromethane at -60 °C. The reaction mixture was filtered into one equivalent of $(p\text{-Tol})_3PAuC{\equiv}CH$ (**13**) in dichloromethane at -60 °C and the mixture was stirred for a further 3 h. The solvent was evaporated under reduced pressure affording complex (**17**) as an orange solid as formulated in the following equation.

$$(p\text{-Tol})_3PAuCl + AgBF_4 \longrightarrow [(p\text{-Tol})_3PAu]BF_4 + AgCl$$

$$(p\text{-Tol})_3PAuC{\equiv}CH + [(p\text{-Tol})_3PAu]BF_4 \longrightarrow$$

(**13**) $[(p\text{-Tol})_3PAuC{\equiv}CH]\cdot\{[(p\text{-Tol})_3P\ Au]BF_4\}$ (**17**)

5.4.1 Characterization of $[(p\text{-Tol})_3PAuC{\equiv}CH]\cdot\{[(p\text{-Tol})_3PAu]BF_4\}$ (17)

The $^{31}P\{^1H\}$-NMR spectrum of complex (**17**) showed two characteristic signals at chemical shifts at δ_P 40.61 and δ_P 32.11 ppm at room temperature in CD_2Cl_2. Both signals were slightly broadened at RT, but at -90 °C sharpened to 39.41 ppm (s) and 31.21 ppm (s), respectively. The chemical shifts for the starting reagents $(p\text{-Tol})_3PAuC{\equiv}CH$ (**13**) and $[(p\text{-Tol})_3PAu]Cl$ in CD_2Cl_2 at -90 °C were δ_P 40.4 and δ_P 31.6 respectively (**Figure 5-11**). The chemical shift at 40.608 ppm at RT therefore can be assigned to the phosphorus atom of the $(p\text{-Tol})_3PAuC{\equiv}CH$ unit and the shift of $\delta_P = 32.108$ to the phosphorus atom of the $[(p\text{-Tol})_3PAu]BF_4$ unit.

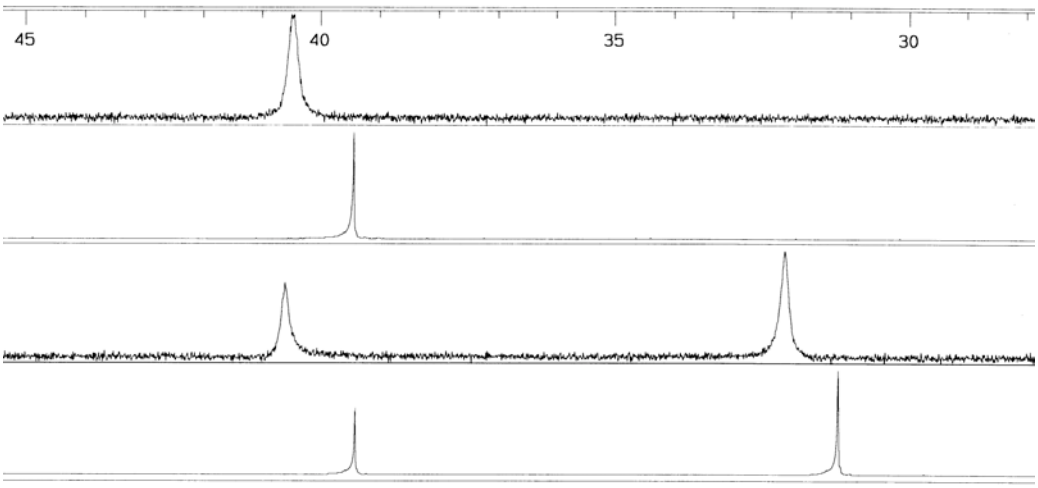

Figure 5-11. Comparison of the $^{31}P\{^{1}H\}$-NMR spectra of [(*p*-Tol)$_3$PAuC≡CH] (**13**) and [(*p*-Tol)$_3$PAuC≡CH]·{[(*p*-Tol)$_3$PAu]BF_4} (**17**) measured at different temperatures [from top to botton: (**13**) 20.0 ° C, 40.45ppm; (**13**) -90 °C, 39.433 ppm; (**17**) 24.7 °C, 40.61 and 32.11 ppm, and (**17**) -90 °C, 39.410 and 31.21 ppm, all measured in CD_2Cl_2].

The aromatic region of the $^{13}C\{^{1}H\}$-NMR of complex (**17**) showed only one group of signals at room temperature, which split into two groups of signals for the different (*p*-Tol)$_3$P units at -90 °C (**Figure 5-12**).

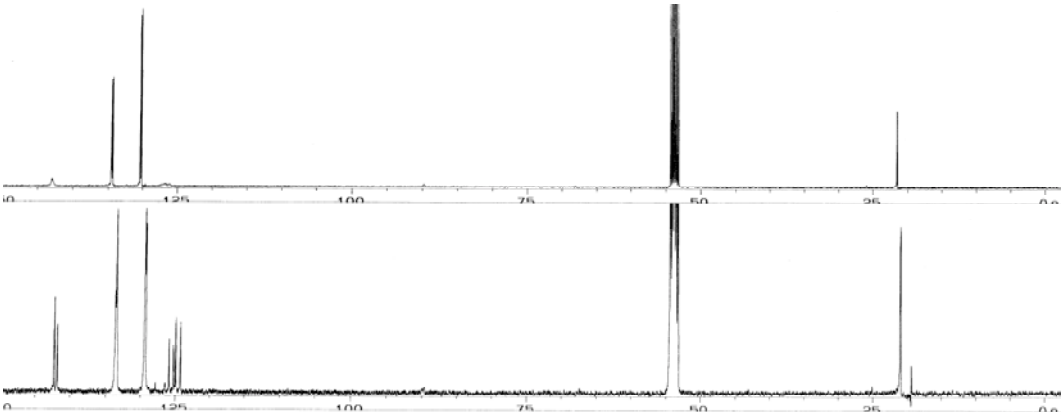

Figure 5-12. $^{13}C\{^{1}H\}$-NMR spectra of [(*p*-Tol)$_3$PAuC≡CH]·{[(*p*-Tol)$_3$PAu]BF_4} (**17**) measured at different temperature (above: 23.9 ° C; below: -90 °C in CD_2Cl_2).

The signal at 127.074 ppm (d) with $^{2}J_{CP}$= 139.7 Hz at -90 °C was easily characterized as belonging to the the carbon atom of the Au<u>C</u>≡CH unit (**Figure 5-13**). The corresponding chemical shift for the terminal carbon atom in the AuC≡<u>C</u>H unit was found at 89.723 ppm (m) at RT, together with weak signals near 89.818 ppm (m) at -90 °C (**Figure 5-14**).

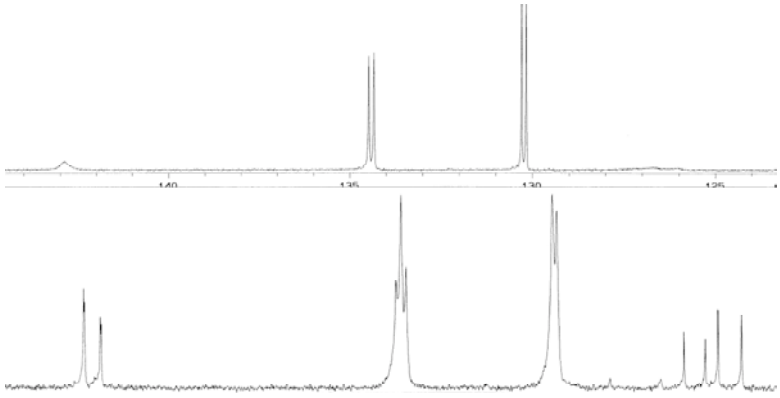

Figure 5-13. $^{13}C\{^{1}H\}$-NMR spectra (aromatic region) of $[(p\text{-Tol})_3PAuC{\equiv}CH]\cdot\{[(p\text{-Tol})_3PAu]BF_4\}$ (**17**) measured at different temperature (above: 23.9 ° C; below: -90 °C in CD_2Cl_2).

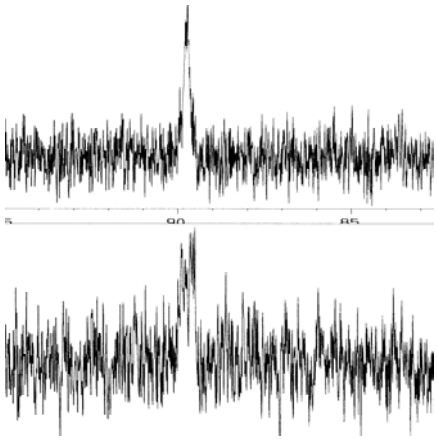

Figure 5-14. $^{13}C\{^{1}H\}$-NMR spectra (Au$C{\equiv}\underline{C}$H) of $[(p\text{-Tol})_3PAuC{\equiv}CH]\cdot\{[(p\text{-Tol})_3PAu]BF_4\}$ (**17**) measured at different temperature (above: 23.9 ° C; below: -90 °C in CD_2Cl_2).

For the $\underline{C}H_3$ carbon atom, two signals were observed at RT (δ = 21.572 and 21.557 ppm with a difference of 1.6 Hz), but at -90 °C only one major resonance at 20.974 ppm was left shifted, slightly upfield (**Figure 5-15**).

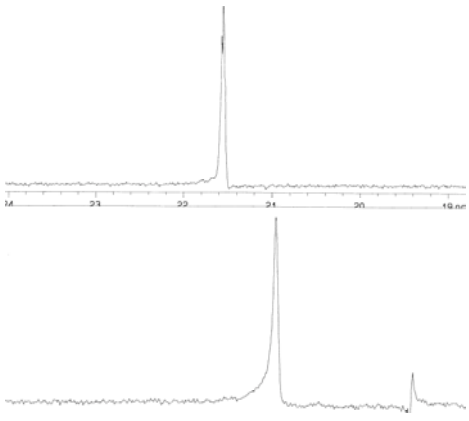

Figure 5-15. $^{13}C\{^{1}H\}$-NMR spectra (-$\underline{C}H_3$) of $[(p\text{-Tol})_3PAuC{\equiv}CH]\cdot\{[(p\text{-Tol})_3PAu]BF_4\}$ (**17**) measured at different temperature (above: 23.9 ° C; below: -90 °C in CD_2Cl_2).

The ^{1}H-NMR spectrum showed one doublet resonance for the AuC≡C<u>H</u> unit of complex (**17**) at 1.659 ppm with a coupling constant J of 5.88 Hz at RT. For the C<u>H</u>$_3$ proton atoms there was one singlet resonance at 2.32 ppm at RT, near the signal at 2.297 ppm for the C<u>H</u>$_3$ group of complex (**13**) at RT.

There is no significant difference between the spectra of complex (**17**) and the starting material at RT and low temperature. At low temperature (-90 °C) the NMR spectrum of the complex (**17**) showed well defined signals. The variable temperature NMR indiciates fluxionality at room temperature relative to the NMR timescale which is suppressed on cooling. It therefore appears that there is no reaction between the components, other than reversible ligand exchange.

5.5 Reaction of (*p*-Tol)$_3$PAuC≡CH and [(*p*-Tol)$_3$PAu]SbF$_6$

A suspension of [(tri(*p*-tolyl)phosphine]gold chloride [(*p*-Tol)$_3$PAu]Cl with one equivalent of $AgSbF_6$ in dichloromethane was stirred at -60 °C. The reaction mixture was filtered into one equivalent of (*p*-Tol)$_3$PAuC≡CH (**13**) in dichloromethane at -60 °C and the mixture stirred for 3 h. The solvent was evaporated under reduced pressure affording complex (**18**) as an orange solid, shown in the following equations.

$$(p\text{-Tol})_3\text{P AuCl} + \text{AgSbF}_6 \longrightarrow [(p\text{-Tol})_3\text{PAu}]\text{SbF}_6 + \text{AgCl}$$

$$(p\text{-Tol})_3\text{PAuC}{\equiv}\text{CH} + [(p\text{-Tol})_3\text{PAu}]\text{SbF}_6 \longrightarrow$$

(**13**) $[(p\text{-Tol})_3\text{PAuC}{\equiv}\text{CH}]\cdot\{[(p\text{-Tol})_3\text{PAu}]\text{SbF}_6\}$ (**18**)

5.5.1 Characterization of [(*p*-Tol)$_3$PAuC≡CH]·{[(*p*-Tol)$_3$PAu]SbF$_6$} (18)

The stretching band *v*(CH) of (AuC≡CH) for compound (**18**) was observed at 3190.9 cm^{-1} in the IR spectrum. In the Raman spectrum only broad signals were observed over the whole spectrum and no characteristic peaks could be identified.

The ^{31}P{^{1}H}-NMR spectrum of complex (**18**) showed one sharp signal at δ_P 44.17 and one broad signal at δ_P 35.67 ppm at room temperature in CD_2Cl_2. On cooling the peak at δ_P 44.17 ppm was shifted upfield to δ_P 42.64 ppm at -90 °C. The peak at δ_P 35.67 ppm slowly disap-

peared and a new peak appeared at δ_P 31.75 ppm below -10 °C. With further cooling below -60 °C the broad peak totally disappeared with concomitant sharpening of the peak at δ_P 31.19 (**Figure 5-16**). The chemical shift for the peak at 31.75 is assumed to pertain to the [(*p*-Tol)$_3$PAu]SbF$_6$ unit, while the chemical shifts for the peaks at δ_P 42.64 is assigned to the [(*p*-Tol)$_3$PAuC≡CH unit. In comparison with the pure complex (*p*-Tol)$_3$PAuC≡CH (**13**) the phosphorus-NMR signals were not very different [δ_P 40.45 (at 20 °C) and δ_P 39.43 (-90 °C)]. It therefore appears that [(*p*-Tol)$_3$PAu]SbF$_6$ and (*p*-Tol)$_3$PAuC≡CH (**13**) give no reaction.

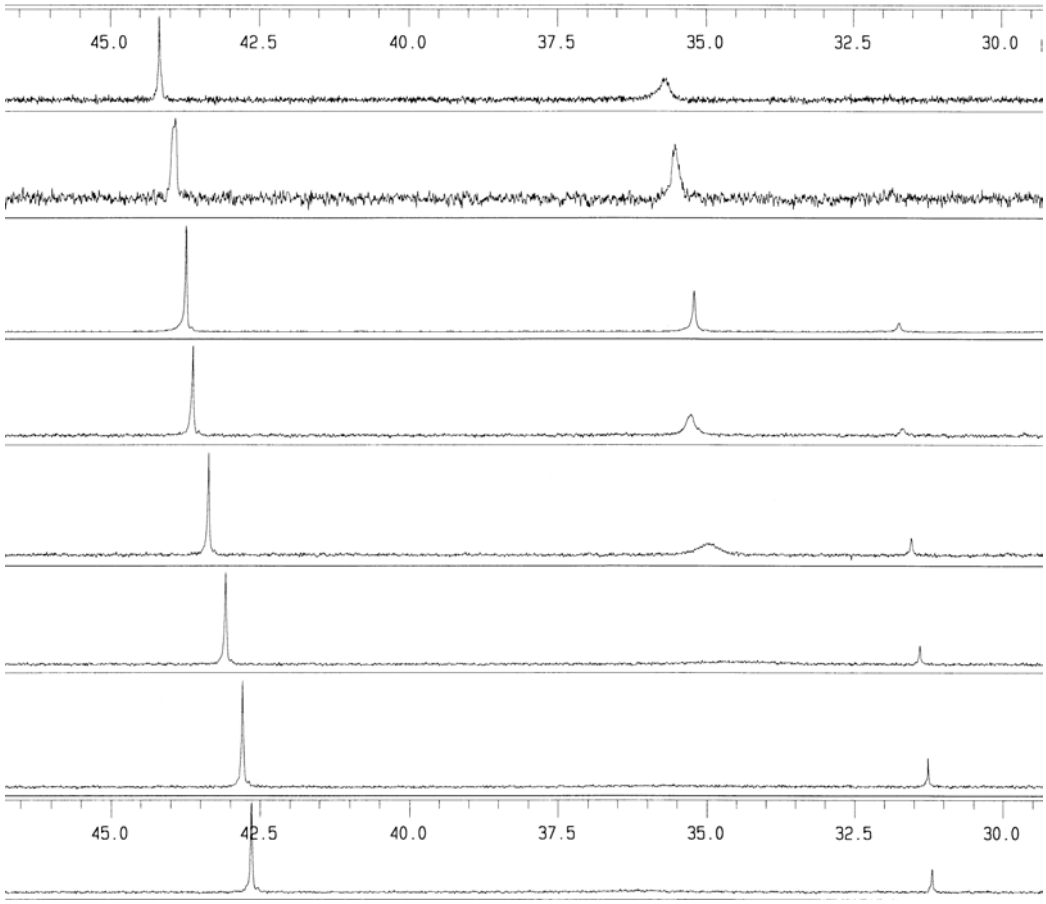

Figure 5-16. Dynamic $^{31}P\{^1H\}$-NMR spectra of [(*p*-Tol)$_3$PAuC≡CH]·{[(*p*-Tol)$_3$PAu]SbF$_6$} (**18**) measured at different temperature (from top to botton: 25 °C, 44.17 and 35.67 ppm; 0 °C, 43.91, 35.53 ppm; -10 °C, 43.74, 35.21, 31.75 ppm; -20 °C, 43.62, 35.21, 31.69 ppm; -40 °C, 43.35, 35.00, 31.54 ppm; -60 °C, 43.07, 34.63, 31.39 ppm; -80 °C, 42.79, 31.26 ppm; -90 °C, 42.64 and 31.20 ppm in CD_2Cl_2).

The $^{13}C\{^1H\}$-NMR spectra of complex (**18**) showed two separate sets of signals for two different [(*p*-Tol)$_3$PAu] units at room temperature (**Figure 5-17**).

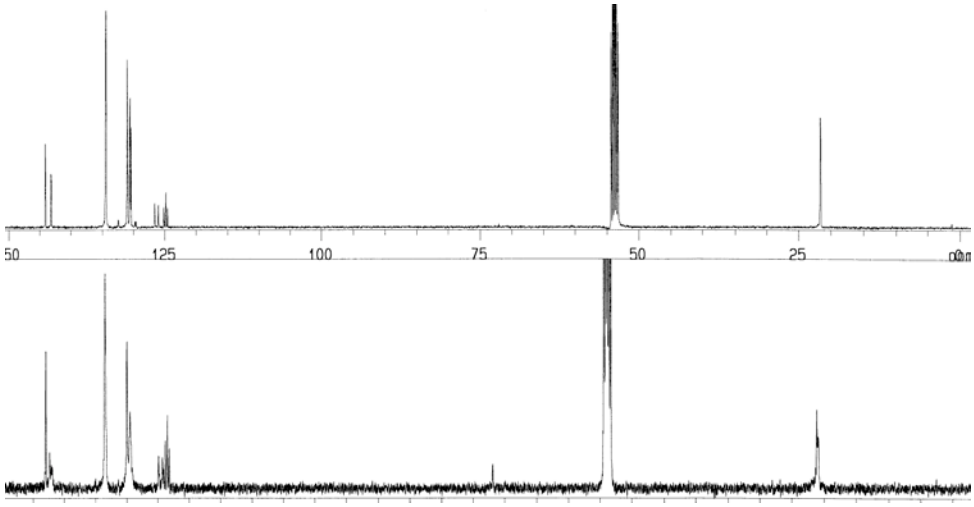

Figure 5-17. $^{13}C\{^{1}H\}$-NMR spectra of $[(p\text{-Tol})_3PAuC{\equiv}CH]\cdot\{[(p\text{-Tol})_3PAu]SbF_6\}$ (**18**) measured at different temperature (above: 27 ° C; below: -90 °C in CD_2Cl_2).

Interestingly only one group of signals exhibits the normal doublet multiplicity for the i-, m- and o-C for the *p*-Tol carbon atoms. The other group of signals exhibit pseudo triplets with smaller splitting (**Figure 5-18)**.

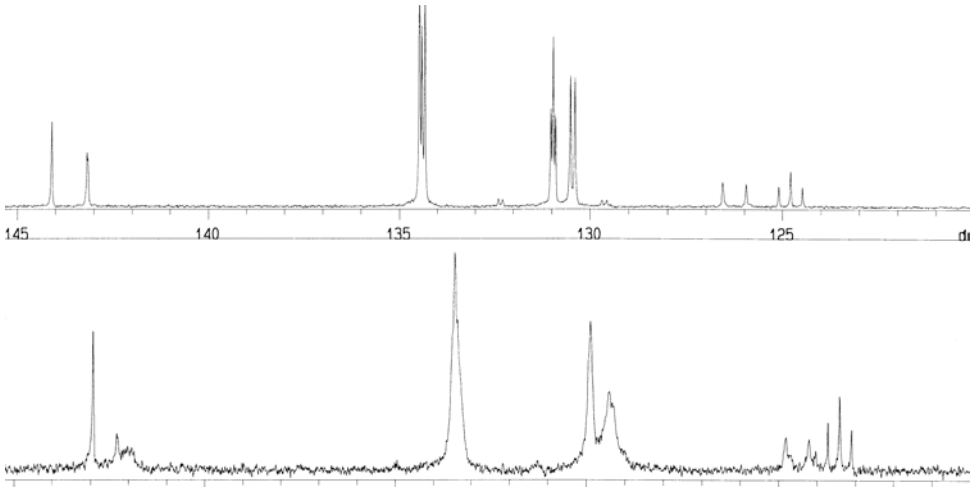

Figure 5-18. $^{13}C\{^{1}H\}$-NMR spectra (aromatic region) of $[(p\text{-Tol})_3PAuC{\equiv}CH]\cdot\{[(p\text{-Tol})_3PAu]SbF_6\}$ (**18**) measured at different temperature (above: 27 ° C; below: -90 °C in CD_2Cl_2).

The triplet splitting was observed also at low temperature (-90 °C). These resonances are tentatively assigned to AXX' spin systems of the cation $[(p\text{-Tol})_3PAuP(p\text{-Tol})_3]^+$ which arises from ligand redistribution. A signal for the carbon atom Au<u>C</u>≡CH with a typical $^2J_{CP}$ of ca. 140 Hz was not found in the aromatic region at RT and low temperature, but the signal of a carbon atom was observed shifted significantly upfield to δ = 72.07 (s) at 27 °C. By cooling down the peak was split into a triplet at δ = 71.89 ppm (t) with J = 9 Hz at -90 °C (**Figure 5-19**). It can be tentatively assigned to a [PAuC≡CAuP] unit, again as an AXX' multiplet.

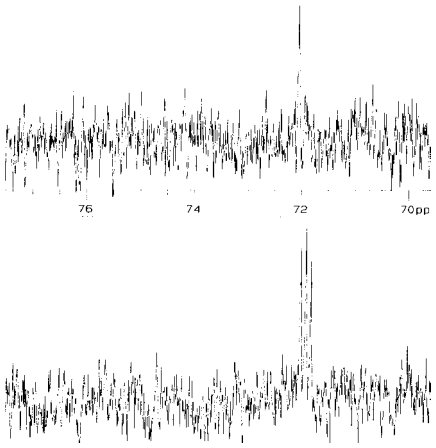

Figure 5-19. $^{13}C\{^{1}H\}$-NMR spectra (AuC≡CH region) of $[(p\text{-Tol})_3PAuC{\equiv}CH]\cdot\{[(p\text{-Tol})_3PAu]SbF_6\}$ (**18**) measured at different temperature (above: 27 ° C; below: -90 °C in CD_2Cl_2).

Similarly two signals were observed for the CH_3 group at RT (δ = 21.67 ppm and 21.57 ppm with J = 9.7 Hz). The peaks were split into a doublet and a triplet at -90 °C (**Figure 5-20**), the latter being assigned to $[(p\text{-Tol})_3PAuP(p\text{-Tol})_3]^+$.

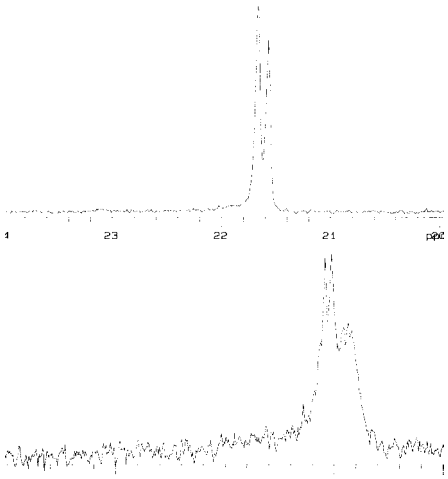

Figure 5-20. $^{13}C\{^{1}H\}$-NMR spectra (-CH_3 region) of $[(p\text{-Tol})_3PAuC{\equiv}CH]\cdot\{[(p\text{-Tol})_3PAu]SbF_6\}$ (**18**) measured at different temperature (above: 27 ° C; below: -90 °C in CD_2Cl_2).

In summary it appears that the reaction of $[(p\text{-Tol})_3PAu]SbF_6$ and $(p\text{-Tol})_3PAuC{\equiv}CH$ (**13**) does not give a 1 : 1 complex. Through exchange reactions symmetrical species are formulated including $[(p\text{-Tol})_3PAuP(p\text{-Tol})_3]^+$ and $[(p\text{-Tol})_3PAuC{\equiv}CAuP(p\text{-Tol})_3]$, with some of the starting materials still present.

5.6 Summary

Among the gold acetylide complexes with (phosphine)gold tetrafluoroborates and hexafluoro-antimonates, the products of the reaction of $(Et_3P)AuC{\equiv}CAu(PEt_3)$ with one equivalent of $[(Et_3P)Au]BF_4$ analyzed well for the expected composition $[(Et_3P)AuC{\equiv}CAu(PEt_3)]\cdot\{[(Et_3P)Au]BF_4\}$ (**15**), but failed to yield a suitable crystal for X-ray analysis. The proposed structure for the complex $[(Et_3P)AuC{\equiv}CAu(PEt_3)]\cdot\{[(Et_3P)Au]BF_4\}$ (**15**) suggests a symmetrical addition of type **I** (**Figure 5-1**).

Similarly, the 1: 2 complex $[(Et_3P)AuC{\equiv}CAu(PEt_3)]\cdot 2\{[(Et_3P)Au]BF_4\}$ (**16**) from the reaction of $(Et_3P)AuC{\equiv}CAu(PEt_3)$ with two equivalents of $[(Et_3P)Au]BF_4$ analyzed well, but also failed to yield a suitable crystal for X-ray analysis.

$(p\text{-Tol})_3PAuC{\equiv}CH$ appears to give no adduct with $[(p\text{-Tol})_3PAu]BF_4$ or $[(p\text{-Tol})_3PAu]SbF_6$.

6 Conclusions

In recent years several experimental investigations and theoretical calculations have demonstrated that most gold(I) compounds form oligomers with closer-than-normal Au--Au distances in the crystal, indicating an attractive interaction between the metal centers. This thesis traced these phenomena in the families of complexes with triple-bonded ligands, i.e. cyanides, isocyanides and acetylides.

6.1 Bis(triphenylphosphoranylidene)ammonium dicyanoaurate(I)

The first section of this work focused on structural and spectroscopic studies of $[Ph_3PNPPh_3]^+[AuCl_2]^-(CH_2Cl_2)$ (**1**), $[(Ph_3P)_2N]^+[Au(CN)_2]^-(CH_2Cl_2)_{0.5}$ (**2**) and $[(Ph_3P)_2N]^+(BF_4)^-(CH_2Cl_2)$ (**3**). In the crystals of these complexes there was no evidence for interionic association. The crystal structure of $[PPN]^+[Au(CN)_2]^-$ (**2**) is closely related to that of the dichloroaurate(I) salt $[PPN]^+[AuCl_2]^-(CH_2Cl_2)$ (**1**), the crystals of which have very similar cell constants and the same space group.

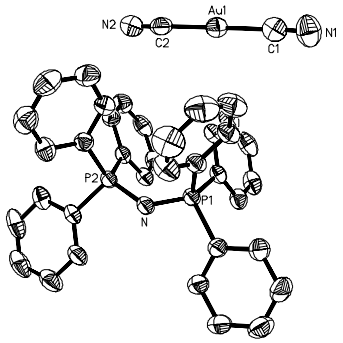

Spectroscopic studies have demonstrated that anion association in aqueous solutions of $M[Au(CN)_2]$ salts are very weak and not manifested in the concentration-dependent IR and NMR spectra with standard resolution. The anions are also not associated in the crystal, where very large and flexible $[PPN]^+$ cations could give room for oligomerization.

In the detailed theoretical and luminescence studies of Patterson *et al.*, it was found that the estimated free energy of dimerization (through Au--Au contacts) to give dianions $[Au(CN)_2]_2^{2-}$ in an ionic structure is not enough to induce aggregation against Coulomb forces.

The present work with $[(Ph_3P)_2N]^+[Au(CN)_2]^-(CH_2Cl_2)_{0.5}$ (**2**) has shown that aurophilic interactions between anions $[Au(CN)_2]^-$ can be maintained only in structures where there is additional support from contacts with counterions or interstitial solvent molecules. Coordinative or hydrogen bonds provide an ideal combination, as demonstrated in several previous studies. Bulky cations with the cationic centers shielded by organic groups as in $[Ph_3PNPPh_3]^+$ do not provide such support and therefore the anions remain separated with a preference for contacts to solvate molecules as in $[(Ph_3P)_2N]^+[Au(CN)_2]^-(CH_2Cl_2)_{0.5}$ (**2**).

6.2 (^{t}Butyl-isocyanide)gold(I) Iodide

In the second section of this work, the structures of the isonitrile gold(I) complexes ^{t}butylisonitrile gold(I) iodide (**4**), methylisonitrile gold(I) chloride and iodide {[MeNCAuX], X = (Cl, I)}, were investigated by quantum-chemical calculations of model systems in order to compare the results with previously obtained computational data on the analogous phosphine systems {$[H_3PAuX]_2$, X = (H, F, Cl, Br, I, -CN, CH_3, -SCH_3)]}.

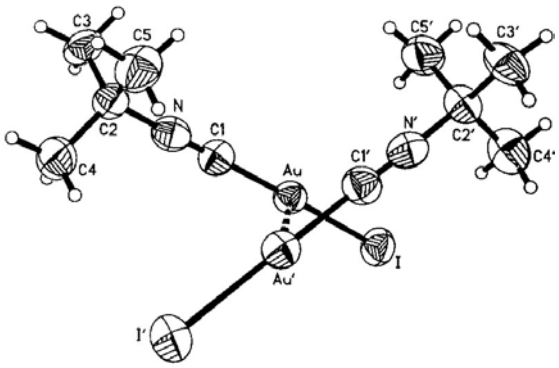

The monomer-monomer interaction at a relatively large distance in (RNC)AuX dimers with antiparallel orientation of monomers was found to be mainly a result of the dominating long-range dipole-dipole attraction and the short-range steric ("Pauli") repulsion. The short but weak monomer-monomer interaction in the perpendicular case is a result of the less dominating steric repulsion and the dipoleinduced dipole attraction, which is weaker than the dipole-dipole attraction of the antiparallel case. The necessary condition to make these effects experimentally observable is an aurophilic correlation attraction, which is not significantly influenced by the type of ligands (methylisonitrile and phosphine). All these results apply to the gas phase and may not necessarily reflect the interaction in a crystal.

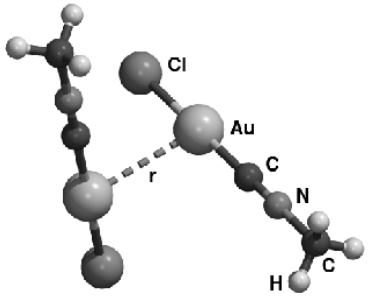

6.3 Mono- and Digoldacetylide Complexes

In the third section of this work gold(I) acetylides were studied with spectroscopic and structural techniques. The aurophilicity concept suggests that mono- and dinuclear gold acetylide complexes LAuC≡CAuL (**A)** and LAuC≡CH (**B**, L = tertiary phosphine donor ligand) should have a rich supramolecular chemistry. All compounds of the type **A** reported in the literature were found to be monomers, however, probably owing to the presence of bulky ligands L. In the present work complexes of gold acetylides with five different phosphorus ligands featuring a variety of cone angles [PEt_3, PMe_3, PMe_2Ph, $PMePh_2$ and $(p\text{-Tol})_3P$] were therefore prepared and structurally characterized.

In this preparative work, product mixtures of types **A** and **B** were obtained and identified by their analytical and spectral data. The prominent and least soluble complexes were isolated by fractional crystallization and their structures determined. The dinuclear complex with the larger phosphine (PEt_3) was found to be a monomer with a "weight-lifting gear" structure of D_3 symmetry.

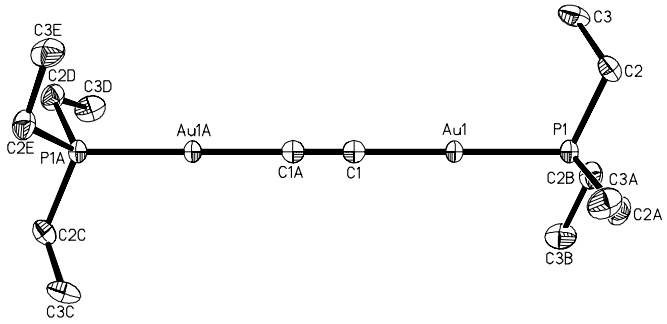

By contrast, the complex with the smallest phosphine (PMe_3) could be shown to be a zig-zag chain polymer in which molecular units with inversion symmetries are linked in a head-to-tail

pattern via aurophilic contacts [3.047(8) Å]. The folding of the chain arises from a dihedral angle P-Au--Au'-P' of 118.2° which minimizes steric interference of the PMe_3 ligands.

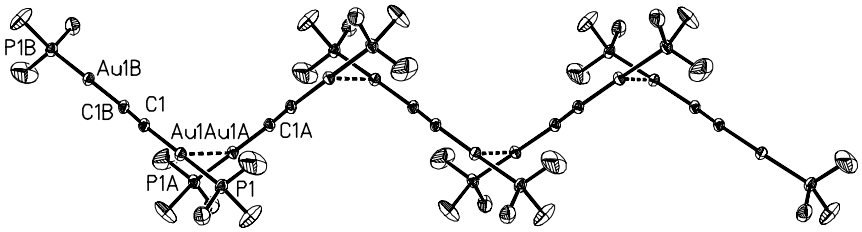

A closely related structure has been found for the dimethylphenylphosphine complex (Me_2PhP) with the Au--Au contact slightly longer at 3.1680(3) Å and the dihedral angle P-Au--Au'-P' at 112.0°.

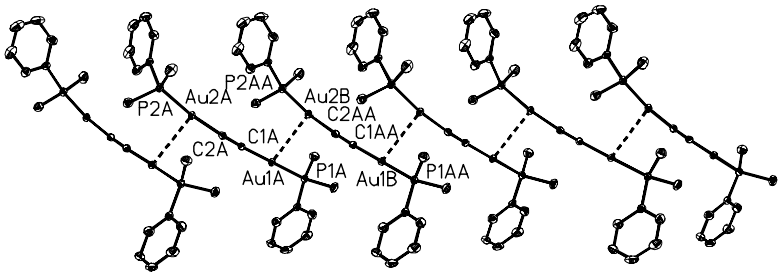

Similar angular units have been found for the complex [(Me_2PhP)AuC≡CH] of type **B,** which forms dimers with an Au--Au' distance of 3.0316(3) Å and a dihedral angle of 111.7°. The dinuclear complex with PMe_2Ph ligands could not be crystallized.

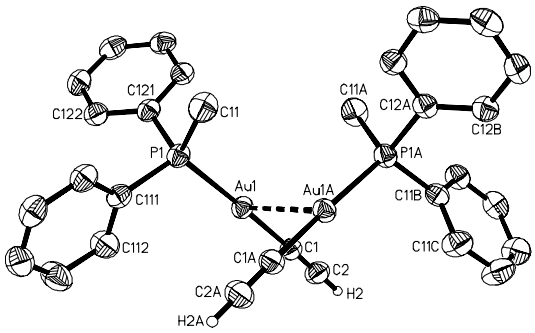

As the second structurally characterized compound of type **B**, complex (p-Tol)$_3$PAuC≡CH (**13**) was obtained. The molecules are not associated owing to steric hindrance. The molecular

axis P1-Au1-C1 of one of two independent molecules in the asymmetric unit is closer to linearity compared to the slightly bent P-Au-C axis found in complex (Ph_2MeP)AuC≡CH (**11**), while that of Au1-C1-C2 is more distorted. The C≡C, Au-C and Au-P distances are similar to those found in complex (**11**) of type **B,** and those in the three compounds of type **A**. This indicates that the structure of a (R_3P)AuC≡CH unit is not strongly influenced by H/Au substitution at the terminal end of the acetylene group.

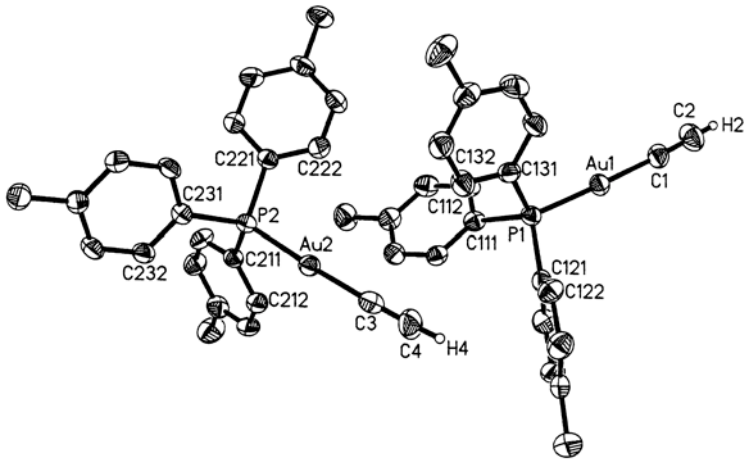

The observations made in the various preparations suggest that an efficient dimerization and/or low solubility of the mononuclear complexes (**B**) may retard the formation of the dinuclear complexes (**A**) quite considerably. This seems to be true for ($MePh_2$)AuC≡CH, which was obtained practically without any dinuclear by-product. By contrast, under similar experimental conditions, the reaction with (Et_3P)AuCl gave exclusively the dinuclear complex. This complex is not associated, and the monomer is aurated further without steric hindrance. There are no quantitative data available to support this more qualitative observation.

In summary it could be shown that monogold and digold acetylides (AuC≡CH and AuC≡CAu) with small tertiary phosphine ligands undergo oligomerization to form dimers or polymers, respectively, through short aurophilic bonding. The compounds have a common structural pattern with very similar angular units in the dimers and in the zig-zag one-dimensional supramolecular aggregates. The energy associated with the aurophilic interactions is estimated to be of the order of 8 - 11 kcal,[178] comparable to the energy of hydrogen bonds. The Au--Au contacts are therefore significant in determining the solid state structure. The photophysical properties of the new compounds, under standard conditions and under pressure, are presently under investigations.

6.4 Adducts of Gold Acetylide Complexes

In a study of the adduct formation between gold acetylide complexes as donors and $[(R_3P)Au]^+$ units as acceptors, the reaction of $(Et_3P)AuC{\equiv}CAu(PEt_3)$ with one equivalent of $[(Et_3P)Au]BF_4$ yielded a product which analyzed well for the expected complex $[(Et_3P)AuC{\equiv}CAu(PEt_3)]\cdot\{[(Et_3P)Au]BF_4\}$ (**15**), but could not be crystallized for X-ray analysis. A proposed structure for the complex is the symmetrical organization as shown in this formula :

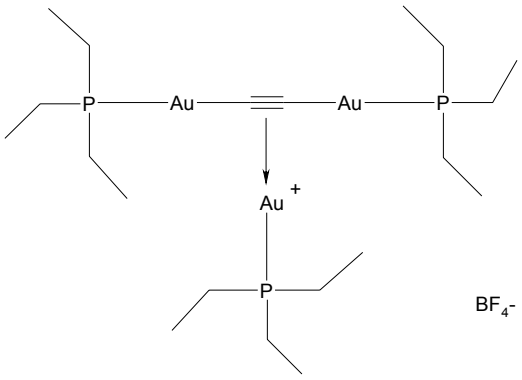

Similarly, the digoldacetylide donor coordinated to two acceptors $[(Et_3P)AuC{\equiv}CAu(PEt_3)]\cdot 2\{[(Et_3P)Au]BF_4\}$ (**16**) could be synthesized from the components in the ratio 1 : 2. The complex analyzed well for the proposed formula (below) (**16**), but again no crystals for X-ray analysis were obtained.

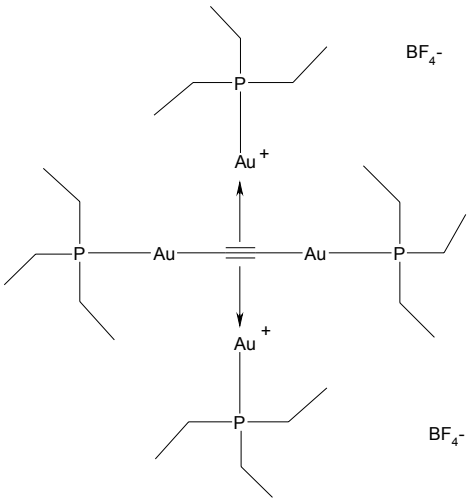

$[(p\text{-Tol})_3PAuC{\equiv}CH]$ and $[(p\text{-Tol})_3PAu]BF_4$ or $[(p\text{-Tol})_3PAu]SbF_6$ gave no well-defined addition compounds.

7 Experimental

7.1 General Techniques and Methods

All experiments were routinely carried out in an atmosphere of dry and pure nitrogen. Solvents were dried and kept under nitrogen. All glassware was oven-dried and filled with nitrogen. Standard equipment was used throughout.

7.1.1 Elemental Analysis (EA)

Elemental analyses were performed in the microanalytical laboratory of Anorganisch-chemisches Institut der Technischen Universität München (director: Mr. Barth).

7.1.2 Melting Point Measurements

The melting points were measured in a Fa. Büchi (Model 510) instrument.

7.1.3 Mass Spectra (MS)

Mass spectra were measured in a Fa. Finnigan (MAT 90) instrument. For ionization the "Fast Atom Bombardment" technique was used (FAB, solvent: 4-nitrobenzylalcohol).

7.1.4 Infrared Spectroscopy (IR)

The IR spectra were recorded employing nujol and KBr windows in a perkin Elmer FT-IR 1650 instrument. The vibrational frequencies are given in wavenumbers (cm^{-1}) and described as vs (very strong), s (strong), m (medium), w (weak) and sh (shoulder).

7.1.5 Raman Spectroscopy

The Raman spectra were measured using crystalline powders in a Renishaw Raman Spectrometer Serie 1000 instrument and a Bio-Rad Raman spectrometer. The vibrational frequencies are given in wavenumbers (cm^{-1}) and described as vs (very strong), s (strong), m (medium), w (weak) and sh (shoulder).

7.1.6 Nuclear Magnetic Resonance Spectroscopy (NMR)

NMR spectra were measured in the following spectrometers. The solvent residual signal was used as an internal standard for ^{1}H- and ^{13}C (^{1}H-coupled/decoupled)-NMR under the given frequencies. ^{31}P-NMR shifts are quoted relative to external aqueous H_3PO_4 (85 %).

^{1}H-NMR:	JEOL-GX270 (270.2 MHz)
	JEOL-GX400 (399.8 MHz)
^{13}C-NMR:	JEOL-GX270 (67.9 MHz)
	JEOL-GX400 (100.5 MHz)
^{31}P{H}-NMR:	JEOL-GX270 (109.4 MHz)
	JEOL-GX400 (161.8 MHz)

7.1.7 Crystal Structure Determinations

Crystal data were collected using a Nonius DIP 2020 system with monochromated Mo-K_α (λ=0.71073 Å) radiation at -130 °C. The structures were solved by direct methods (SHELXS-97) and refined by full matrix least-squares calucations on F^2(SHELXL-97)[183a].

Non-hydrogen atoms were refined with anisotropic displacement parameters. Hydrogen atoms were placed in idealized positions and refined using a riding model with fixed isotropic contributions. The acetylenic hydrogen in ($MePh_2P$)AuC≡CH was located and also refined using a riding model with fixed isotropic contributions. Further information on crystal data, data collection and structure refinement are summarized in the corresponding tables. Important interatomic distances and angles are shown in the corresponding figure captions.

The function minimized was:

$$wR2 = \{[\sum w(F_0^2-F_c^2)^2]/\{[\sum w(F_0^2)^2]\}^{1/2}$$

$$w = 1/[\sigma^2(F_0^2)+(ap)^2+bp]$$

[183] a) Sheldrick, G. M., SHELX-97, Programs for crystal structure analysis; University of Göttingen: Germany 1997. b) Spek, A. L., Acta Crystallogr., Sect A, **1990**, 46, 194.

$p = (F_0^2+2F_c^2)/3$; a = 0.0466, b= 0.98.

[$(Et_3P)AuC{\equiv}CAu(PEt_3)$], 0.0081; [$(Me_3P)AuC{\equiv}CAu(PMe_3)$], 0.0000

[$(Me_2PhP)AuC{\equiv}CAu(PPhMe_2)$], 0.0195 ; [$(MePh_2P)AuC{\equiv}CH$]; 12.45

[$(Et_3P)AuC{\equiv}CAu(PEt_3)$], 57.73; [$(Me_3P)AuC{\equiv}CAu(PMe_3)$], 20.97

[$(Me_2PhP)AuC{\equiv}CAu(PPhMe_2)$] 11.50; [$(MePh_2P)AuC{\equiv}CH$].

7.2 Starting Material

Tetrachloroauric acid was obtained from Fa. Degussa AG, Hanau. The following compounds were prepared following literature procedures. The tertiary phosphines were commercially available.

(tht)AuCl	[184]
Me_3P	Fulka
$(Me_3P)AuCl$	[185]
$(Et_3P)AuCl$	[185]
Me_2PhP	Acros
$(Me_2PhP)AuCl$	[185]
Ph_2MeP	Acros
$(Ph_2MeP)AuCl$	[185]
$(p\text{-Tol})_3P$	Fluka
$[(p\text{-Tol})_3P]AuCl$	[185]

[184] a) Dash, K. C., Schmidbaur, H., Chem. Ber. **1973**, 106, 1221. b) Uson, R., Laguna, A., Vicente, J., J. Organomet. Chem. **1977**, 131, 471.

[185] a) Schmidbaur, H., Brachthäuser, B., Steigelmann, O., Beruda, H., Chem. Ber. **1992**, 125, 2705. b) Mann, F. G., Wells, A. F., Purdie, D., J. Chem. Soc. **1937**, 1828.

7.3 Synthesis and Characterization of Bis(triphenylphoranylidene)-ammonium dicyanoaurate(I)

7.3.1 Bis(triphenylphosphoranylidene)ammonium dichloroaurate(I) (1)

$[PPN]^+[AuCl_2]^-$ was prepared from (tht)AuCl (0.560 g, 1.72 mmol) and [PPN]Cl (0.998 g, 1.72 mmol) in 30 mL of dichloromethane as described in the literature;[145,146] yield 1.18 g (84 %).

7.3.2 Bis(triphenylphosphoranylidene)ammonium dicyanoaurate(I) (2)

A solution of $[PPN]^+[AuCl_2]^-$ (0.620 g, 0.696 mmol) in 10 mL of dichloromethane was treated with an aqueous solution (10 mL) of $K^{13}CN$ (0.104 g, 1.57 mmol) for 4 h at room temperature with vigorous stirring. The organic phase was separated and washed twice with 5 mL of dichloromethane. The combined organic phases were back extracted twice with 5 mL of water and were dried over $MgSO_4$. The product remained after evaporation of the solvent in a vacuum, yield 0.47 g (87 %).

$^{13}C_2{}^{12}C_{36}H_{30}AuN_3P_2$:		calcd.:	C 58.06	H 3.83	N 5.32
(789.58 g/mol)		found:	C 57.98	H 3.86	N 5.15
MS (FAB) [m/z]:		537.7	$[PPN]^+$		
NMR(0.097M in CD_2Cl_2, RT)					
^{1}H-NMR (CD_2Cl_2, 25 °C):	Ar-H	7.2-7.6	m		
^{13}C(^{1}H-coupled)-NMR:	Ar-C	126.9-	m		
(CD_2Cl_2, 25 °C)		132.6			
	^{13}CN	151.3	s		
^{31}P{^{1}H}-NMR:		22.3	s		
(CD_2Cl_2, 25 °C)					
IR (Nujol), cm^{-1}:		2140.1	$\nu[Au(^{12}CN)_2]^-$		
		2098.3	$\nu[Au(^{13}CN)_2]^-$		

Crystal data for $[(Ph_3P)_2N]^+[Au(CN)_2]^-(CH_2Cl_2)_{0.5}$ **(2)**:

Empirical formula:	$C_{38.5}H_{31}AuClN_3P_2$
Formula weight (g/mol):	830.02
Crystal system:	monoclinic
Space group:	$P2_1/n$
Unit cell dimensions:	a = 9.1488(1) Å, α = 90.00°
	b = 24.1213(3) Å, β = 105.034(1)°
	c = 16.8338(2) Å, γ = 90.00°
Z:	4
Volume, Å^3:	3587.8(1)
μ(Mo-Kα), cm^{-1}:	42.94
Reflections collected / unique:	88429 / 7762 [R = 0.055]
Absorption correction:	DELABS
*wR*2:	0.1079
R [I ≥ 2σ (I)]:	0.0407 for 7762 reflections and 424 parameters
Weighting scheme:	a = 0.0466, b= 0.98

7.3.3 Bis(triphenylphosphoranylidene)ammonium tetrafluoroborate (3)

This compound was obtained from the reaction of equimolar quantities of bis(triphenylphosphoranylidene)ammonium chloride and silver tetrafluoroborate in dichloromethane in virtually quantitative yield. After filtration the product was isolated from the filtrate by evaporation of all volatiles. The product shows the PPN cation as the parent peak in the mass spectrum (FAB, m/e = 538.3). The $^{31}P\{^1H\}$ NMR spectrum (in CD_2Cl_2 at 20 °C) has the cation resonance at δ = 22.40 ppm. Single crystals of the dichloromethane solvate (1:1) were obtained from dichloromethane solution upon layering with pentane at -20 °C.

Crystal data for $[(Ph_3P)_2N]^+(BF_4)(CH_2Cl_2)$ **(3)**:

Empirical formula:	$C_{37}H_{32}BCl_2F_4NP_2$
Formula weight (g/mol):	710.29
Crystal system:	triclinic
Space group:	$P\bar{1}$
Unit cell dimensions:	a = 9.495(2) Å, α = 90.28(2)°
	b = 10.635(4) Å, β = 94.59(1)°

	c = 17.020(2) Å, γ = 93.50(2)°
Z:	2
Volume, $Å^3$:	1709.9(8)
μ(Mo-Kα), cm^{-1}:	3.34
Reflections collected / unique:	7384 / 7384
Absorption correction:	DELABS
*wR*2:	0.0984
R [I ≥ 2σ (I)]:	0.0465 for 7384 reflections and 424 parameters
Weighting scheme:	a = 0.0641, b= 0.00

The occupation of the solvent molecule CH_2Cl_2 in the crystals of **2** was reduced to 0.5 due to the very large atomic displacement parameters.

7.4 Synthesis and Characterization of (^{t}Butyl-isocyanide)gold(I) Iodide

7.4.1 Preparation of ^{13}C-labeled ^{t}butylisocyanide

Following literature procedures[186] the isonitrile was prepared from ^{t}butylamine (26 mL, 17.94 g, 0.24 mmol), chloroform-^{13}C (0.667 mL, 1.0 g, 8.27 mmol), chloroform-^{12}C (9 mL, 13.5 g, 0.113 mol), and benzyl-triethylammonium chloride (0.25 g) in 37.5 mL of dichloromethane, and sodium hydroxide (37.5 g, 0.938 mol) in 40 mL of water. After 4 h of reflux with stirring and cooling to 20 °C, ice water (100 mL) was added to the reaction mixture. The aqueous phase was extracted with dichloromethane (12.5 mL) and the combined organic phase washed with water (12.5 mL) followed by 12.5 mL of a 5 % [w/w] aqueous sodium chloride solution. The solution was dried over $MgSO_4$ and distilled under nitrogen; b.p. 85 °C, 6.65 g yield (66 %).

^{13}C{^{1}H}-NMR:	$\underline{C}H_3$	30.65	s
($CDCl_3$, 20 °C)	$\underline{C}Me_3$	54.08	t, J = 5.3 Hz
	$\underline{C}N$	152.47	t, J = 8.8 Hz
IR (Nujol), cm^{-1}:		2134.7	ν(C≡N)

[186] Gokel, G. W., Widera, R. R., Werner, W. P., Org. Synth. **1976**, 55, 96.

7.4.2 Preparation of ^{13}C-labeled (^{t}butylisocyanide)gold(I) chloride and iodide

0.468 g of ^{t}BuNC (0.64 mL, 5.63 mmol) and (tetrahydrothiophene)gold(I) chloride (1.80 g, 5.63 mmol) were dissolved in dichloromethane (40 mL) at 20 °C under nitrogen.[157] After 1 h of stirring a clear solution was obtained. The volume of this solution was reduced to 2mL in a vacuum to precipitate the product. This was filtered and dried under vacuum: 1.41 g, yield (80 %).

^{13}C{^{1}H}-NMR:	$\underline{C}H_3$	29.83	s
(CD_2Cl_2, 20 °C)	$\underline{C}Me_3$	59.60	t, J = 4.0 Hz
	Au$\underline{C}$	132.49	t, J = 24.2 Hz

7.4.3 Preparation of ^{13}C-labeled (^{t}butylisocyanide)gold(I) iodide (4)

0.7 g of (^{t}BuNC)AuCl (2.22 mmol) was dissolved in dichloromethane (10 mL) and treated with a solution of KI (0.366 g, 2.22 mmol) in water (10 mL). The mixture was stirred at 0 °C for 3 h. The phases were separated, the aqueous phase washed with dichloromethane (2 × 5 mL) and the combined organic phase extracts were washed with water (2 × 5 mL), dried over $MgSO_4$ and evaporated to dryness in a vacuum: 0.6 g yield (70 %), m.p. 85 °C.

C_5H_9NAuI :	calcd.:	C 14.76	H 2.23	N 3.44
(406.99 g/mol)	found:	C 15.07	H 2.28	N 3.52

MS (CI) [m/z]:	406.7	(3%)	$[M]^+$
^{1}H-NMR (CD_2Cl_2, 25 °C):	$C\underline{H}_3$	1.54	s
^{13}C(^{1}H-coupled)-NMR:	$\underline{C}H_3$	29.72	s
(CD_2Cl_2, 25 °C)	$\underline{C}Me_3$	59.19	s
	Au$\underline{C}$	142.48	t, J = 21.9 Hz
IR (KBr), cm^{-1}:	2239.2	ν(C≡N)	
IR (Nujol), cm^{-1}:	2235.8	ν(C≡N)	

Crystal data for (^{t}BuNC)AuI **(4)**:

Empirical formula:	C_5H_9NAuI
Formula weight (g/mol):	407.0
Crystal system:	monoclinic, colorless crystal
Space group:	*C*2/*c*
Unit cell dimensions:	a = 12.413(2) Å, α = 90.00°
	b = 11.977(1) Å, β = 97.68(2)°
	c = 12.448(2) Å, γ = 90.00°
Z:	8
Volume, Å^3:	1834.0(4)
μ(Mo-Kα), cm^{-1}:	71.073
Density (ρ_{calc}), gcm^{-3}:	2.948
F(000):	1424
Reflections collected / unique:	2501 / 1973 [R_{int} = 0.0547]
Absorption correction:	DELABS
*R*1	0.0473
*wR*2:	0.1142
ρ_{fin} (max/min), eÅ^{-3}:	+2.151 / -1.279
Weighting scheme:	a = 0.0676, b= 0.00

7.5 Synthesis and Characterization of Mono- and Digoldacetylide Complexes

7.5.1 General Preparative Method

A suspension of ca. 10 mmol of the (phosphine)gold chloride in ethanol (100 mL) is saturated with acetylene gas at -60 °C for 1 h. Following this a solution of sodium ethanolate [freshly prepared by dissolving sodium metal (11 mmol) in ethanol (20 mL)] is added slowly with stirring. Acetylene is bubbled through the reaction mixture for another 3 h. On warming the mixture becomes clear followed by the formation of a precipitate. This is filtered off, washed with water and dried in a vacuum. This product is a mixture of compounds (**A** and **B**) for R_3P = Me_3P, Me_2PhP and $MePh_2P$, but only pure **A** for R_3P = Et_3P. The major component can be separated by fractional crystallization from dichloromethane/*n*-pentane. Single crystals can be grown for the pure components from dichloromethane carefully layered with *n*-pentane.

7.5.2 Reaction of (Trimethylphosphine)gold Chloride and Acetylene Gas

A suspension of the (trimethylphosphine)gold chloride [(Me_3P)AuCl], (3.0 g, 9.8 mmol), in ethanol (100 mL) was saturated with acetylene gas at -60 °C for 1h. Following this a solution of sodium ethanolate (prepared by dissolving sodium metal (0.27 g, 11 mmol) in ethanol (25 mL)) was added slowly with stirring. Acetylene gas was bubbled through the reaction mixture for another 3 h. On warming the mixture became clear followed by the formation of a precipitate. This was filtered off, washed with water and dried in a vacuum. This pale yellow powder (1.22 g, 4.09 mmol, yield 41.8 %)) was characterized as the component (Me_3P)AuC≡CH (**5**).

A second component was crystallized from the mother liquor at ca. -35 °C, washed with water, dissolved in CH_2Cl_2 and dried in a vacuum. This yellow crystalline powder (0.76 g, 1.33 mmol, yield 27.2 %) was characterized as (Me_3P)AuC≡CAu(PMe_3) (**6**)**.** Single crystals were grown from dichloromethane carefully layered with *n*-pentane.

7.5.2.1 Characterization of [(Trimethylphosphine)gold]acetylene (5)

(Me_3P)AuC≡CH (**5**), 1.22 g, 4.09 mmol, yield 41.8 %, pale yellow solid, m.p. 111-112 °C.

$C_5H_{10}AuP$:		calcd.:	C 20.15	H 3.38	P 10.39
(298.07 g/mol)		found:	C 20.12	H 3.37	P 10.01
^{1}H-NMR (CD_2Cl_2, 25 °C):	$C\underline{H}_3$	1.48	d, 9H, $^2J_{CP}$ = 9.9 Hz		
	C≡C$\underline{H}$	2.09	s, 1H		
^{13}C(^{1}H-coupled)-NMR:	$\underline{C}H_3$	31.0	dq, $^1J_{CP}$ = 35 Hz, $^1J_{CH}$ = 128.2 Hz		
(CD_2Cl_2, 25 °C)	C≡$\underline{C}$H	90.4	dd, $^1J_{CH}$ = 227.3 Hz, $^3J_{CP}$ = 12.9 Hz		
	Au$\underline{C}$	128.3	dd, $^2J_{CH}$ = 38.7 Hz, $^2J_{CP}$ = 143.4 Hz		
^{31}P{^{1}H}-NMR:		1.03	s		
(CD_2Cl_2, 25 °C)					
IR (Nujol), cm^{-1}:		1971.1	w, *ν*(C≡C)		
		3272.2	w, *ν*(CH), (-Au-C≡CH)		
		3258.8			
Raman (powder sample) :		1973.8	s, *ν*(C≡C)		
(cm^{-1})					

7.5.2.2 Characterization of Bis[(trimethylphosphine)gold]acetylene (6)

$(Me_3P)AuC{\equiv}CAu(PMe_3)$ (**6**), 0.76 g, 1.33 mmol, yield 27.2 %, yellow solid, m.p. 206-207°C.

$C_8H_{18}Au_2P_2$:	calcd.:	C 16.85	H 3.18	P 10.87
(570.10 g/mol)	found:	C 16.75	H 3.21	P 9.18

		%	
MS (FAB) [m/z]:	1065.8	2.62	$[2M - Me_3P + H]^+$
	843.7	27.95	$[M + Me_3PAu]^+$
	767.6	6.98	$[M + Au]^+$
	571.5	28.51	$[M + H]^+$
	349.4	74.99	$[(Me_3PAuPMe_3]^+$
	273.3	59.05	$[Me_3PAu]^+$
	147.2	100.0	

^{1}H-NMR (CD_2Cl_2, 25 °C):	$C\underline{H}_3$	1.49	d, $^2J_{HP}$ = 9.9 Hz
$^{13}C(^1H$-coupled)-NMR:	$\underline{C}H_3$	15.81	dq, $^1J_{CP}$ = 35.9 Hz, $^1J_{CH}$ = 130.9 Hz
(CD_2Cl_2, 25 °C)	Au$\underline{C}$	206.7	dd, $^2J_{CP}$ = 12.0 Hz, $^3J_{CP}$ = 5.5 Hz,
$^{31}P\{^1H\}$-NMR:		1.03	s
(CD_2Cl_2, 25 °C)			
Raman (powder sample) :		1999.3	ν(C≡C)
(cm^{-1})		1921.9	w

Crystal data for $(Me_3P)AuC{\equiv}CAu(PMe_3)$ (**6**):

Empirical formula:	$C_8H_{18}Au_2P_2$	
Formula weight (g/mol):	570.10	
Crystal system:	tetragonal	
Space group:	*P*4/*ncc*	
Unit cell dimensions:	a = 15.8161(2) Å,	α = 90.00°
	b = 15.8161(2) Å,	β = 90.00°
	c = 10.9850(2) Å,	γ = 90.00°
Z:	8	

Volume, $Å^3$:	2747.9(1)
μ(Mo-Kα), cm^{-1}:	215.21
Density (ρ_{calc}), gcm^{-3}:	2.756
F(000):	2032
Crystal size, mm:	0.35 × 0.30 × 0.10
Θ-range for data collection, °:	3.43 to 27.25
Reflections collected / unique:	67236 / 1540 [R_{int} = 0.080]
Absorption correction:	DELABS
T_{min} / T_{max}:	0.389 / 0.790
Refined parameters:	55
*R*1	0.0448
*wR*2:	0.0990
Goodness-of-fit on F^2	1.390
ρ_{fin} (max/min), $eÅ^{-3}$:	2.686 / -1.101

7.5.3 Reaction of (Triethylphosphine)gold Chloride and Acetylene Gas

A suspension of (triethylphosphine)gold chloride [$(Et_3P)AuCl$, 2.32 g, 6.6 mmol] in ethanol (130 mL) was saturated with acetylene gas at -60 °C for 1 h. A solution of sodium ethanolate [freshly prepared by dissolving sodium metal (0.16g, 7.0 mmol) in ethanol (20 mL)] was then added slowly with stirring. Acetylene gas was bubbled through the reaction mixture for another 3 h. On warming the yellow mixture became clear followed by the formation of a white precipitate. This very fine suspension could not be filtered off or separated by the centrifugation method. Therefore this suspension was evaporated to dryness in a vacuum. The obtained pale yellow substance was washed with water and recrystallized from CH_2Cl_2. The white crystalline material (2.03 g, 3.10 mmol, yield 93.76 %) was characterized as the complex $(Et_3P)AuC{\equiv}CAu(PEt_3)$ (**8**)**.** The component $(Et_3P)AuC{\equiv}CH$ (**7**) was observed as a small by-product in trace ^{13}C-NMR and Raman spectroscopy. Single crystals of (**8**) were grown from dichloromethane carefully layered with *n*-pentane.

7.5.3.1 Characterization of [(Triethylphosphine)gold]acetylene (7)

$(Et_3P)AuC{\equiv}CH$ (**7**) ($C_8H_{16}AuP$, 340.16 g/mol) was not isolated from the product mixture.

$C_8H_{16}AuP$:

(340.16 g/mol)

MS (FAB) [m/z]:		341.4	$[M + H]^+$
$^{13}C(^1H$-coupled)-NMR:	C≡CH	88.76	vw
(CD_2Cl_2, 25 °C)			
Raman (powder sample) :		1974	vw, *ν*(C≡C), AuC≡CH
(cm^{-1})			

7.5.3.2 Characterization of Bis[(triethylphosphine)gold]acetylene (8)

(Et_3P)AuC≡CAu(PEt_3) (**8**), 2.03 g, 3.10 mmol, yield 93.76 %, white solid, m.p. 180-181 °C.

$C_{14}H_{30}Au_2P_2$:	calcd.:	C 25.70	H 4.62	P 9.47
(654.25 g/mol)	found:	C 25.25	H 4.38	P 8.87

		%	
MS (FAB) [m/z]:	1506.4	28.45	$[2M + Au]^+$
	1388.2	1.20	$[2M - Et_3P + Au]^+$
	1192.1	5.30	$[2M - Et_3P + H]^+$
	970.0	100.0	$[M + Et_3PAu]^+$
	851.7	17.99	$[M + Au]^+$
	655.7	20.14	$[M + H]^+$
	433.6	93.29	$[Et_3PAuPEt_3]^+$
	315.4	71.31	$[Et_3PAu]^+$

^1H-NMR (CD_2Cl_2, 25 °C):	C<u>H</u>$_3$	1.05	dt, $^3J_{HP}$ = 18 Hz, $^3J_{HH}$ = 7.6 Hz
	C<u>H</u>$_2$	1.70	dq, $^2J_{HP}$ = 8.1 Hz, $^3J_{HH}$ = 7.5 Hz
$^{13}C(^1H$-coupled)-NMR:	<u>C</u>H$_3$	8.90	dq, $^2J_{CP}$ = 4.6 Hz, $^1J_{CH}$ = 128.2 Hz
(CD_2Cl_2, 25 °C)	<u>C</u>H$_2$	18.04	dt, $^1J_{CP}$ = 32.3 Hz, $^1J_{CH}$ = 130 Hz
	Au<u>C</u>	150.0	br., s
$^{31}P\{^1H\}$-NMR:		39.20	s
(CD_2Cl_2, 25 °C)			
Raman (powder sample) :		2009.1	*ν*(C≡C)
(cm^{-1})		1921.6	

Crystal data for $(Et_3P)AuC{\equiv}CAu(PEt_3)$:

Empirical formula:	$C_{14}H_{30}Au_2P_2$
Formula weight (g/mol):	654.25
Crystal system:	cubic
Space group:	$Pa\ \bar{3}$
Unit cell dimensions:	a = 12.3718(1) Å, α = 90.00°
	b = 12.3718(1) Å, β = 90.00°
	c = 12.3718(1) Å, γ = 90.00°
Z:	4
Volume, Å^3:	1893.7(1)
μ(Mo-Kα), cm^{-1}:	156.31
Density (ρ_{calc}), gcm^{-3}:	2.295
F(000):	1208
Crystal size, mm:	0.40 × 0.30 × 0.20
Θ-range for data collection, °:	3.14 to 26.58
Reflections collected / unique:	53486 / 704 [R_{int} = 0.076]
Absorption correction:	DELABS
T_{min} / T_{max}:	0.468 / 0.827
Refined parameters:	28
*R*1	0.0245
*wR*2:	0.0537
Goodness-of-fit on F^2	1.265
ρ_{fin} (max/min), eÅ^{-3}:	0.727 / -1.208

7.5.4 Reaction of [(Dimethylphenyl)phosphine]gold Chloride and Acetylene Gas

A suspension of (dimethylphenylphosphine)gold chloride [$(Me_2PhP)AuCl$], (3.0 g, 8.1 mmol), in ethanol (100 mL) was saturated with acetylene gas at -60 °C for 1 h. Following this a solution of sodium ethanolate [freshly prepared by dissolving sodium metal (0.22 g, 9.5 mmol) in ethanol (20 mL)] was slowly added with stirring. Acetylene was bubbled through the reaction mixture for another 3 h. On warming the yellow mixture became clear and a white precipitate formed. This was filtered off, washed with water, redissolved in CH_2Cl_2 and dried in a vacuum. The white product (0.65g, 1.81 mmol, yield 22.4 %) was characterized as $(Me_2PhP)AuC{\equiv}CH$ (**9**).

The mother liquor (an EtOH solution) was dried in a vacuum and the residue washed with water and dissolved in CH_2Cl_2. Through recrystallisation at low temperature a white crystalline product (2.01 g, 2.89 mmol, yield 71.5 %) was obtained and characterized as the complex $(Me_2PhP)AuC{\equiv}CAu(PPhMe_2)$ (**10**). Single crystals of (**10**) were grown from dichloromethane carefully layered with *n*-pentane.

7.5.4.1 Characterization of [(Dimethylphenylphosphine)gold]acetylene (9)

$(Me_2PhP)AuC{\equiv}CH$ (**9**), 0.65g, 1.81 mmol, yield 22.4 %, white solid, m.p. 157°C.
$C_{10}H_{21}AuP$:
(360.03 g/mol)

MS (FAB) [m/z]:		1029.4	36.27 $[M - H + 2Me_2PhPAu]^+$
		891.3	17.24 $[M - H + Me_2PhPAu + Au]^+$
		695.3	9.38 $[M + Me_2PhPAu]^+$
		473.3	79.43 $[Me_2PhPAuPPhMe_2]^+$
		335.2	100.0 $[Me_2PhPAu]^+$
^{1}H-NMR (CD_2Cl_2, 25 °C):	$C\underline{H}_3$	1.73	d, $^2J_{HP}$ = 7.6 Hz, 6H
		7.46-7.75	m, 5H, Ph
^{13}C(^{1}H-coupled)-NMR:	$\underline{C}H_3$	15.70	qdq, $^1J_{CH}$ = 131.0 Hz, $^1J_{CP}$ = 34.6 Hz, $^3J_{CH}$ = 3.1 Hz
	$C{\equiv}\underline{C}H$	90.47	d, $^1J_{CH}$ = 228.4 Hz
(CD_2Cl_2, 25 °C)	$Au\underline{C}$	128.6	dd, $^2J_{CH}$ = 143.4 Hz, $^2J_{CP}$ = 38.7 Hz
	m-$\underline{C}_{3/5}$	129.5	dd, $^3J_{C,P}$ = 10.8 Hz
	p-$\underline{C}_4$	131.7	dd, $^4J_{CP}$ = 2.3 Hz
	o-$\underline{C}_{2/6}$	132.5	dd, $^2J_{CP}$ = 13.1 Hz
	i-$\underline{C}_1$	134.2	d, $^1J_{CP}$ = 53.0 Hz
	$Au\underline{C}$	148.3	br. s
^{31}P{^{1}H}-NMR:		12.9	s
(CD_2Cl_2, 25 °C)			

IR (Nujol), cm^{-1}:	1963.6	w, *v*(C≡C)	
	1973.8		
	3274.6	w, *v*(CH), (-Au-C≡CH)	

7.5.4.2 Characterization of Bis[(dimethylphenylphosphine)gold]acetylene (10)

$(Me_2PhP)AuC{\equiv}CAuP(PhMe_2)$ (**10**), 2.01 g, 2.89 mmol, yield 71.5%, m.p. 181-182°C, white solid.

$C_{18}H_{22}Au_2P_2$:	calcd.:	C 31.14	H 3.19	P 8.92
(694.23 g/mol)	found:	C 31.16	H 3.27	P 8.77

		%	
MS (FAB) [m/z]:	1447.4	2.95	$[2M - Me_2PhP + Au]^+$
	1251.4	2.05	$[2M - Me_2PhP + H]^+$
	1029.4	54.62	$[M + Me_2PhPAu]^+$
	891.3	16.08	$[M + Au]^+$
	695.3	24.32	$[M + H]^+$
	473.3	77.22	$([Me_2PhPAuPPhMe_2]^+)$
	335.2	100.0	$[Me_2PhPAu]^+$

^{1}H-NMR (CD_2Cl_2, 25 °C):	C<u>H</u>$_3$	1.73	d, $^2J_{HP}$ = 7.6 Hz, 6H
		7.46-7.75	m, 5H, Ph

^{13}C(^{1}H-coupled)-NMR:	<u>C</u>H$_3$	15.70	qdq, $^1J_{CH}$ = 131.0 Hz, $^1J_{CP}$ = 34.6 Hz, $^3J_{CH}$ = 3.1 Hz
(CD_2Cl_2, 25 °C)	m-<u>C</u>$_{3/5}$	129.5	dd, $^3J_{CP}$ = 10.8 Hz
	p-<u>C</u>$_4$	131.7	dd, $^4J_{CP}$ = 2.3 Hz
	o-<u>C</u>$_{2/6}$	132.5	dd, $^2J_{CP}$ = 13.1 Hz
	i-<u>C</u>$_1$	134.2	d, $^1J_{CP}$ = 53.0 Hz
	Au<u>C</u>	148.3	br. s

^{31}P{^{1}H}-NMR:		33.212	s

(CD_2Cl_2, 25 °C)

Raman (powder sample) : (cm^{-1})	1998.3	s, ν(C≡C)

Crystal data for $(Me_2PhP)AuC{\equiv}CAuP(PhMe_2)$ (**10**):

Empirical formula:	$C_{18}H_{22}Au_2P_2$	
Formula weight (g/mol):	694.23	
Crystal system:	orthorhombic	
Space group:	*Pbca*	
Unit cell dimensions:	a = 12.848(1) Å,	α = 90.00°
	b = 11.433(1) Å,	β = 90.00°
	c = 25.581(1) Å,	γ = 90.00°
Z:	8	
Volume, $Å^3$:	3757.6(5)	
μ(Mo-Kα), cm^{-1}:	157.63	
Density (ρ_{calc}), gcm^{-3}:	2.454	
F(000):	2544	
Crystal size, mm:	0.50 × 0.45 × 0.30	
Θ-range for data collection, °:	3.17 to 27.25	
Reflections collected / unique:	93336 / 4169 [R_{int} = 0.076]	
Absorption correction:	DELABS	
T_{min} / T_{max}:	0.438 / 0.814	
Refined parameters:	199	
*R*1	0.0252	
*wR*2:	0.0610	
Goodness-of-fit on F^2	1.299	
ρ_{fin} (max/min), $eÅ^{-3}$:	0.964 / -1.031	

7.5.5 Reaction of (Diphenylmethylphosphine)gold Chloride and Acetylene Gas

A suspension of (diphenylmethylphosphine)gold chloride [(Ph_2MeP)AuCl], (3.0 g, 6.9 mmol) in ethanol (100 mL) was saturated with acetylene gas at -60 °C for 1 h. Subsequently a solution of sodium ethanolate [freshly prepared by dissolving sodium metal (0.18 g, 8 mmol) in ethanol (20 mL)] was slowly added with stirring. Acetylene was bubbled through the reaction

mixture for another 3 h. On warming the white mixture became clear and a white precipitate formed. This was filtered off, washed with water, resolved in CH_2Cl_2 and dried in a vacuum. The white product (0.91 g, 2.15 mmol, yield 31.0 %) was characterized as (Ph_2MeP)AuC≡CH (**11**).

The mother liquor (an EtOH solution) was evaporated in a vacuum and the residue washed with water and dissolved in CH_2Cl_2. Through recrystallisation at low temperature a white crystalline product (1.33 g, 1.625 mmol, yield 46.9 %) was obtained and characterized as (Ph_2MeP)AuC≡CAu($PMePh_2$) (**12**)**.** Single crystals of (**11**) were grown from dichloromethane carefully layered with *n*-pentane.

7.5.5.1 Characterization of (Diphenylmethylphosphine)gold]acetylene (11)

($MePh_2P$)AuC≡CH (**11**), 0.91 g, 2.15 mmol, yield 31.0 %, m.p. 215°C, white solid.

$C_{15}H_{14}AuP$:	calcd.:	C 42.67	H 3.34	P 7.34
(422.20 g/mol)	found:	C 42.50	H 3.32	P 7.06

		%	
MS (FAB) [m/z]:	1215.9	10.10	$[M - H + 2Ph_2MePAu]^+$
	1041.7	1.85	$[2M + Au]^+$
	843.6	1.51	$[2M + H]^+$
	819.6	32.49	$[M + Ph_2MePAu]^+$
	619.4	1.46	$[M + Au]^+$
	597.5	67.50	$[Ph_2MePAuPMePh_2]^+$
	423.4	3.99	$[M + H]^+$
	397.2	100.0	$[Ph_2MePAu]^+$

^{1}H-NMR (CD_2Cl_2, 25 °C):	C≡C<u>H</u>	1.62	s, 1H
	C<u>H</u>$_3$	2.06	d, $^2J_{HP}$ = 8.8 Hz, 3H
	Ar-<u>H</u>	7.45-7.63	m, 10H

^{13}C(^{1}H-coupled)-NMR:	<u>C</u>H$_3$	14.07	dq, $^1J_{CH}$ = 132.8 Hz, $^1J_{CP}$ = 34.5 Hz
(CD_2Cl_2, 25 °C)	C≡<u>C</u>H	90.06	dd, $^1J_{CH}$ = 228.6 Hz, $^3J_{CP}$ = 2.3 Hz
	Au<u>C</u>	127.85	d, $^2J_{CP}$ = 39.7 Hz

	m-$\underline{C}_{3/5}$	129.34	dm, $^1J_{CH}$ = 164 Hz
	p-$\underline{C}_4$	131.49	dt, $^1J_{CH}$ = 138 Hz, $^4J_{CP}$ = 7.0 Hz
	i-$\underline{C}_1$	132.16	d, $^1J_{CP}$ = 54.6 Hz
	o-$\underline{C}_{2/6}$	133.11	dm, $^1J_{CH}$ = 153 Hz
$^{31}P\{^1H\}$-NMR:		26.08	s
(CD_2Cl_2, 25 °C)			
IR (Nujol):		1978.5	w, *ν*(C≡C)
(cm^{-1})		3279.6	w, *ν*(CH), (-Au-C≡CH)
Raman (powder sample) :		1981.8	s, *ν*(C≡C)
(cm^{-1})			

Crystal data for ($MePh_2P$)AuC≡CH (**11**):

Empirical formula:	$C_{15}H_{14}AuP$	
Formula weight (g/mol):	422.20	
Crystal system:	monoclinic	
Space group:	*C*2/*c*	
Unit cell dimensions:	a = 22.0202(3) Å,	α = 90.00°
	b = 7.0904(1) Å,	β = 96.550(1)°
	c = 17.7718(7) Å,	γ = 90.00°
Z:	8	
Volume, $Å^3$:	2756.6(1)	
μ(Mo-Kα), cm^{-1}:	107.64	
Density (ρ_{calc}), gcm^{-3}:	2.035	
F(000):	1584	
Crystal size, mm:	0.50 × 0.30 × 0.20	
Θ-range for data collection, °:	3.20 to 27.17	
Reflections collected / unique:	38989 / 2862 [R_{int} = 0.042]	
Absorption correction:	DELABS	
T_{min} / T_{max}:	0.503 / 0.842	
Refined parameters:	155	
*R*1	0.0217	
*wR*2:	0.0560	

Goodness-of-fit on F^2	1.099
ρ_{fin} (max/min), e$Å^{-3}$:	2.032 / -0.772

7.5.5.2 Characterization of Bis[(diphenylmethylphosphine)gold]acetylene (12)

(MePh$_2$P)AuC≡CAuP(Ph$_2$Me) (**12**), 1.33 g, 1.625 mmol, yield 46.9 %, m.p. 215°C, white solid.

$C_{28}H_{26}Au_2P_2$:	calcd.:	C 41.09	H 3.20	P 7.57
(818.39 g/mol)	found:	C 39.60	H 3.18	P 7.50

		%	
MS (FAB) [m/z]:	1633.0	1.53	$[2M - Ph_2Me + Au]^+$
	1437.2	1.13	$[2M - Ph_2Me + H]^+$
	1215.3	36.64	$[M + Ph_2MeAu]^+$
	1015.2	9.87	$[M + Au]^+$
	819.2	17.97	$[M + H]^+$
	597.2	57.17	$[Ph_2MePAuPMePh_2]^+$
	397.2	100.0	$[Ph_2MePAu]^+$

^{1}H-NMR (CD_2Cl_2, 25 °C):	C<u>H</u>$_3$	2.06	d, $^2J_{HP}$ = 8.8 Hz, 3H
	Ar-<u>H</u>	7.45-7.63	m, 10H

^{13}C(^{1}H-coupled)-NMR:	<u>C</u>H$_3$	14.1	dq, $^1J_{CH}$ = 132.8 Hz, $^1J_{CP}$ = 34.5 Hz
(CD_2Cl_2, 25 °C)	m-C$_{3/5}$	129.3	dm, $^1J_{CH}$ = 164 Hz
	p-C$_4$	131.5	dt, $^1J_{CH}$ = 138 Hz, $^4J_{CP}$ = 7.0 Hz
	i-C$_1$	132.2	d, $^1J_{CP}$ = 54.6 Hz
	o-C$_{2/6}$	133.1	dm, $^1J_{CH}$ = 153 Hz
	Au<u>C</u>	147.4	br. s

^{31}P{^{1}H}-NMR:	27.53	s
(CD_2Cl_2, 25 °C)		
Raman (powder sample) :	2001.6	s, ν(C≡C)
(cm^{-1})	1918.1	

7.5.6 Reaction of [Tri(*p*-tolyl)phosphine]gold Chloride and Acetylene Gas

A suspension of tri(*p*-tolyl)phosphine)gold chloride [(p-Tol)$_3$PAuCl], (2.0 g, 3.7 mmol) in ethanol (100 mL) was saturated with acetylene gas at -60 °C for 1 h. Subsequently a solution of sodium ethanolate [freshly prepared by dissolving sodium metal (0.09 g, 3.9 mmol) in ethanol (10 mL)] was slowly added with stirring. Acetylene was bubbled through the reaction mixture for another 3 h. On warming the mixture became a clear solution and a white precipitate formed. This was filtered off, washed with water, dissolved in CH_2Cl_2 and dried in a vacuum. The white product (1.34 g, 1.31 mmol, yield 70.8 %) was characterized as (*p*-Tol)$_3$PAuC≡CH (**13**). Single crystals of (**13**) were grown from dichloromethane carefully layered with *n*-pentane.

7.5.6.1 Characterization of [Tri(*p*-tolyl)phosphinegold]acetylene (13)

(*p*-Tol)$_3$PAuC≡CH (**13**), 1.34 g, 1.31 mmol, yield 70.8 %, m.p. 145°C, white solid.

$C_{23}H_{22}AuP$:	calcd.:	C 52.48	H 4.21	P 5.88
(526.37 g/mol)	found:	C 52.28	H 4.33	P 5.93

		%	
MS (FAB) [m/z]:	1249.6	0.54	$[2M + Au]^+$
	1223.5	1.98	$[M - H + (p\text{-Tol})_3PAu + Au]^+$
	1027.5	10.44	$[M + (p\text{-Tol})_3PAu]^+$
	805.5	19.73	$[(p\text{-Tol})_3PAuP(p\text{-Tol})_3]^+$
	527.4	9.98	$[M + H]^+$
	501.4	100.0	$[(p\text{-Tol})_3PAu]^+$

^{1}H-NMR (CD_2Cl_2, 25 °C):	C≡C<u>H</u>	1.62	s, 1H
	C<u>H</u>$_3$	2.36	s, 9H
	m-<u>H</u>$_{3/5}$	7.25	dd, $^3J_{HH}$= 8.1, $^4J_{HP}$= 1.8
	o-<u>H</u>$_{2/6}$	7.42	dd, $^3J_{HH}$= 8.1, $^3J_{HP}$= 13.3
^{1}H-NMR (CD_2Cl_2, -90 °C):	C≡C<u>H</u>	1.68	s
	C<u>H</u>$_3$	2.32	s
	m-<u>H</u>$_{3/5}$	7.23	dd, $^3J_{HH}$= 7.9, $^4J_{HP}$= 1.6
	o-<u>H</u>$_{2/6}$	7.32	dd, $^3J_{HH}$= 7.9, $^3J_{HP}$= 12.0

$^{13}C(^{1}H$-coupled)-NMR:	$\underline{C}H_3$	21.52	qt, $^{1}J_{CH}$ = 127 Hz, $^{3}J_{CH}$ = 3.7 Hz
(CD_2Cl_2, 25 °C)	C≡$\underline{C}$H	89.7	d, $^{1}J_{CH}$= 227 Hz
	Au$\underline{C}$	127.93	d, $^{2}J_{CP}$= 39.7 Hz
	i-$\underline{C}_1$	127.08	dt, $^{1}J_{CP}$= 58.1 Hz, $^{3}J_{CH}$= 8.30
	m-$\underline{C}_{3/5}$	130.06	ddq, $^{1}J_{CH}$= 161.35, $^{3}J_{CP}$= 11.52, $^{3}J_{CH}$= 5.53
	o-$\underline{C}_{2/6}$	134.30	ddd, $^{1}J_{CH}$= 163.19, $^{2}J_{CP}$=13.83, $^{3}J_{CH}$= 6.45
	p-$\underline{C}_4$	142.3	s
$^{13}C\{^{1}H\}$-NMR:	$\underline{C}H_3$	20.89	s
(CD_2Cl_2, -90 °C)	C≡$\underline{C}$H	89.69	d, $^{3}J_{CP}$= 26.5 Hz
	Au$\underline{C}$	127.02	d, $^{2}J_{CP}$= 139.0 Hz
	i-$\underline{C}_1$	125.43	d, $^{1}J_{CP}$= 58.6 Hz
	m-$\underline{C}_{3/5}$	129.24	d, $^{3}J_{CP}$= 12.0
	o-$\underline{C}_{2/6}$	133.52	d, $^{2}J_{CP}$= 13.7
	p-$\underline{C}_4$	141.76	d, $^{4}J_{CP}$= 2.4
$^{31}P\{^{1}H\}$-NMR:		40.45	s
(CD_2Cl_2, 25 °C)			
$^{31}P\{^{1}H\}$-NMR:		39.43	s
(CD_2Cl_2, -90 °C)			
IR (Nujol):			
(cm^{-1})		3275.5	vw, *ν*(CH), (-Au-C≡CH)
Raman (powder sample) :		1981.8	s, *ν*(C≡C)
($cm^{-}1$)			

Crystal data for (*p*-Tol)$_3$PAuC≡CH (**13**):

Empirical formula:	$C_{23}H_{22}AuP$	
Formula weight (g/mol):	526.34	
Crystal system:	monoclinic	
Space group:	$P2_1/c$	
Unit cell dimensions:	a = 9.4175(2) Å,	α = 90.00°
	b = 21.9742(4) Å,	β = 97.312(1)°
	c = 19.7824(5) Å,	γ = 90.00°

Z:	8
Volume, $Å^3$:	4060.52(15)
μ(Mo-Kα), cm^{-1}:	73.27
Density (ρ_{calc}), gcm^{-3}:	1.722
F(000):	2032
Crystal size, mm:	0.40 × 0.40 × 0.05
Θ-range for data collection, °:	3.14 to 26.58
Reflections collected / unique:	131597 / 7990 [R_{int} = 0.064]
Absorption correction:	DELABS
T_{min} / T_{max}:	0.330 / 0.758
Refined parameters:	459
*R*1	0.0356
*wR*2:	0.0857
Goodness-of-fit on F^2	1.066
ρ_{fin} (max/min), $eÅ^{-3}$:	1.115 / -1.028

7.5.6.2 Characterization of Bis[tri(*p*-tolyl)phosphinegold]acetylene (14)

(*p*-Tol)$_3$PAuC≡CAuP(*p*-Tol)$_3$ (**14**) was not isolated from the product mixture and only characterized in solution.

$C_{44}H_{42}Au_2P_2$:
(1026.70 g/mol)

$^{13}C(^1H$-coupled)-NMR:			
(CD_2Cl_2, 25 °C)	C≡C	147.86	br
$^{31}P\{^1H\}$-NMR:		40.44	s
(CD_2Cl_2, 25 °C)			

7.6 Synthesis and Characterization of Addition Products

7.6.1 Preparation and Characterization of [(Et$_3$P)AuC≡CAu(PEt$_3$)]·{[(Et$_3$P)Au]BF$_4$} (15)

A suspension of (triethylphosphine)gold chloride [(Et$_3$P)AuCl] (0.214 g, 0.61 mmol) and

$AgBF_4$ (0.120 g, 0.61 mmol) in THF (40 mL) was stirred for 2 h at -60 °C. The reaction mixture was filtered into $(Et_3P)AuC{\equiv}CAu(PEt_3)$ (**8**, 0.40 g, 0.61 mmol) in THF at -60 °C and the mixture stirred for a further 3 h. The solvent was evaporated under vacuum to afford an orange solid.

$[(Et_3P)AuC{\equiv}CAu(PEt_3)]\cdot\{[(Et_3P)Au]BF_4\}$ (**15**), orange solid, m.p. 86-87 °C.

(A : the parent axle unit; L : the ligand unit)

$C_{20}H_{45}Au_3BF_4P_3$:		calcd.:	C 22.74	H 4.29	P 8.80
(1056.20 g/mol)		found:	C 22.45	H 4.10	P 8.28
			%		
MS (FAB) [m/z]:		1504.1	7.36	$[2\ Et_3PAuCCAuPEt_3 + Au]^+$	
		968.6	100.0	$[M - BF_4^-]^+$	
		850.6	17.89	$[M - Et_3P - BF_4^-]^+$	
		654.8	9.38	$(Et_3P)AuCCAu(PEt_3)$	
		433.1	89.28	$[Et_3PAuPEt_3]^+$	
		315.1	57.10	$[Et_3PAu]^+$	
^{1}H-NMR (CD_2Cl_2, 25 °C):	A/L-C$\underline{H}_3$	1.154	dt, $^3J_{HP}$ = 18.3, $^3J_{HH}$ = 7.7		
	A-C$\underline{H}_2$	1.883	dq, $^2J_{HP}$ = 9.5, $^3J_{HH}$ = 7.7		
	L-C$\underline{H}_2$	1.937	dq, $^2J_{HP}$ = 4, $^3J_{HH}$ = 7.3		
^{13}C(^{1}H-coupled)-NMR:	L-$\underline{C}H_3$	8.969	qt, $^1J_{CH}$ = 129, $^2J_{CH}$ = 5		
(CD_2Cl_2, 25 °C)	A-$\underline{C}H_3$	9.107	qt, $^1J_{CH}$ = 129, $^2J_{CH}$ = 4		
	L-$\underline{C}H_2$	17.210	tdq, $^1J_{CH}$ = 131, $^1J_{CP}$ = 18, $^2J_{CH}$ = 2		
	A-$\underline{C}H_2$	17.788	tdq, $^1J_{CH}$ = 130, $^1J_{CP}$ = 34, $^2J_{CH}$ = 2		
		149.516	w, m		
	Au$\underline{C}$	156.174	S		
^{31}P{^{1}H}-NMR:	A-P	34.525	s		
(CD_2Cl_2, 25 °C)	L-P	47.615	s		
		79.611	s		

7.6.2 Preparation and Characterization of $[(Et_3P)AuC{\equiv}CAu(PEt_3)]\cdot\{[(Et_3P)Au]BF_4\}_2$ (16)

A suspension of (triethylphosphine)gold chloride [$(Et_3P)AuCl$] (0.321 g, 0.92 mmol) and $AgBF_4$ (0.178 g, 0.92 mmol)) in THF (75 mL) was stirred for 2 h at -60 °C. The reaction mixture was filtered with a canula into $(Et_3P)AuC{\equiv}CAu(PEt_3)$ (**8**, 0.30 g, 0.46 mmol), and the mixture stirred under the same conditions for a further 3 h. The solvent was evaporated under vacuum affording an orange oil.

$[(Et_3P)AuC{\equiv}CAu(PEt_3)]\cdot\{[(Et_3P)Au]BF_4\}_2$ (**16**), orange oil.

$C_{26}H_{60}Au_4B_2F_8P_4$:	calcd.:	C 21.42	H 4.15	P 8.50
(1458.13 g/mol)	found:	C 22.50	H 4.15	P 7.32
		%		

MS (FAB) [m/z]:	968.6	1.58	$[M - Et_3PAu - 2(BF_4)^-]^+$	
	664.6	2.11		
	433.1	100.0	$[Et_3PAuPEt_3]^+$	
	315.1	61.93	$[Et_3PAu]^+$	

^{1}H-NMR (CD_2Cl_2, 25 °C):	A-C<u>H</u>$_3$	1.192	dt, $^3J_{HP}$ = 19.4, $^3J_{HH}$ = 7.7	
	L-C<u>H</u>$_3$	1.203	dt, $^3J_{HP}$ = 18.7, $^3J_{HH}$ = 7.7	
	A/L-C<u>H</u>$_2$	1.936	dq, $^2J_{HP}$ = 10.6, $^3J_{HH}$ = 7.7	
^{13}C(^{1}H-coupled)-NMR:	L-<u>C</u>H$_3$	9.106	qt, $^1J_{CH}$ = 129, $^2J_{CH}$ = 5	
(CD_2Cl_2, 25 °C)	A-<u>C</u>H$_3$	9.391	qt, $^1J_{CH}$ = 129, $^2J_{CH}$ = 4	
	L-<u>C</u>H$_2$	17.4	t, $^1J_{CH}$ = 129	
	A-<u>C</u>H$_2$	17.788	tdq, $^1J_{CH}$ = 131, $^1J_{CP}$ = 36, $^2J_{CH}$ = 2	
	Au<u>C</u>	163.970	s	
^{31}P{^{1}H}-NMR:		36.098	s	
(CD_2Cl_2, 25 °C)		47.468	s	
		79.488	s	

7.6.3 Preparation and Characterization of $[(p\text{-}Tol)_3PAuC{\equiv}CH]\cdot\{[(p\text{-}Tol)_3PAu]BF_4\}$ (17)

A suspension of [tri(*p*-tolyl)phosphine]gold chloride [$(p\text{-}Tol)_3PAuCl$] (0.350 g, 0.65 mmol)

and $AgBF_4$ (0.128 g, 0.65 mmol) in dichloromethane (50 mL) was stirred for 2 h at -60 °C. The reaction mixture was filtered using a canula into (*p*-Tol)$_3$PAuC≡CH (0.333 g, 0.63 mmol) in dichloromethane at -60 °C, and the mixture was stirred for a further 3 h. The solvent was evaporated under vacuum affording a orange solid.

[(*p*-Tol)$_3$PAuC≡CH]·{[(*p*-Tol)$_3$PAu]BF_4} (**17**), orange solid.
$C_{44}H_{43}Au_2BF_4P_2$:
(1114.51 g/mol)

^{1}H-NMR (CD_2Cl_2, -90 °C):	C≡C<u>H</u>	1.659	d, J = 5.88
	C<u>H</u>$_3$	2.32	s
	m-H$_{3/5}$	7.233	d, $^3J_{HH}$= 8
	o-H$_{2/6}$	7.319	dd, $^3J_{HH}$= 8, $^3J_{HP}$= 13
^{13}C-NMR:	A/L-<u>C</u>H$_3$	21.565	d, J= 1.6
(CD_2Cl_2, 25 °C)	C≡<u>C</u>H	68.118	vw
		89.723	m
	A/L-i-C$_1$	126.364	d, $^1J_{CP}$ = 69.1
	A/L-m-C$_{3/5}$	130.231	d, J = 12.1
	A/L-o-C$_{2/6}$	134.397	d, $^2J_{CP}$ = 13.7
	A/L-p-C$_4$	142.893	m, br
^{13}C-NMR:	A-<u>C</u>H$_3$	20.974	s
(CD_2Cl_2, -90 °C)	L-<u>C</u>H$_3$	19.418	
	C≡<u>C</u>H	89.818	m
	L-i-C$_1$	124.49	d, $^1J_{CP}$ = 65.9
	A-i-C$_1$	125.46	d, $^1J_{CP}$ = 58.6
	A/L-m-C$_{3/5}$	129.281	d, $^3J_{CP}$= 12
	L-o-C$_{2/6}$	133.399	d, $^2J_{CP}$ = 13.7
	A-o-C$_{2/6}$	133.535	d, $^2J_{CP}$ = 13.6
	L-p-C$_4$	141.767	d, $^4J_{CP}$= 2.4
	A-p-C$_4$	142.222	d, $^4J_{CP}$= 2.4
	Au<u>C</u>≡CH	127.074	d, $^2J_{CP}$= 139.7

$^{31}P\{^{1}H\}$-NMR (25 °C):	32.108	s
(CD_2Cl_2)	40.608	s
$^{31}P\{^{1}H\}$-NMR(-90 °C):	31.212	s
(CD_2Cl_2)	39.410	s

7.6.4 Preparation and Characterization of [(*p*-Tol)$_3$PAuC≡CH]·{[(*p*-Tol)$_3$PAu]SbF$_6$} (18)

A suspension of [tri(*p*-tolyl)phosphine]gold chloride [(*p*-Tol)$_3$PAuCl] (0.31 g, 0.58 mmol) and $AgSbF_6$ (0.20 g, 0.58 mmol) in dichloromethane (50 mL) was stirred for 2 h at -60 °C. The reaction mixture was filtered into (*p*-Tol)$_3$PAuC≡CH (0.30g, 0.57 mmol) in dichloromethane at -60 °C, and the mixture stirred for a further 3 h. The solvent was evaporated under vacuum affording a brown solid.

[(*p*-Tol)$_3$PAuC≡CH]·[(AuP(*p*-Tol)$_3$)$^+$(SbF_6)$^-$] (**18**), 0.7 g, brown solid, mp 115 °C.

$C_{44}H_{43}Au_2F_6P_2Sb$:	calcd.:	C 41.83	H 3.43	P 4.90
(1263.44 g/mol)	found:	C 43.64	H 3.68	P 5.23

		%	
MS (FAB) [m/z]:	2264.5	1.16	[(*p*-Tol)$_3$PAu]$_4$C$_2$SbF$_6$]$^+$
	1764.2	3.90	[(*p*-Tol)$_3$PAu]$_3$C$_2$HSbF$_6$
	1535.5	33.5	
	1029.3	37.2	[(*p*-Tol)$_3$PAu]$_2$C$_2$H
	806.8	74.82	[(*p*-Tol)$_3$PAuP(p-Tol)$_3$]$^+$
	501.9	100	[(*p*-Tol)$_3$PAu]$^+$

^{1}H-NMR (CD_2Cl_2, 23 °C):	C≡C<u>H</u>	1.973	s
	C<u>H</u>$_3$	2.32	s
	m-<u>H</u>$_{3/5}$	7.233	d, $^3J_{HH}$= 8
	o-<u>H</u>$_{2/6}$	7.319	dd, $^3J_{HH}$= 8, $^3J_{HP}$= 13

^{13}C-NMR:	A-<u>C</u>H$_3$	21.572	s
(CD_2Cl_2, 25 °C)	L-<u>C</u>H$_3$	21.668	s
	C≡<u>C</u>H	72.069	s
	L-i-<u>C</u>$_1$	124.792	t, $^1J_{CP}$= 30.95

	A-i-$\underline{C}_1$	126.256	d, $^1J_{CP}$ = 61.8
	L-m-$\underline{C}_{3/5}$	130.454	d, $^3J_{CP}$= 12.1
	A-m-$\underline{C}_{3/5}$	130.961	t, J = 6.05
	L-o-$\underline{C}_{2/6}$	134.393	t, J = 7.65
	A-o-$\underline{C}_{2/6}$	133.393	d, $^2J_{CP}$ = 15.3
	L-p-$\underline{C}_4$	143.16	d, $^4J_{CP}$ = 2.4
	A-p-$\underline{C}_4$	144.098	s
^{13}C-NMR:	A-$\underline{C}H_3$	20.870	t, J= 4.0
(CD_2Cl_2, -90 °C)	L-$\underline{C}H_3$	21.06	d, J= 5.6
	C≡$\underline{C}$H	71.885	t, J= 9.25
	L-i-$\underline{C}_1$	123.411	t, $^1J_{CP}$= 30.90
	A-i-$\underline{C}_1$	124.50	d, $^1J_{CP}$ = 60.3
	L-m-$\underline{C}_{3/5}$	129.389	m
	A-m-$\underline{C}_{3/5}$	129.883	s
	L-o-$\underline{C}_{2/6}$	133.419	m
	A-o-$\underline{C}_{2/6}$	133.419	m
	L-p-$\underline{C}_4$	142.294	d
		142.015	m
	A-p-$\underline{C}_4$	142.916	s
^{31}P{^{1}H}-NMR (25 °C):		35.673	br
(CD_2Cl_2)		44.173	s
^{31}P{^{1}H}-NMR (-90 °C)		31.197	s
(CD_2Cl_2)		42.635	s
IR (Nujol):		1917.7	w, *ν*(C≡C)
(cm^{-1})		3190.9	w, *ν*(CH), (-Au-C≡CH)

8 Appendix

Table 8-1. Selected characterization data for the complexes of the type LAuC≡CAuL (A) from the reference literature.

		mp °C	Raman ν(C≡C) cm^{-1}	^{31}P ppm	^{1}H CH ppm	^{13}C Au-C ppm	^{13}C ppm	Au--Au	Ref.
1	$[RAuC{\equiv}CAuR]^{2-}$								Nast 1981
2	$Ph_3PAuC{\equiv}CAuPPh_3{\cdot}3CHCl_3$	de-comp. >60	2040						Cross 1986
3	(*p*-Tol)$_3$PAuC≡CAuP(*p*-tol)$_3{\cdot}2CH_2Cl_2$	110-115		40.7 $CDCl_3$					Cross 1986
4	(p-$MeOC_6H_4$)$_3$PAuC≡CAuP(p-$MeOC_6H_4$)$_3{\cdot}2CHCl_3$	125		38.3					Cross 1986
5	(*m*-Tol)$_3$PAuC≡CAuP(*m*-Tol)$_3$							monomer	Bruce 1988
6	(*m*-Tol)$_3$PAuC≡CAuP(*m*-Tol)$_3{\cdot}C_6H_6$							monomer	Bruce 1988
7	$Ph_3PAuC{\equiv}CAuPPh_3{\cdot}2C_6H_6$							monomer	Bruce 1988
8	$NpPh_2PAuC{\equiv}CAuPPh_3Np{\cdot}2CHCl_3$		2007 vs	38.0, s CD_2Cl_2	6.9-8.4			monomer	Müller 1994
9	$Np_2PhPAuC{\equiv}CAuPPhNp_2{\cdot}6CHCl_3$		2012 vs	30.7, s CD_2Cl_2	7.0-8.7			monomer	Müller 1994
10	$Fc_2PhPAuC{\equiv}CAuPPhFc_2{\cdot}4EtOH$		2003 vs	31.4, s CD_2Cl_2	7.9-8.7	145.0, dd $^{1}J_{CP}$=136	$^{2}J_{CP}$=21	monomer	Müller 1994
11	$Np_3PAuC{\equiv}CAuPNp_3{\cdot}CH_2Cl_2$		2008 vs						Müller 1994
12	$Ph_3PAuC{\equiv}CAuPPh_3{\cdot}2H_2O$		2002 vs	43.4	7.3-7.6	134.2,131.1,128.8			Müller 1994
13	$Cy_3PAuC{\equiv}C\text{-}ph\text{-}{\equiv}CAuPCy_3$		2113 2111-R	57.5		α137.6,d $^{2}J_{CP}$=131	β103.6, d $^{3}J_{CP}$=24		Chao 2002
14	$Cy_3PAuC{\equiv}C\text{-}ph\text{-}ph\text{-}{\equiv}CAuPCy_3$		2107-R						Chao 2002
15	$Me_3PAuC{\equiv}CAuPMe_3$	206-207	1999.3	1.03	1.49 $^{2}J_{HP}$=9.9	206.7, dd $^{2}J_{CP}$=12.0	$^{3}J_{CP}$=5.5	3.0747(8)	Liau 2003
16	$Et_3PAuC{\equiv}CAuPEt_3$	180-181	2009.1	39.20		150.0, br, s		6.959	Liau 2003
17	$(PhMe_2)PAuC{\equiv}CAuP(Me_2Ph)$	181-182	1998.3	33.21	1.73	148.3, br, s		3.1680(3)	Liau 2003
18	$(MePh_2)PAuC{\equiv}CAuP(Ph_2Me)$	106-107	2001.6						Liau 2003
19	$Vi_3PAuC{\equiv}CAuPVi_3$		1995.3						Liau 2003

Table 8-2. Selected characterization data for the complexes of the type LAuC≡CH (B) from the reference literature.

		mp °C	IR ν(C≡C) cm^{-1}	IR ν(CH) cm^{-1}	^{31}P ppm	^{1}H CH ppm	^{13}C Au-C ppm	^{13}C CH ppm	Ref.
1	$K[Au(C{\equiv}CH)_2]$								Nast 1964
2	$K_2[HC{\equiv}CAuC{\equiv}CAuC{\equiv}CH]$								Nast 1964
3	$iPr_3PAuC{\equiv}CH$	66	1978	3284	66.1	1.95, d, $^{4}J_{PH}$=5.2	150.26,s	88.65,d $^{3}J_{CP}$=22.9	Werner 1984
4	$[Ph_4P]_2[HC{\equiv}CAuC{\equiv}CAuC{\equiv}CH]$		1963						Nast 1981
5	$Ph_3PAuC{\equiv}CH$		1975	3278	41.9	1.75			Cross 1986
6	$NpPh_2PAuC{\equiv}CH$				40.3 s		125.6-135.5, m	90.8, s	Müller 1994
7	$BpPh_2PAuC{\equiv}CH$				42.0 s	1.8 s	127.1-144.3, m	89.9, s	Müller 1994
8	$[N(PPh_3)_2][HC{\equiv}CAuC{\equiv}CH]$	225	1962 w	3266 vw		1.37 s	127.02 s	87.10	Vicente 1995
9	$Ph_3PAuC{\equiv}CH$	168	1982	3272	42.4 s	1.83 s			Vicente 1995
10	$(p\text{-}MeOC_6H_4)_3PAuC{\equiv}CH$	123	1982	3268	37.9 s	1.81, d $^{4}J_{PH}$=4.8	126.3,d $^{2}J_{CP}$=140	90.48,d $^{3}J_{CP}$=26.2	Vicente 1995
11	$[N(PPh_3)_2][ClAuC{\equiv}CH]$	192	1975 (1982w)	3282 (3270 vw)	20.9 s	1.63 s		87.75 s (83.75 s)	Vicente 1995/ 1997
12	$[N(PPh_3)_2][BrAuC{\equiv}CH]$	186	1980 w	3266 vw	21.7 s	1.65, s		83.37 s	Vicente, 1995/ 1997
13	$[N(PPh_3)_2][IAuC{\equiv}CH]$	185	1964 w	3268 vw		1.63, s		82.20 s	Vicente 1997
14	$Me_3PAuC{\equiv}CH$	111-112	1971.1 (1973.8, Raman)	3272.2	1.03	2.09 s	128.3,d $^{2}J_{CP}$=38.7	90.4,d $^{3}J_{CP}$=12.9	Liau 2003
15	$Et_3PAuC{\equiv}CH$		(1974.0 Raman)					88.76	Liau 2003
16	$(Me_2Ph)PAuC{\equiv}CH$	157		14.06			127.90	90.5,d	Liau 2003
17	$(MePh_2)PAuC{\equiv}CH$	106-107	1978.5 (1981.8, Raman)	3279.6		1.62 s	127.8,d $^{2}J_{CP}$=39.7	90.1,d $^{3}J_{CP}$=2.3	Liau 2003
18	$(p\text{-}Tol)_3PAuC{\equiv}CH$ (RT)		(1983.5, Raman)	3275.5	40.4	1.62	127.93, d $^{2}J_{CP}$=39.7	89.7 $^{1}J_{CP}$=227	Liau 2003
	$(p\text{-}Tol)_3PAuC{\equiv}CH$ (-90°C)				39.4	1.566 $^{4}J_{PH}$=27.4	127.01, d $^{2}J_{CP}$=139.0	89.747 89.687 $^{3}J_{CP}$=26.5	

Table 8-3. Selected characterization data for the complexes of the type LAuC≡CR' (C) from the reference literature.

		Mp °C	IR ν(C≡C) cm^{-1}	^{31}P ppm	^{1}H ppm	C≡C Å	Au-C Å	Au-P Å	Au--Au Å	struc-ture	Ref.
1	$[AuC{\equiv}C^tBu]_4$	150									Coates 1962
2	$Et_3PAuC{\equiv}CPh$		2109 (KBr)								Coates 1962
3	$^nBuNCAuC{\equiv}CPh$										
4	$Me_3PAuC{\equiv}C^tBu$										
5	$Ph_3PAuC{\equiv}CPh$	80-85	2123 vw 2129 vw								Coates 1962
6	$^iPrNH_2AuC{\equiv}CPh$		2122-2125			1.21	1.94		3.274 3.722	Infinite zigzag	Cor-field 1967
7	$Ph_3PAuC{\equiv}CC_6F_5$	235-236	2130			1.197 (16)	1.993 (14)	2.274 (3)	>5.0	monom er	Bruce 1984
8	$Ph_3PAuC{\equiv}CPh$					1.18(2) 1.16(2)	1.97(2) 2.02(2)	2.276(5) 2.282(4)	3.379 (1)		Bruce 1986
9	$Ph_3PAuC{\equiv}CMe$	148-150	2120	41.8 $CDCl_3$	1.98 $CDCl_3$						Cross 1986
10	$Ph_3PAuC{\equiv}CEt$	154-155	2115	41.1 s	1.27 2.40						Cross 1986
11	$Ph_3PAuC{\equiv}CF_3$	155	2128	41.2							Cross 1986
12	$Ph_3PAuC{\equiv}CPh$	163-165	2118	42.3							Cross 1986
13	$(p\text{-Tol})_3PAuC{\equiv}CPh$	146-148	2120	40.2							Cross 1986
14	$Fc_2PhPAuC{\equiv}CPh$			32.1 s		1.172 (21)	2.011 (15)	2.274 (4)			Müller 1994
15	$Ph_3PAuC{\equiv}CPh$	135-138		42.6 s							Müller 1994
16	$MePh_2PAuC{\equiv}CPh$			26.9 s	2.1,d $^2J_{PH}$=10						Müller 1994
17	$(H_3N)AuC{\equiv}CPh$		2112								Mingos 1995
18	$\{[Au(C{\equiv}C^tBu)]_6\}_2$		2002 1983 1964 (KBr)		1.2 0.5				3.304-3.301		Mingos 1995